

TKK Dissertations 29  
Espoo 2006

**ELECTROCHEMILUMINESCENT AND  
CHEMILUMINESCENT LABELS FOR  
BIOAFFINITY ASSAYS**

Doctoral Dissertation

**Qinghong Jiang**



**Helsinki University of Technology  
Department of Chemical Technology  
Laboratory of Inorganic and Analytical Chemistry**

TKK Dissertations 29  
Espoo 2006

# **ELECTROCHEMILUMINESCENT AND CHEMILUMINESCENT LABELS FOR BIOAFFINITY ASSAYS**

Doctoral Dissertation

**Qinghong Jiang**

Dissertation for the degree of Doctor of Science in Technology to be presented with due permission of the Department of Chemical Technology for public examination and debate in Auditorium Ke 2 at Helsinki University of Technology (Espoo, Finland) on the 21st of April, 2006, at 12 noon.

**Helsinki University of Technology  
Department of Chemical Technology  
Laboratory of Inorganic and Analytical Chemistry**

**Teknillinen korkeakoulu  
Kemian tekniikan osasto  
Epäorgaanisen ja analyttisen kemian laboratorio**

Distribution:

Helsinki University of Technology  
Department of Chemical Technology  
Laboratory of Inorganic and Analytical Chemistry  
P.O. Box 6100 (Kemistintie 1 A)  
FI - 02015 TKK  
FINLAND  
URL: <http://www.chemistry.tkk.fi/eokem/>  
Tel. +358-9-451 2590  
Telefax +358-9-462 373  
E-mail: [jiang.qinghong@tkk.fi](mailto:jiang.qinghong@tkk.fi)

© 2006 Qinghong Jiang

ISBN 951-22-8106-6  
ISBN 951-22-8107-4 (PDF)  
ISSN 1795-2239  
ISSN 1795-4584 (PDF)  
URL: <http://lib.tkk.fi/Diss/2006/isbn9512281074/>

TKK-DISS-2118

Otamedia Oy  
Espoo 2006



HELSINKI UNIVERSITY OF TECHNOLOGY P. O. BOX 1000, FI-02015 TKK <a href="http://www.tkk.fi">http://www.tkk.fi</a>		ABSTRACT OF DOCTORAL DISSERTATION	
Author QINGHONG JIANG			
Name of the dissertation Electrochemiluminescent and Chemiluminescent Labels for Bioaffinity Assays			
Date of manuscript		Date of the dissertation 21 <sup>th</sup> April, 2006	
<input type="checkbox"/> Monograph		<input checked="" type="checkbox"/> Article dissertation (summary + original articles)	
Department	Department of Chemical Technology		
Laboratory	Laboratory of Inorganic and Analytical Chemistry		
Field of research	Electrochemiluminescence and chemiluminescence		
Opponent(s) (Instructor)	<b>Dmitri Papkovsky</b> (University College Cork) Supervisor		
Abstract <p>This thesis describes the electrochemiluminescence (ECL) of luminophores generated by cathodic pulse polarization of oxide film-coated electrodes in aqueous medium, and the chemiluminescence (CL) of luminophores induced by the dissolution of oxide film-covered aluminum or magnesium in appropriate aqueous medium. Their extremely sensitive ECL and CL signals allow these luminophores to be used as labels in bioaffinity assays, such as immunoassays and DNA probe assays. In this work, three types of luminophores were studied: organic luminophores, transition metal chelates, and lanthanide chelates. Studies show the hot electron-induced ECL excitation method provides a basis for time-resolved measurements. Thus, novel immunoassays and DNA-probe assays can be developed in which a combination of time-resolution and wavelength discrimination is applied in the simultaneous detection of several different labels. Some applications of immunoassays based on Tb(III) chelate labels and hot electron-excited ECL at insulating film-coated electrodes were demonstrated. Present studies widen the choices for electrochemiluminescent and chemiluminescent labels in immunoassays.</p>			
Keywords: electrochemiluminescence, chemiluminescence, label, bioaffinity, hot electron			
ISBN (printed)	951-22-8106-6	ISSN (printed)	1795-2239
ISBN (pdf)	951-22-8107-4	ISSN (pdf)	1795-4584
ISBN (others)		Number of pages	97p+app.87
Publisher Laboratory of Inorganic and Analytical Chemistry, Tkk			
Print distribution Laboratory of Inorganic and Analytical Chemistry, Tkk			
<input type="checkbox"/> The dissertation can be read at <a href="http://lib.tkk.fi/Diss/2006/isbn9512281074">http://lib.tkk.fi/Diss/2006/isbn9512281074</a>			



## ABSTRACT

This thesis describes the electrochemiluminescence (ECL) of luminophores generated by cathodic pulse polarization of oxide film-coated electrodes in aqueous medium, and the chemiluminescence (CL) of luminophores induced by the dissolution of oxide film-covered aluminum or magnesium in appropriate aqueous medium. Their extremely sensitive ECL and CL signals allow these luminophores to be used as labels in bioaffinity assays, such as immunoassays and DNA probe assays in place of radioactive and enzymatic labels. In this work, the weight is on the exploration of usable electrochemiluminescent labels and electrochemiluminescence in general.

Three types of luminophores were studied: organic luminophores, transition metal chelates, and lanthanide chelates. The ECL mechanisms of the luminophores were of interest. In principle, the tunnel emission of hot electrons into the aqueous electrolyte, which successively generate hydrated electrons, is the common initial step for ECL of all the studied luminophores. All of the present label molecules (except luminol) seem most efficiently to be excited by a route in which the label is first one-electron oxidized (or reduced) and the resulting radical is immediately reduced (or oxidized) by the primary or secondary radicals of the system. The ECL systems are characterized by the coreactant involved, the thickness of oxide film, and pH of the buffer solution.

The hot electron-induced ECL excitation method provides a basis for time-resolved measurements. Thus, novel immunoassays and DNA-probe assays can be developed in which a combination of time-resolution and wavelength discrimination is applied in the simultaneous detection of several different labels.

Some applications of immunoassays based on Tb(III) chelate labels and hot electron-excited ECL at insulating film-coated electrodes were demonstrated. The assays were reasonably sensitive and it was shown that it is possible to develop both non-competitive and competitive immunoassays based on the detection of hot electron-induced ECL of labels.

ECL of organic luminophores and metal chelates with different characteristic emission properties can be induced by hot electron excitation method in aqueous medium. Present studies widen the choices for electrochemiluminescent and chemiluminescent labels in immunoassays.

## PREFACE

It has been exciting, fruitful, and enjoyable for me to spend four years at the Laboratory of Inorganic and Analytical Chemistry of Helsinki University of Technology. I am sure it will become one of the most treasured memories of my life.

I would like to express my deepest gratitude to my supervisor, Prof. Sakari Kulmala, for giving me the opportunity to work in the group of Analytical Chemistry at the Helsinki University of Technology. He has given me much support but also freedom during my four-year journey of scientific and personal development. His creative ideas and amazing productivity in ECL research impressed me deeply.

My heartfelt thanks to Johanna Suomi, the finest of friends in the group of Analytical Chemistry, for the wonderful time we spent doing experiments shoulder by shoulder in the lab, for all the help she gave me, and for valuable discussions not least those on Finnish culture that we had during lunch time. Many thanks as well to Timo Alakleme, from the laboratory of Analytical Chemistry at the University of Turku, for guiding me e.g. in the use of LS-50B luminescence spectrometer and other apparatus and for oxidizing the Al electrodes with different oxide film thicknesses, and to Markus Håkansson and Anna-Maria Spehar for sharing their ideas and helping me to improve my language skills. Special thanks to Antti J. Niskanen for kindly oxidizing most of the silicon electrodes I needed and sharing his knowledge of silicon wafers. Thanks to Tiina Ylinen, for helping with the literatures search.

Finally, I would like to thank my dear husband and son for their all-out support and endless love. It was they who gave me the strength to endure all those lonely days and nights. Also warm thanks to my parents and my parents-in-law for taking care of my son when I was away. Completion of this thesis would not have been possible without the encouragement and understanding of my family.

Kathleen Ahonen assisted with the language of the thesis and financial aid was provided by the Research Foundation of Helsinki University of Technology. Chinese Government Award For Outstanding PhD Students Abroad was obtained in 2006.



## List of publications

- I. J. Suomi, M. Håkansson, Q. Jiang, M. Kotiranta, M. Helin, A.J. Niskanen, S. Kulmala, **Time-Resolved Detection of Electrochemiluminescence of Luminol**, *Anal. Chim. Acta*, 541 (2005) 167-169.
- II. M. Helin, Q. Jiang, H. Ketamo, M. Håkansson, A.-M. Spehar, S. Kulmala, T. Ala-Kleme, **Electrochemiluminescence of Coumarin Derivatives Induced by Injection of Hot Electrons into Aqueous Electrolyte Solution**, *Electrochim. Acta*, 51 (2005) 725-730.
- III. Q. Jiang, A.M. Spehar, M. Håkansson, J. Suomi, T. Ala-Kleme, S. Kulmala, **Hot Electron-Induced Cathodic Electrochemiluminescence of Rhodamine B at Disposable Oxide-Coated Aluminum Electrodes**, *Electrochim. Acta*, 51(2006) 2706-2714.
- IV. Q. Jiang, M. Håkansson, J. Suomi, T. Ala-Kleme, S. Kulmala, **Cathodic Electrochemiluminescence of Lucigenin Induced at Disposable Oxide-Coated Aluminum Electrode**, *J. Electroanal. Chem.*, Submitted.
- V. Q. Jiang, J. Suomi, M. Håkansson, A. Niskanen, M. Kotiranta, S. Kulmala, **Cathodic Electrogenated Chemiluminescence of Ru(bpy)<sub>3</sub><sup>2+</sup> Chelate at Oxide-Coated Heavily Doped Silicon Electrodes**. *Anal. Chim. Acta*, 541 (2005) 159-165.
- VI. Q. Jiang, M. Kotiranta, K. Langel, J. Suomi, M. Håkansson, A.-M. Spehar, T. Ala-Kleme, J. Eskola, S. Kulmala, **Ruthenium(II) Tris-(2,2'-bipyridine) Chelate as a Chemiluminophore in Extrinsic Lyoluminescences of Aluminum and Magnesium in Aqueous Solution**, *Anal. Chim. Acta*, 541 (2005) 179-186.
- VII. Q. Jiang, S. Sun, M. Håkansson, K. Langel, T. Ylinen, J. Suomi, S. Kulmala, **Electrochemiluminescence and Chemiluminescence of a Carboxylic Acid Derivative of Ruthenium(II) Tris-(2,2'-bipyridine)**

**Chelate Synthesized for Labeling Purposes**, *J. Lumin.*, 118 (2006) 265-271.

- VIII. Q. Jiang, M. Håkansson, A.-M. Spehar, J. Ahonen, T. Ala-Kleme, S. Kulmala, **Hot Electron-Induced Time-Resolved Electrogenerated Chemiluminescence of a Europium(III) Label in Fully Aqueous Solutions**. *Anal. Chim. Acta*, 558 (2006) 302-309.
- IX. T. Ala-Kleme, S. Kulmala, Q. Jiang, **Generation of Free Radicals and Electrochemiluminescence from Simple Aromatic Molecules in Aqueous Solutions**, *Lumin.*, in press.
- X. J. Eskola, P. Mäkinen, L. Oksa, K. Loikas, M. Nauma, Q. Jiang, M. Håkansson, J. Suomi, S. Kulmala, **Competitive Immunoassay by Hot Electron-Induced Electrochemiluminescence Detection and Using a Semiautomatic Electrochemiluminometer**, *J. Lumin.*, 118 (2006) 238-244.

## **Authors' contribution to the attached scientific papers**

The author has participated in the research and writing of 17 scientific publications at the Helsinki University of Technology. Ten of the most relevant of these are included in this thesis. Dr. Johanna Suomi and Prof. Kulmala were the primary authors of paper I; the present author participated in the measurements and in the writing of the manuscript. The experiments reported in paper II were planned by Prof. Kulmala and Dr. Timo Ala-Kleme, and the author participated in the work and wrote up the results in the appropriate form for publication. The experiments in papers III-VIII were designed by the present author together with Prof. Kulmala, and most of the measurements were carried out by her. She also wrote the original manuscripts. The work of paper IX was carried out in collaboration with Dr. Ala-Kleme and Prof. Kulmala, who were the main authors. Paper X was written on the basis of the results of the group by the author and Prof. Kulmala together with Jarkko Eskola. Papers V-VI will be also included in the thesis by Markus Håkansson.

# Electrochemiluminescent and chemiluminescent labels for bioaffinity assays

## CONTENTS

List of symbols and abbreviations .....	8
1. Introduction.....	10
2. Principles of bioaffinity assays .....	11
3. Principles of chemiluminescence and electrochemiluminescence .....	14
3.1 Principles of chemiluminescence.....	14
3.2 Principles of electrochemiluminescence.....	16
3.2.1 General mechanism of electrochemiluminescence.....	17
3.2.2 Hot electron-induced ECL.....	19
3.3 Applications of chemiluminescent and electrochemiluminescent luminophores as labels.....	21
3.3.1 Organic luminophores as labels.....	21
3.3.2 Transition metal chelates as labels.....	23
3.3.3 Lanthanide chelates as labels.....	25
4. Aims of the research .....	27
5. Experimental .....	27
5.1 Reagents.....	27
5.2 Instrumentation .....	29
6. Results and discussion .....	30
6.1 Hot electron emission and common primary species of luminophore ECL at conductor/insulator/electrolyte tunnel junction electrodes .....	30
6.2 Organic luminophores.....	34
6.2.1 Long-lived ECL of luminol .....	35
6.2.2 Cathodic ECL of coumarin derivatives.....	37
6.2.3 Hot electron-induced ECL of rhodamine B.....	41
6.2.4 Hot electron-induced ECL of lucigenin.....	46
6.3 Transition metal chelates .....	52
6.3.1 ECL of $\text{Ru}(\text{bpy})_3^{2+}$ induced at oxide film-coated silicon electrodes and CL of $\text{Ru}(\text{bpy})_3^{2+}$ .....	52
6.3.2 ECL of carboxylate derivative of $\text{Ru}(\text{bpy})_3^{2+}$ .....	63
6.4 Lanthanide chelates and their aromatic moieties.....	67
6.4.1 ECL of lanthanide chelates and their aromatic moieties .....	67
6.4.2 Chemiluminescence of Tb(III) chelates induced at aluminum surface in alkaline aqueous solution.....	79
6.5 Immunoassays using ECL labels .....	81
6.5.1 Competitive immunoassay of thyroxin.....	81
6.5.2 Non-competitive immunoassay of hTSH.....	83
7. Conclusions.....	85
References:.....	88
Reprints of original publications.....	99

## List of symbols and abbreviations

Ab	antibody
Ag	antigen
ABEI	aminobutylethylisoluminol
AHEI	aminohexylethylisoluminol
Ar	aromatic luminophores
BADE	9,9'-bis(acridinium-N,N'-diacetic acid) ethyl ester
biim	biimidazole
bpym	bipyrimidine
CB	conduction band
C/I/E	conductor/insulator/electrolyte
CL	chemiluminescence
CLIA	CL immunoassay
dmbp	4,4'-dimethyl-2,2'-bipyridine
dmphen	4,7-dimethyl-9,10-phenanthroline
DMF	Dimethylformamide
DNA	deoxyribonucleic acid
ECL	electrochemiluminescence = electrogenerated chemiluminescence
$e_{aq}^-$	hydrated electron
$E_c$	conduction band edge
$E_{cs}^{oxide}$	conduction band edge at oxide surface
ECLIA	ECL immunoassay
$e_{quasifree}^-$	hot dry electron
$E_F$	Fermi level
$e_{SS, ins}^-$	less energetic electrons via the surface states
$E_V$	valence band edge
$E_{vs}^{oxide}$	valence band edge at oxide surface
F-center (in metal oxides)	two electrons trapped in an $O^{2-}$ vacancy
$F^+$ -center (in metal oxides)	one electron trapped in an $O^{2-}$ vacancy
HIV-1	human immunodeficiency virus-1
hTSH	human thyroid stimulation hormone
IRMA	immunoradiometric assay
$L_{ox}$	one-electronically oxidized ligand L
$L_{Re}$	one-electronically reduced ligand L
M/I/M	metal/insulator/metal junction
$^3MLCT$	metal-to-ligand charge transfer excited triplet state
NHS ester	N-hydroxysuccinimide ester
$Ox^\bullet$	one-electron oxidant
PAHs	polyaromatic hydrocarbons
PCR	polymerase chain reaction
phen	phenanthroline
PL	photoluminescence
PTFE	Polytetrafluoroethylene
RNA	ribonucleic acid
RSD	relative standard deviation
SCE	saturated calomel electrode
SHE	standard hydrogen electrode
SPBA	N,N-di-(3-sulfopropyl)-9,9'-bisacridinium

ssDNA	single-stranded DNA
Transitions	
${}^5D_4 \rightarrow {}^7F_j$ of Tb(III)	${}^5D_4 \rightarrow {}^7F_{6,5,4,3,2,1,0}$
TR-ECL	time- resolved electrogenerated luminescence
$VO^{2-}$	an $O^{2-}$ vacancy
$\phi_{cl}$	quantum yield
$\phi_c$	fraction of reacting molecules giving an excitable molecule
$\phi_e$	fraction of molecules in an electronically excited state
$\phi_f$	fraction of excited molecules that return to the ground state by emitting a photon.

## 1. Introduction

An emission of light ( ultra-violet, visible, infrared), which occurs when a molecule in an excited state relaxes radiatively to its ground state is called luminescence. In general, almost all light emissions not induced by a hot incandescent body, such as a black body, can be called luminescence. The various types of luminescence differ from the source of energy to obtain the excited state. When the excited state is produced by photons, luminescence is classified as photoluminescence (PL) (including fluorescence and phosphorescence). In chemiluminescence (CL), the excitation energy is provided by a chemical reaction. Electrochemiluminescence (ECL), also known as electrogenerated chemiluminescence, is a type of luminescence in which at least one of the reactants resulting in the luminescence via more or less simple pathway is electrically produced at an electrode. ECL normally involves the generation of reactive intermediates from stable precursors in bulk solution at the surface of an electrode, and reaction of these intermediates to form excited states that emit light.

In CL and ECL, where the excitation step does not require irradiation of the sample, there are no problems with light scattering or source instability, as frequently encountered in photoluminescence. High background signals due to unselective photoexcitation are not a problem either. Thus, a highly sensitive detection can be achieved with simple instrumentation. CL and ECL thus provide a versatile, ultrasensitive tool with a wide range of applications in fields as diverse as biotechnology, pharmacology, molecular biology, and clinical and environmental chemistry.<sup>1,2,3</sup>

Both CL detection and ECL detection have been widely applied in bioaffinity assays, such as in immunoassays and DNA-probe assays, in which photoluminescent, chemiluminescent and electrochemiluminescent labels have largely replaced radioactive labels. In many cases, the analytical sensitivity of CL- and ECL- based immunoassays is comparable to or better than that obtained with radioactive labels, especially in the field of clinical chemistry. In addition, chemiluminescent and electrochemiluminescent labels are typically extremely stable, with shelf-lives in

excess of one year at room temperature. Detection limits are at sub-picomolar level, and detection can be made in a wide linear dynamic range extending over several orders of magnitude.<sup>4</sup> Unlike radioactive labels, CL and ECL are suitable for non separation protocols.<sup>5,6</sup> With them, the problems with reagent storage, handling and disposal are reduced. Moreover, their small size allows multiple labeling of the same molecule without affecting the immunoreactivity or hybridization of the probes.

Present thesis describes novel CL and ECL labels excited by highly energetic reductants including hot electrons injected from oxide film-covered electrodes in aqueous medium. The analytical applicability of lanthanide labels is also demonstrated in immunoassay formats.

## **2. Principles of bioaffinity assays**

The ability to determine the presence of drugs, intermediate metabolites, and biopolymers in body fluids, cells, and tissue specimens is of great importance in the life sciences. However, the wide range of chemical structures and the complexity of the physiological function of biomolecules create considerable problems in the analysis of these substances. Bioaffinity assays play a vital role in the quantitative analysis of molecules of biological interest.

A bioaffinity assay is an assay based on an interaction between a ligand and a receptor. Both the ligand and the receptor are biomolecules (proteins, antibodies, haptens, enzymes, oligonucleotides). Note: it is usual to describe the small molecule in affinity interactions as a ligand. If the interacting molecules are an antigen and an antibody, the bioaffinity assay is called an immunoassay. Affinity interactions—between antigen and antibody, protein and nucleic acid, chemoreceptor and ligand etc., and hybridization of complementary strands of ssDNA—are among the most important biochemical processes in nature.<sup>7</sup> Affinity interactions are the basis for the design of bioanalytical assays.

Immunoassays are the more common type of bioaffinity assays. Basically, an immunoassay exploits the unique specificity of an antibody (Ab) binding an antigen



(Ag) in order to selectively recognize and determine analytes that are either antibodies or antigens.<sup>8</sup> An antibody is a protein that is produced by the body in response to an “invading” (foreign) substance, or antigen, which the body is trying to “fight off” (eliminate or reduce) by mounting an immune response. The specificity of antibody-antigen binding is determined by the amino acids of the complementarity-determining regions. High selectivity can be obtained because other interfering compounds in the sample are not recognized in an immunoassay.

The vast majority of immunoreactions are monitored via a labeled antigen (Ag\*) or antibody (Ab\*). Labels include radioactive compounds, enzymes that cause a change of color in a solution, and luminophores that produce light through chemical reactions. The label can be applied, during the manufacture of the reagent, to either the antibody or antigen. Analysis is achieved by measuring some physical or chemical properties associated with the label, thereby allowing the construction of a standard curve that represents a measured physical signal as a function of labeled compound. Unknown analyte concentrations are extracted from this calibration curve.

Immunoassay methods that do not require separation of the bound Ab-Ag\*(or Ab\*-Ag) complex from free Ab and Ag\* (or free Ab\*, Ag) are referred to as homogeneous immunoassay (Fig.1a), while those that do require separation are referred to as heterogeneous one (Fig.1b-d). Homogeneous methods are generally applied to the measurement of small analytes such as abused and therapeutic drugs. Change in the activity of the label upon antibody binding makes possible a selective detection of the label (and the antigen) (Fig. 1a). Since no separation is involved, the number of procedural steps is reduced, and so the time required per assay. Additionally, since the physical transfer step is circumvented, potential sample loss related to this step is eliminated. Even though the sensitivity of homogeneous assays tends to be lower, and the dynamic range of homogeneous assay is generally modest,<sup>9</sup> homogeneous assays are usually preferred to heterogeneous unless sensitivity is an important issue.

The measurement of analyte in an immunoassay is achieved by using either a competitive (Fig. 1a, c, d) or a noncompetitive format (Fig. 1b). In competitive formats, unlabelled analyte (antigen) in the test sample is measured by its ability to compete with labeled antigen in the immunoassay. The unlabeled antigen blocks the

ability of the labeled antigen to bind because that binding site on the antibody is already occupied by unlabeled antigen. Thus, in a competitive immunoassay, less label measured in the assay means more of the unlabeled (test sample) antigen is present. In the competitive format, the amount of antigen in the test sample is inversely related to the amount of label measured. Competitive immunoassay formats can use either one-step or two-step method.

Noncompetitive assay formats, in which the measurement of labeled analyte is directly proportional to the amount of antigen present in the sample, generally provide the highest level of assay sensitivity and specificity. In a typical example of a noncompetitive immunoassay, an antigen is sandwiched between two antibodies (Fig. 1b). One of the antibodies, the coating antibody, is immobilized onto a solid phase, and the other (the detecting antibody) is labeled. As also with the competitive, noncompetitive assay formats can utilize either one step or two steps methods. The two-step assay format differs from the one-step in employing washing steps in which the sandwich binding complex is isolated and washed to remove excess unbound labeled reagent and any other interfering substances.

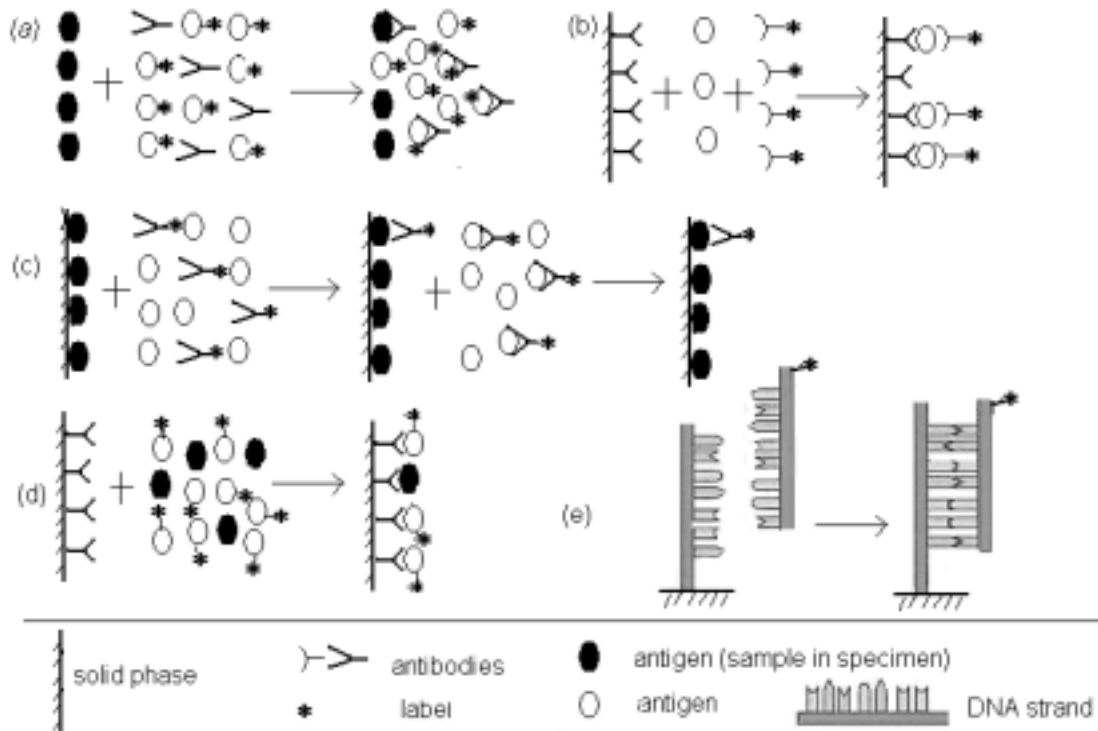


**Fig. 1** Five general immunoassay formats: (a) homogeneous competitive immunoassay (b) heterogeneous non-competitive immunoassay (c) heterogeneous competitive immunoassay (d) heterogeneous competitive immunometric assay (e) DNA-probe assay.<sup>10, 11</sup>

DNA-probe assay, another important type of bioaffinity assay, has found widespread use in the field of molecular diagnostics.<sup>12</sup> Molecular diagnostics, which is based on the analysis of genomic sequences, offers a highly sensitive and quantitative method for the detection of infectious disease pathogens and genetic variation. DNA probe assay (Fig. 1e) provides a method for the analysis of specific gene sequences based on DNA hybridization. The target gene sequence is identified by a DNA probe that forms a double-stranded complex with its complementary nucleic acid. DNA probes are single-stranded oligonucleotides, bound with labels to provide detectable signals for DNA hybridization.

The most widely used labels in bioaffinity assay are photoluminescent labels, chemiluminescent labels, radioactive labels and enzymatic labels. CL- and ECL-based immunoassays, relying on direct or indirect detection via luminescence, offer high sensitivity and broad linear range, in combination with the high specificity of the immunogenic reaction. For use as a CL or ECL label, a compound must fulfill four requirements: 1) it must be capable of participating in a CL or ECL reaction; 2) it must be attachable to the antigen or antibody, to form a stable reagent until the reaction is triggered; 3) it must retain a high quantum yield and the necessary kinetics after coupling; 4) it must not significantly alter the physico-chemical properties of the molecule to which it is attached, in particular its immunological activity. Since most analytes are not naturally luminescent, and there is an urgent need for a wide variety of analytical applications, the design, synthesis and characterization of luminescent molecules are under intense study.

### **3. Principles of chemiluminescence and electrochemiluminescence**

#### **3.1 Principles of chemiluminescence**

Chemiluminescence is observed when the excited product of an exoergic chemical reaction relaxes to its ground state with emission of photons.<sup>13</sup> A chemical reaction produces energy in sufficient amount to induce the transition of an electron from its ground state to an excited electronic state. The energy levels are identical with those

involved in fluorescence. The electronic transition is often accompanied by vibrational and rotational changes in the molecule. The excited molecule can also lose energy by undergoing chemical reactions, by collisional deactivation, internal conversion or inter-system crossing. These radiationless processes are undesirable from the analytical point of view when they compete with chemiluminescence.

In a CL reaction, A and B react to form a product C, some fraction of which is present in an electronically excited state,  $C^*$ , which subsequently relaxes to the ground state emitting a photon:



The fraction of molecules emitting a photon on return to the ground state is the quantum yield ( $\phi_{cl}$ ). It is the product of three ratios:

$$\phi_{cl} = \phi_c \cdot \phi_e \cdot \phi_f \quad (2)$$

where  $\phi_c$  is the fraction of reacting molecules giving an excitable molecule and accounts for the yield of the chemical reaction,  $\phi_e$  is the fraction of such molecules in an electronically excited state and relates to the efficiency of the energy transfer and  $\phi_f$  is the fraction of these excited molecules that return to the ground state by emitting a photon. Hence, the chemiluminescence takes place at the rate of a chemical reaction, and the emission intensity is affected by a combination of chemical reaction rate and luminescence considerations.

The presence of suitable molecules (enhancers) may increase the intensity and duration of light emission, thereby improving the analytical performance of the CL reaction.<sup>14</sup>

CL offers the unique feature that light is emitted by a specific reaction involving the analyte or label (in bioaffinity assays). Without the typical background emission of fluorescence, the background signal is reduced and the detection limits improved. Since minor changes in a weak signal are more easily observed than minor changes in a strong signal, chemiluminescence is extremely sensitive (limit of detection in

zeptomole amounts,  $10^{-21}$  mol).<sup>15</sup> Another advantage of the CL method is the relatively simple instrumentation required. No excitation light source is needed (unlike for fluorescence and phosphorescence) and no monochromator (often not even a filter). Only a single light detector is needed to detect the light emitted from CL reactions. Normally, all that is needed is a photomultiplier tube, sufficiently sensitive in the spectral region of interest.

Some shortcomings have to be considered as well. A CL reagent may yield significant emission not just for more than one analyte or label, i.e. selectivity may be restricted. Moreover, CL emission intensity may be sensitive to a variety of environmental factors, such as temperature, solvent, ionic strength, pH and other species present in the system.

### 3.2 Principles of electrochemiluminescence

Electrochemiluminescence (ECL) can be described as chemiluminescence produced as a result of electrochemical reactions. Both CL and ECL often involve the production of light by species that undergo highly energetic electron transfer reactions. However, luminescence in CL is initiated and controlled by the mixing of reagents or careful manipulation of fluid flow. In ECL, luminescence is initiated and controlled by switching on or sweeping electrode potential. ECL has unique advantages over CL in that the reactants for luminescence are produced *in situ* in the vicinity of an electrode surface to which appropriate potential is applied.<sup>16-19</sup> This *in situ* generation of reactants allows the detection of a wider range of analytes.<sup>11, 20</sup>

ECL has been known for a long time. Reports date back as far as 1927 for the light emission of Grignard compounds at appropriate potentials,<sup>21</sup> and 1929 for the ECL of luminol<sup>22</sup>. Since the first detailed study in the mid-1960s,<sup>23,24</sup> a great number of research papers and patents have been published. Many of these focus on the reaction mechanisms and characteristics of ECL, especially ECL of polyaromatic hydrocarbons (PAHs) and metal complexes.<sup>25-27</sup> Recently, most attention has been paid to the application of ECL-active species as labels on biological molecules, such as in immunoassays and DNA analysis.<sup>21</sup> Commercial systems have been developed

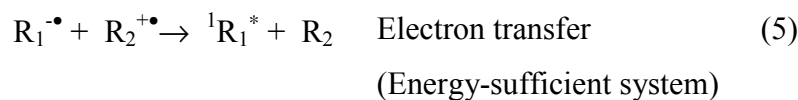
that use ECL to detect clinically important analytes (e.g.,  $\alpha$ -fetoprotein, digoxin, thyrotropin, and various antibodies) with high sensitivity and selectivity.<sup>28</sup>

### 3.2.1 General mechanism of electrochemiluminescence

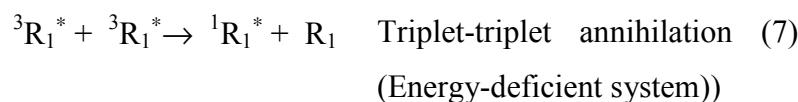
In general, ECL excitation pathways are closely related to their corresponding photoluminescent excitation pathways.<sup>29-31</sup> An essential difference is that the energy for generation of excited state species in ECL derives from an electrochemical reaction instead of specific light absorption in photoluminescence. The typical ECL of organic species (e.g. PAHs) in organic solvents originates in an energetic electron-transfer reaction between an oxidized and a reduced species, both of which are generated at an electrode by alternate pulsing of the electrode potential.<sup>29-31</sup> The general formula is as follows:<sup>29-32</sup>



either:



or:



followed by:



In energy-sufficient systems, formation of the excited singlet state  ${}^1R^*$  is energetically accessible, whereas, in energy-deficient systems, only the excited triplet state  ${}^3R^*$  is generated via the redox reaction. The emitting species  ${}^1R^*$  is formed via triplet-triplet annihilation (7). In fact, the excited species can be either  ${}^1R_1^*$  or  ${}^1R_2^*$ , depending on their relative energies. In energy-sufficient systems, light may also be produced by both routes, but the energy-sufficient system will predominate. In principle, ECL

reactions can be carried out at two separate but closely located electrodes, or at a single electrode using an alternating potential. Either  $R_1$  or  $R_2$  can be the analyte in the system.

The energetics of the ECL system is related to the formal redox potentials of the oxidized radical  $R_2^{+\bullet}$  and reduced radical  $R_1^{-\bullet}$  involved in the ECL excitation step (5 or 6). The enthalpies ( $\Delta H^\circ$ ) of the excitation steps can be calculated with the following equation according to basic thermodynamics:<sup>33</sup>

$$\Delta H^\circ = \Delta G^\circ + T\Delta S^\circ = nF(E^\circ(R_2^{+\bullet}/R_2) - E^\circ(R_1/R_1^{-\bullet})) - 0.16 \text{ eV} \quad (9)$$

Where  $E^\circ(R_2^{+\bullet}/R_2)$  and  $E^\circ(R_1/R_1^{-\bullet})$  represent the standard potentials of the oxidant and the reductant of the excitation step (or electrode potential if heterogeneous electron transfer occurs), respectively. The precise value for  $T\Delta S^\circ$  is unknown, but it is estimated to be about -0.16 eV.<sup>33</sup> For an energy-sufficient system, the  $\Delta H^\circ$  of the excitation step is larger than the energy required to produce the excited singlet state  $^1R_1^*$  from the ground state. If  $\Delta H^\circ$  is just sufficient for the generation of  $^3R_1^*$ , the ECL system is an energy-deficient system.

ECL can be generated in a two- or one-step method. In the two-step potential sweep method, cyclic voltammetry technique is commonly utilized to obtain potentials at which the reactants can be produced and then ECL reaction occurs.<sup>34, 35</sup> A working electrode, usually a metal or glassy carbon electrode, is immersed in a solution, and the electrode potential is swept to the value at which an oxidized (or reduced) radical product is formed, and kept at this value for a certain time (few  $\mu\text{s}$  or s). After this, the reverse process takes place. As a result of this two-step potential sweep, both oxidized radicals and reduced radicals exist in the diffusion layer near the electrode surface and can react with each other to form the excited state. ECL can also be obtained with two different electrodes that are close enough to allow the electrogenerated radicals to interdiffuse and undergo annihilation to emit light (e.g., eq. 5 or 6).<sup>36,37</sup>

In the one-step potential method, ECL is generated in the presence of a coreactant, and the electrode typically oxidizes or reduces the reagents in a single potential step.

A coreactant is a species that can produce a radical intermediate that can react with an ECL luminophore to produce excited states upon electrochemical oxidation or reduction. Oxalate ion ( $\text{C}_2\text{O}_4^{2-}$ ) was the first coreactant to be used<sup>38</sup> and it produces the strong reductant  $\text{CO}_2^{\bullet-}$  upon oxidation in aqueous solution:



If an ECL luminophore (L) can be oxidized at the same potential to produce another radical,  $\text{L}^{\bullet+}$ , the  $\text{L}^{\bullet+}$  and  $\text{CO}_2^{\bullet-}$  can react to produce an excited state capable of emitting light. Oxalate is often referred to as an oxidative coreactant owing to its ability to form a strong reducing species upon electrochemical oxidation. The strategy of coreactant ECL is used in analytical and biotechnology applications.<sup>28,39</sup>

There are many extensively applied coreactants, such as peroxodisulfate ion ( $\text{S}_2\text{O}_8^{2-}$ ) in  $\text{Ru}(\text{bpy})_3^{2+}$  system,<sup>40,41</sup> and hydrogen peroxide in luminol alkaline medium system applications.<sup>42,43</sup> Use of the coreactant ECL format widens the usable potential window of a conventional metal electrode, which, especially in aqueous medium, is restricted by cathodic hydrogen evolution and anodic oxygen evolution reactions and their overvoltages.<sup>44</sup>

With conventional metal electrodes, ECL of organic luminophores generally takes place only in organic solvents from which water and dissolved oxygen have been rigorously excluded to prevent quenching of ECL reactions. This requirement limits the application of ECL in biochemical analysis. Moreover, the available potential range at conventional metal electrodes in water is too narrow for simultaneously generation of two species (i.e. radical anions and cations) needed for annihilation ECL. Another problem is that one-electron oxidized or reduced radical luminophores are normally extremely unstable in aqueous solutions.

### 3.2.2 Hot electron-induced ECL

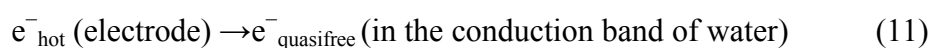
An alternative ECL system, which is of greater technical simplicity for certain applications than the conventional one, can be created at metal electrodes covered with oxide of aluminum, gallium, tantalum, magnesium, and silicon.<sup>45-49</sup> The use of



oxide-covered cathodes widens the potential window and the wider window is, the more energetic the light emissions can be.<sup>50-52</sup>

It has been proposed that oxide-covered electrodes can act as cold cathodes during cathodic pulse polarization and tunnel-emit hot electrons into an aqueous electrolyte. These generate hydrated electrons and oxidizing radicals from coreactants such as dissolved oxygen, and peroxodisulfate.<sup>45,53,54</sup> Studies in nonaqueous, e.g., acetonitrile, have provided experimental evidence for the production of hot electrons from a Ta<sub>2</sub>O<sub>5</sub>-covered Ta electrode.<sup>47,55</sup> The mechanism of hot electron excited ECL at oxide-covered electrodes is distinctly different from that of the conventional ECL described above. Here, hot electron denotes an electron possessing higher energy in aqueous solution than an electron heterogeneously transferred to an electrolyte solution from an active metal electrode in conventional ECL.

During the high amplitude cathodic pulse polarization of an oxide-covered electrode, hot electrons in metal with sufficient energy may enter the conduction band of water through the oxide layer/solution interface and turn into hydrated electrons after thermalization and solvation.<sup>56,57</sup> A general mechanism of hot electron-induced ECL at oxide-covered electrode may consist of either oxidation-initiated reductive pathways (13a-b) or reduction-initiated oxidative pathways (14a-b) as described below:<sup>45, 58, 59</sup>



Here, Ox<sup>•</sup> is one-electron oxidant, which could be produced from coreactants or just the F<sup>+</sup>-center existing in oxide film.<sup>53</sup>

The simultaneous presence of highly reducing and oxidizing species in the vicinity of the electrode surface makes it possible to generate ECL from luminophores that cannot be excited at conventional metal cathodes in fully aqueous solutions. This type of ECL also provides a means to simultaneously excite several luminophores emitting in different spectral region.<sup>60</sup> In addition, ECL luminophores with different luminescence lifetimes can be excited simultaneously and discriminated by a time-resolved measurement technique.<sup>61,62</sup> Thus, wavelength or time discrimination or a combination of these, can be exploited in discrimination of the electrochemiluminescence signals emerging from different luminophores.

### **3.3 Applications of chemiluminescent and electrochemiluminescent luminophores as labels**

Clinical analysis, in which analytes specific to human biological activity are determined, has received much interest over the past decades.<sup>63,64</sup> Because of the advantages of CL and ECL methods including ultrasensitive detection limits, rapid assays, and wide linear calibration ranges, CL and ECL are quite commonly applied in bioaffinity assays, such as in DNA probe assays and immunoassays.<sup>65</sup>

In both immunoassays and DNA assays, the label is covalently linked to either the antigen or antibody by chemical modification of the label, antigen or antibody or by conjugation with a bifunctional reagent. ECL immunoassays (ECLIA) have a potential advantage over more conventional CL (CLIA) immunoassays in that not only can an ECL reaction be controlled and manipulated by change in the applied potential, but also a wide range of formats can be readily developed in homogeneous immunoassay format. The CL and ECL labels can be classified into organic luminophores, transition metal chelates, and lanthanide chelates on the basis of their natures. These are discussed below.

#### **3.3.1 Organic luminophores as labels**

The diverse optical and redox properties of organic luminophores have found for them a great number of practical applications as labels in bioaffinity assays. In principle,

many of the common organic labels (e.g. fluorescein derivatives, coumarine derivatives, and methyl chloroformate) used in fluoroimmunoassay could be applied as ECL labels with hot-electron excitation.<sup>60,66,67,68</sup> In addition, some organic compounds (such as hemin<sup>69</sup>) themselves possessing catalytic ECL activity, even when conjugated to a protein, have been proposed as labels for bioassays.

Luminol and isoluminol (Fig. 2a,2b) were the first compounds to be used as CL labels,<sup>70,71</sup> but acridinium ester and derivatives of lucigenin are more sensitive (Fig. 2c).<sup>72</sup> Luminol-type chemiluminescence derivatization reagents (e.g. isoluminol derivatives: AHEI, ABEI) are among the most popular pure organic luminophores, and they have been extensively investigated for labeling other molecules in immunoassays<sup>73</sup>. Luminol and luminol-type CL derivatization reagents could also be utilized as ECL labels.<sup>74-76</sup> It has been proposed that the ECL reaction mechanism of luminol in alkaline medium is similar to its CL reaction.<sup>77, 78</sup>

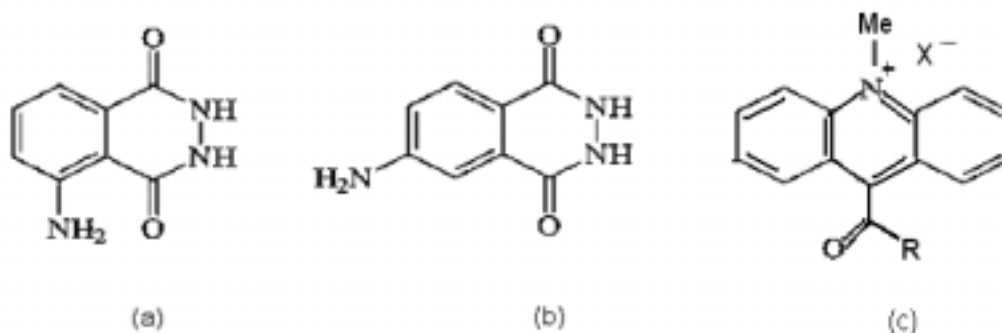


Fig. 2 Molecular structure of (a) luminol, (b) isoluminol, (c) acridinium ester.

As labels, luminol and luminol-type CL derivatization reagents can be coupled with amines, carboxylic acids, amino acids and peptides.<sup>79</sup> The biomolecules of interest, can be sensitively detected by competitive immunoassays. For example, methamphetamine and amphetamine in human serum<sup>80</sup> or urine<sup>81</sup> can be sensitively detected down to 20 pmol/ml with isoluminol isothiocyanate (4-isothiocyanatophthalhydrazide; ILITC) as label and CE technique glycylglycine can be detected at low to sub-fmol level.<sup>82</sup> Tripeptides have been detected at about 100 fmol levels with ABEI as an electrochemiluminescent label.<sup>83</sup> It is worth noting that isoluminol derivatives (such as ABEI) do not markedly lose their chemiluminescence efficiency if conjugated with proteins.<sup>84</sup>

Acridinium derivatives provide very sensitive detection due to their high quantum yields and low background signals (no need for catalysts). Acridinium labels have been proposed for ultrasensitive immunoassays of various analytes at the sub-picomolar level: human growth hormone<sup>85,86</sup>, interleukins, interferons and related peptides,<sup>87-90</sup> antibodies<sup>91</sup>, proinsulin<sup>92</sup>, parathyroid hormone-related peptide,<sup>93</sup> apolipoprotein B<sup>94</sup>, and haptens<sup>95-97</sup>. After treatment with activated esters or imidates, the labels easily couple to protein.<sup>98,99</sup> Acridinium derivatives are also suitable for labeling DNA strands for DNA-probe assay. Indeed, after inclusion in the DNA helix, acridinium labels show increased stability toward hydrolysis and no reactivity with nucleophiles such as thiols and sulfites. Various nonseparative determinations of hybridization rate constants and thermodynamic affinities have been based on these properties.<sup>100-102</sup>

### 3.3.2 Transition metal chelates as labels

A large number of transition metal chelates and clusters produce ECL. Amongst the investigated metals are Ru, Os, Re, Ir, Pd, and Mo. Much attention has been paid to Ru(bpy)<sub>3</sub><sup>2+</sup> chelate and its derivatives due to their strong luminescence (not only in aqueous solution but also at physiological pH), good solubility in aqueous solution, and compatibility with a variety of analytes. The label is small enough to allow even multi-labeling of biomolecules without interfering with biological activity. One of the most attractive features of the Ru(bpy)<sub>3</sub><sup>2+</sup> label is that the nondestructive mechanism of Ru(bpy)<sub>3</sub><sup>2+</sup> ECL enhances the signal intensity by producing more than one photon per label. Thus, Ru(bpy)<sub>3</sub><sup>2+</sup> is often used to label other molecules and enable their detection via ECL. Ru(bpy)<sub>3</sub><sup>2+</sup> derivatives are reported to be good labels for both immunoassays<sup>103-106</sup> and DNA-probe assays.<sup>107-110</sup>

With suitable groups attached to bipyridine moieties (Fig. 3), Ru(bpy)<sub>3</sub><sup>2+</sup> can be linked to biologically interesting molecules such as antibodies, haptens, and nucleic acids, where it serves as a label for analysis. The first immunoassay based on the use of tris(2,2'-bipyridyl) ruthenium NHS ester, [4-(*N*-succinimidylpropyl)-4'-methyl-2,2'-bipyridine]bis(2,2'-bipyridine)-ruthenium(II) dihexafluorophosphate<sup>111</sup>, as label was reported in 1991. Thereafter, similar techniques were adopted for the

quantification of PCR-amplified products from viruses, cloned genes and oncogenes;<sup>112</sup> specific amplified DNA sequences based on PCR products;<sup>113</sup> HIV-1 RNA;<sup>114</sup> biotoxoids, viruses and bacterial spores;<sup>115,116</sup> HIV-1 proviral DNA sequences.<sup>117</sup>

In DNA assays, labeling of DNA strands with  $\text{Ru}(\text{bpy})_3^{2+}$  derivatives allows them to be detected with high sensitivity, with detection limits as low as 20 DNA copies per ml in plasma or serum.<sup>118</sup> Even 10 DNA copies were detected for Epstein–Barr virus DNA<sup>119</sup>. The techniques of ECL immunoassay and DNA-probe assays carried out on magnetic beads are commercially available in automated analyzers, e.g. Origen<sup>®</sup> from Igen<sup>120-122</sup> or Elecsys<sup>®</sup> from Boehringer Mannheim<sup>®123-125</sup>.

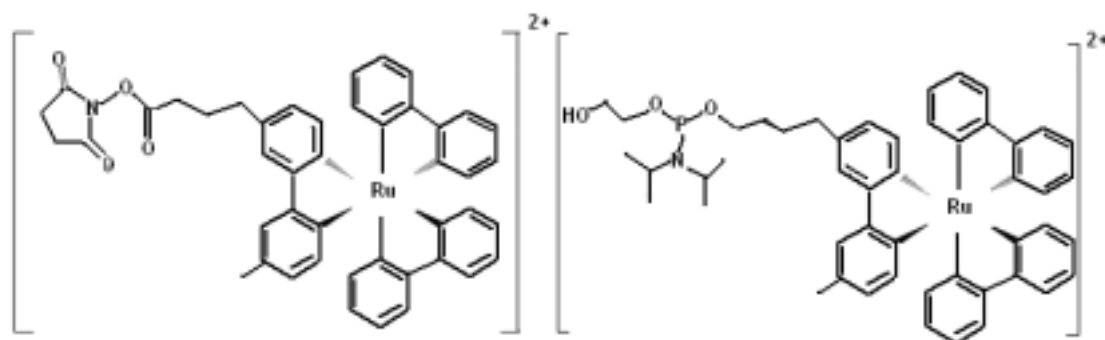


**Fig. 3**  $\text{Ru}(\text{bpy})_3^{2+}$ -NHS ester for ECL labeling of biological molecules (left) and  $\text{Ru}(\text{bpy})_3^{2+}$ -phosphoramidite linker for ECL labeling of DNA and RNA (right).

Even though these labels are already well established for ECL immunoassays and DNA-probe assays, new derivatives are being synthesized and investigated. A number of papers have been published on both mono- and multi-metallic ruthenium systems. The ECL of monometallic ruthenium complexes has also been exploited in systems containing a crown ether moiety covalently bonded to a bipyridyl ligand. As examples,  $\text{Ru}(\text{bpy})_2(\text{CE-bpy})^{2+}$  [CE-bpy is a bipyridine ligand in which a crown ether (15-crown-5) is bound to the bpy ligand in the 3- and 3'-positions]<sup>126</sup> and  $(\text{bpy})_2\text{Ru}(\text{AZA-bpy})^{2+}$  [AZA-bpy = 4-(*N*-aza-18-crown-6-methyl-2,2'-bipyridine)]<sup>127, 128</sup> have been reported. As well, a series of ruthenium bipyridine complexes have been investigated,<sup>129,130</sup> including  $(\text{Ru}(\text{bpy})_2(\text{bpym})^{2+}$ ,  $(\text{Ru}(\text{bpy})_2(\text{biim})^{2+}$ ,  $\text{Ru}(\text{phen})_3^{2+}$ ,  $\text{Ru}(\text{bpy})_2(\text{dmbp})^{2+}$ ,  $\text{Ru}(\text{dmphen})_3^{2+}$ , and  $\text{Ru}(\text{dmbp})_3^{2+}$ . In addition, the efficiency of these complexes as probes with CL or ECL detection has been discussed<sup>129,130</sup>.

The ECL of the bimetallic ruthenium system  $[\text{Ru}(\text{bpy})_2]_2(\text{bphb})^{4+}$  has been studied in an attempt to obtain more intense emission than that of  $\text{Ru}(\text{bpy})_3^{2+}$ .<sup>131</sup> The bphb (=1,4-bis(4'-methyl-2,2'-bipyridin-4-yl)benzene) is capable of binding two independent metal centers through a "bridging ligand" framework. This new kind of complex was proposed as a useful label for bioanalytical applications. ECL experiments have also been performed on dendritic complexes containing two, four, and eight ruthenium units in both homogeneous and heterogeneous assay formats.<sup>132</sup> The ECL in these systems increases linearly with the number of active ruthenium centers.

In addition to ruthenium chelates, a number of other transition metal chelates are potential labels for bioaffinity assays. Osmium polypyridine complexes have better photo stability and lower oxidation potentials than their ruthenium analogues and could be useful in the design of DNA-labeling agents.<sup>133-135</sup> Phenanthroline-based labels have been synthesized,<sup>136</sup> as well chromium complex  $\text{Cr}(\text{bpy})_3^{3+}$ <sup>137</sup> and iridium complexes<sup>138</sup>. However no immunoassay utilizing these labels has yet been described.

### 3.3.3 Lanthanide chelates as labels

Lanthanide ions characteristically have narrow spectral line widths, long luminescence life-time, large Stokes shift, and strong binding force with biological molecules.<sup>139,140</sup> Some lanthanide ions, especially  $\text{Eu}^{3+}$  and  $\text{Tb}^{3+}$ , when bound to a chelator, emit strong photoluminescence. Since each luminescent lanthanide(III) ion has a characteristic emission spectrum, labeling can be done with several lanthanide ions at the same time. The choice of the chelator is key in the preparation of label. Usually, the chelating agent needs to contain an aromatic group for excitation energy absorption. The energy is transferred intramolecularly to the lanthanide ion, enhancing its luminescence. The long lifetime of lanthanide chelates luminescence (ca. 100-2000  $\mu\text{s}$ ) makes them good labels in time-resolved photoluminoimmunoassays<sup>141</sup> and electrochemiluminoimmunoassays<sup>54</sup>.

Like their use as photoluminescent labels, lanthanide ions can also be used as chemiluminescent labels. They react with many biologically active compounds in

replacing Ca, Zn, Mg and Fe cations to provide information on these materials and the biochemical processes occurring therein.<sup>142,143</sup> In addition, ECL of a series of lanthanide chelates, cryptates, and mixed-ligand chelates has been observed.<sup>45,52,144-146</sup> In both CL and ECL, the luminescence occurs via a “ligand-sensitized” route, in which the ligand (coordinated to lanthanide ion) is excited by redox reaction in the presence of a appropriate precursor<sup>45,147,148</sup> or thermal decomposition of peroxide ligand,<sup>145,149</sup> followed by an intermolecular transfer of this excitation energy to f-orbitals of lanthanide metal centers.

Some lanthanide(III) chelates can be detected by cathodic pulse polarization of thin insulating film-coated electrodes at the pM level with the linear calibration curve spanning five to six orders of magnitude of concentration.<sup>45,54,150</sup> The luminescence lifetime of Tb(III) with a multidentate ligand is of the order of 1.7-2.4 ms, thus allowing the efficient use of time-resolved measuring techniques.<sup>45,54</sup> Moreover, the homogeneous assay is applicable because the excitation of the label molecules only occurs at a certain distance from the surface of the insulating film, whereas more distant label molecules are not excited. An ECLIA of human thyroid-stimulating hormone using Tb(III) chelates of 2,6-bis[N,N-bis (carboxymethyl) aminomethyl] –4-(phenylethyl)phenol (an isothiocyanate derivative) as ECL labels and based on hot electron electrochemistry has been reported.<sup>151</sup> In homogeneous immunoassay with 15 min incubation time, a linear calibration range of 0.25 – 324  $\mu$ U/ ml was obtained with time-resolved ECL detection; results were best with labeled antibodies bearing four or five of these Tb(III) chelates per antibody.

Actual immunoassays utilizing hot electron electrochemistry in the detection step of the bioaffinity assay have been demonstrated only a few times,<sup>51, 54, 151, 152</sup> and no commercial reagent kits or instruments are yet available. Some suitable electrochemiluminescent Tb(III) chelates for labeling are commercially available from Perkin-Elmer Life Sciences as isothiocyanate, iodoacetamido, and amino derivatives.

## 4. Aims of the research

CL and ECL labels offer a versatile, ultrasensitive tool for a wide range of applications in diverse fields. They are easily combined with flow-injection analysis or chemical separation techniques such as liquid chromatography or capillary electrophores. In some applications, ECL possesses advantages over conventional CL because of *in situ* generation of reactants, achieved through suitable programming of the potential of the working electrode. One of the most important areas of application for CL and ECL labels is in bioaffinity assays.

In this work, new alternative label substances for CL and cathodic ECL purposes were identified and tested. These included some coumarins, rhodamine B, lucigenin, metal chelates such as carboxylic acid derivative of  $\text{Ru}(\text{bpy})_3^{2+}$ , and an aromatic Eu(III) chelate. In addition to the investigation of the potential use of these labels in bioaffinity assays on the basis of detection sensitivity, studies were made of their CL and ECL mechanisms. Finally, some practical applications of ECLIA based on electrochemiluminescent labels and hot electron-excited ECL at insulating film-covered electrodes were explored.

## 5. Experimental

### 5.1 Reagents

Tris(2,2'-bipyridine) ruthenium(II) chloride hexahydrate ( $\text{Ru}(\text{bpy})_3^{2+}$ ),  $\text{K}_2\text{S}_2\text{O}_8$ ,  $\text{Na}_2\text{B}_4\text{O}_7 \cdot 10\text{H}_2\text{O}$ , HF, HCl,  $\text{H}_2\text{O}_2$ ,  $\text{NaNO}_3$ ,  $\text{NaNO}_2$ ,  $\text{HCOONa}$ ,  $\text{NaBr}$ ,  $\text{NaCl}$ ,  $\text{NaI}$ ,  $\text{NaN}_3$ ,  $\text{HCOONa}$ ,  $\text{NaOH}$ ,  $\text{H}_2\text{SO}_4$ ,  $\text{Na}_2\text{SO}_4$ ,  $\text{HCl}$ ,  $\text{NaCl}$  and  $\text{NaSCN}$  were pro analysi or suprapur products of Merck. Ethanol was a pro analysi grade product from Primalco.  $\text{H}_2\text{O}_2$ , hexammine cobalt(III) chloride, and  $\text{K}_4\text{P}_2\text{O}_8$  were purchased from J.T. Baker, Ventron and Polysciences Inc, respectively.  $\text{EuCl}_3$ , Tween 20, Silver hexafluorophosphate ( $\text{AgPF}_6$ ), ammonium hexafluorophosphate ( $\text{NH}_4\text{PF}_6$ ), and luminol (5-amino-2,3-dihydrophatelazine-1,4-dione) were products of Aldrich. All coumarins—7-hydroxy-4-methylcoumarin, 6,7-dihydroxy-4-methylcoumarin and 7-



amino-4-methylcoumarin— were purchased from Aldrich. Silica gel (200-300 mesh) used for column chromatography was bought from Qingdao Ocean Chemical. Rhodamine B and lucigenin were pro analysi products of Sigma and no purification was made before use. Benzene, toluene, phenol were pro analysi products of Labscan and p-cresol and aniline were pro analysi products of Fluka. The label chelate Tb(III) chelated by  $N^1$ -(4-isothiocyanatobenzyl)diethylenetriamine-  $N^1, N^2, N^3, N^3$ -tetraacetate (commercially available from the present PerkinElmer Life Sciences) was obtained from Wallac Oy (Turku, Finland) and 2,6-bis[ $N,N$ -bis(carboxymethyl)aminomethyl]-4-methylphenol was synthesized as described previously.<sup>51</sup> The safety precautions required in handling of the reagents have been presented previously.<sup>150</sup> All reagents were used as received and quartz-distilled water was used in all solutions.

Planar Al electrodes were cut from nominally 99.9% and 99.5% pure, ca. 0.3 mm thick aluminum bands (Merk Art. 1057, batch 720 K22720857). The bands were covered with 2-3 nm thick natural oxide film<sup>153</sup> and cut into 9.0 mm  $\times$  9.0 mm or 15 mm  $\times$  15 mm pieces to fit into the sample cell. Magnesium electrodes were cut from nominally 99.5 % pure Mg bands (Merck). The oxide film-coated aluminum electrodes of different film thickness were anodically oxidized in neutral ammonium borate.<sup>154</sup>

Antimony-doped n-Si (111) with resistivity of 0.008-0.015  $\Omega$ cm and boron-doped p-Si (100) with resistivity of 0.01-0.02  $\Omega$ cm were purchased from Okmetic Oy (Finland). Insulating oxide films were fabricated on the silicon wafers by thermal oxidation in clean room. First, the wafers were cleaned by a standard RCA-cleaning process with HF dip last. They were then oxidized immediately by thermal oxidation at 850°C in 10% oxygen and 90% nitrogen atmosphere. Loading of the wafers into the furnace was at 700°C in 5% oxygen and 95% nitrogen atmosphere, and temperature was ramped up 10°C/min in the same atmosphere. After oxidation, the temperature was ramped down 4°C/min in 100% nitrogen to 700 °C for unloading. The oxidation times varied for the various thicknesses of the oxide film. The thickness of the oxide film was determined with an ellipsometer using the wavelength 632.8 nm (He-Ne laser).

## 5.2 Instrumentation

The apparatus for ECL measurements included a laboratory-made coulometric pulse generator, a Pine Instruments RD4 potentiostat with a laboratory-made pulse generator, a two-electrode cell, a photon counter unit and a photomultiplier tube (PMT).<sup>45,51,150</sup> The ECL was excited by either the coulometric pulse generator or the potentiostatic pulse generator. The coulometric pulse generator is capable of supplying from 10 to 300  $\mu\text{C}$  pulse with a maximum 10A current and 75 V voltage.<sup>151</sup> Basically, this device allows a capacitor (charged with a preset voltage) to feed current through the electrochemical cell until a preset charge has passed, after which the current feed is cut off. At the moment of cut-off, the pulse generator gives a triggering pulse for a photon counting device, which makes accurate time-resolved measurement possible. The potentiostat pulse generator could deliver both anodic and cathodic pulses, but the coulometric pulse generator with a two-electrode cell can deliver only cathodic or anodic pulses, depending on the chosen polarity of the electrodes.

The ECL intensity was measured through a suitable interference filter, with a photon counting unit,<sup>150</sup> consisting of a photomultiplier, a Stanford Research Systems photon counter, and a Nucleus MCS-II scale card attached to a PC computer. The MCS-II card allows time-resolved measurements and simultaneous measurement of light emitted during the whole period of a pulse. Thus the lifetime of electrogenerated luminescence could also be measured in this way. In principle, only cathodic light emission intensity responds to the concentration of the presence of luminophores.

The ECL spectra were measured in a 1-cm polystyrene cuvette, in which an Al strip working electrode and a Pt wire counter electrode were set between two PTFE support pieces. Measurements were made with an ordinary Perkin-Elmer LS-5 luminometer or LS-50B luminescence spectrometer (with the excitation shutter closed using the widest possible gate time), or with an Ocean Optics USBFL-2000 spectrometer. Photoluminescence measurements were made in quartz cuvettes using a Perkin-Elmer LS-5 luminometer or LS50B luminescence spectrometers. For immunoassays, an Arcus 1230 fluorometer (Wallac Oy, Turku, Finland) was modified to a time-resolved electrochemiluminometer by removing the excitation lamp and

optics and changing the PMT to measure light from one side of a 12-well single strip (from a detachable 96-well microtiter plate) attached in an original Arcus strip rack.

The two-electrode cell was composed of either an Al-cup or Al, Mg, Si-strip working electrode and a Pt-wire counter electrode. The choice of the anode material is not critical as long as the migration of the anodic dissolution products is insignificant in the time scale of the experiment, and in principle any area combination of working and counter electrode can be used for generation of ECL with appropriate voltage pulse amplitude and electrolyte solution. The measurement electrolyte was usually 0.05 M  $\text{Na}_2\text{B}_4\text{O}_7$  buffer, with sodium sulfate occasionally added to reduce the solution IR drop. In some cases, the solution was adjusted to the desired pH with sulfuric acid or sodium hydroxide.

## 6. Results and discussion

### 6.1 Hot electron emission and common primary species of luminophore ECL at conductor/insulator/electrolyte tunnel junction electrodes

Transfer of hot electrons from metal/insulator/metal (M/I/M) junctions into aqueous electrolyte solutions has been reported by Diesing et al.<sup>155</sup> Later, Kulmala and Alakleme<sup>156</sup> proposed that hot electrons can be injected into the conduction band of water from these kind of devices. Analogously, hot electrons can be injected into aqueous solutions through insulating films<sup>157-159</sup> when the negative bias applied to a conductor/insulator/electrolyte (C/I/E) tunnel emitter is of sufficient magnitude to excite the electrons at or above the conduction band of insulating film.<sup>45,48,49,160,161</sup>

At certain threshold voltage, depending on the oxide film thickness, tunnel emission of electrons starts to occur from the base conductor of C/I/E junctions. The required electric field for the tunnel emission must not induce electric breakdown of the film. To  $\text{Al}_2\text{O}_3$ , for instance, critical field strength is from about  $3 \times 10^6$  to  $1 \times 10^7$  V/cm<sup>162</sup>. In our studies, aluminum, magnesium, and silicon electrodes covered with  $\text{Al}_2\text{O}_3$ , MgO and  $\text{SiO}_2$  film were used as C/I/E tunnel-emitters.  $\text{Al}_2\text{O}_3$ , MgO and  $\text{SiO}_2$  films can

withstand high enough electric field to be used as cold cathodes and to emit hot electrons into aqueous solutions.

A general schematic presentation of hot emission in a C/I/E junction emitter is shown in Fig. 4. In the case of very thin oxide films (thickness < ca. 5 nm), hot electrons are transferred across the insulating film by direct tunnel emission, i.e. they tunnel ballistically from an already high energy level through the barrier to an equal energy level in solution, and no considerable loss of electron energy occurs. Thus, the injected 'dry quasifree' hot electrons, with energy above the conduction band edge of water, can become thermalized and hydrated.<sup>48,49,53</sup> In the case of thicker insulating film, Fowler-Nordheim (F-N) tunneling is the predominant tunneling mechanism.<sup>54,159,160</sup> Under this regime, the electrons are first tunneled into the conduction band of the oxide and then heterogeneously transferred to the solution species from the bottom of the conduction band or from somewhat above it at the oxide/solution interface. During transport in the conduction band of the oxide under high electric field, the electrons partly gain energy from the field and partly lose it by inelastic scattering. Finally, not all of the electrons are transferred from the bottom of the conduction band to solution but also from somewhat above the conduction band edge of the oxide.

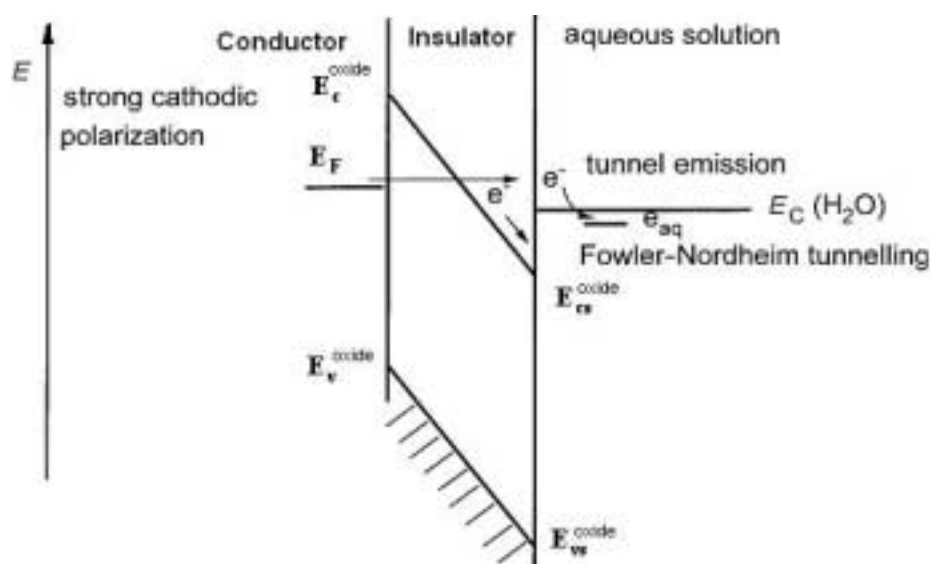
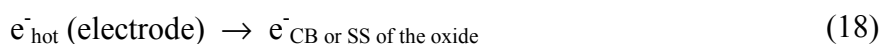


Fig. 4 Schematic presentation of hot electron emission.

Originally, it was assumed that only metals and heavily doped n-type semiconductors could work as conductors in C/I/E tunnel emission electrodes, but very recently we showed that p-type semiconductors are applicable as well (paper V). Thus, reductions at the electrode can be caused by the direct action of 1) dry hot electrons ( $e^-_{\text{quasifree}}$ ), 2) hydrated electrons ( $e^-_{\text{aq}}$ ), 3) electrons heterogeneously transferred from the bottom of the insulator conduction band (CB) or somewhere above it, 4) less energetic electrons via the surface states.<sup>157c</sup> However, strong ECL of luminophores at oxide film-covered electrodes has been observed only in the direct tunnel emission regime,<sup>48</sup> which implies that  $e^-_{\text{quasifree}}$  or  $e^-_{\text{aq}}$  play an important role in ECL pathways as strongly reducing agents ( $E(e^-_{\text{aq}})^\circ = -2.9 \text{ V vs. SHE}$ ).<sup>163</sup>



It is worth noting that the highly cathodic ECL onset potentials measured for different luminophores are about the same even though the redox and luminescence properties of the luminophores are very different.<sup>59,164</sup> Moreover, the ECL onset potential of the oxide-covered aluminum metal is very close to the energy level of the conduction band edge of water (i.e. - 1.3 eV<sup>165</sup> on the physical scale). These findings suggest that the mechanism for ECL of these luminophores involves the same primary process; i.e., the generation of  $e^-_{\text{aq}}$  by hot electron injection into the conduction band of water appears to be common to all these ECL processes.

In another approach, strongly oxidizing species can be directly generated at cathode upon addition of coreactants such as peroxodisulfate ions or hydrogen peroxide. In air-saturated solutions, due to oxygen evolution at the counter electrode, oxyradicals and hydrogen peroxide will be formed if hydrated electrons are produced at the working electrode. The  $\text{O}_2$  concentration of air-saturated electrolyte solutions is close to  $2 \times 10^{-4} \text{ M}$ :<sup>166</sup>





where  $k_{21} = 1.9 \times 10^{10} \text{ l mol}^{-1} \text{ s}^{-1}$ ,  $k_{22} = 1.3 \times 10^{10} \text{ l ml}^{-1} \text{ s}^{-1}$ .<sup>163</sup> In addition, it has been suggested that  $\text{F}^+$ -centers (i.e. one electron trapped in an anion vacancy in aluminum oxide) or corresponding  $\text{E}_1'$ -centers (i.e. one electron trapped in an anion vacancy in silicon dioxide) can act as strong oxidizing species capable of oxidizing hydroxide ions and hydroxyl groups of the oxide surface to hydroxyl radical.<sup>49,54</sup>



The simultaneous presence of reducing agents (i.e. hydrated electrons) and oxidizing agents (e.g. sulfate radicals, hydroxyl radicals) thus creates extremely harsh condition in aqueous solution, condition that allow the generation of chemiluminescence from a variety of luminophores during cathodic pulse polarization of oxide film-covered electrodes. The mechanisms for generation of ECL from different luminophores at oxide-covered electrodes will be discussed in detail below in the context of individual applications.

The oxide film of a oxide film-coated Si electrode can withstand more cathodic potential than the conduction edge of water before the onset of the electric field of tunnel emission in the oxide film.<sup>160</sup> This implies that electrons with higher energy can be injected into aqueous electrolytes from oxide film-coated Si electrode than from oxide film-covered metal electrode. In addition,  $\text{Al}_2\text{O}_3$  film may dissolve due to the hydrogen evolution-induced alkalization of the aluminum electrode surface during prolonged pulse polarization. All these considerations make thin oxide film-coated silicon electrodes a promising material as the working electrode for ECL applications. In principle, various types of luminescent compounds can be thought to be electrically excited on the basis discussed above, such as some organic luminophores and metal chelates which were studied in this work.

## 6.2 Organic luminophores

A large number of ECL-active luminophores exist among organic compounds. In conventional ECL in nonaqueous solutions, light emits from organic luminophores via ion annihilations reaction involving anodically and cathodically generated radicals<sup>167</sup>. With high amplitude cathodic pulse polarization, many aromatic organic compounds (fluorescein, eosin, metalloporphyrins) can be excited to emit light at insulating film-coated electrode in aqueous solution.<sup>60,62,67</sup> The general mechanism involved in the Ox-Red or Red-Ox excitation pathway for aromatic luminophores (Ar) is a bit different from that ECL induced at conventional electrodes.<sup>60,62</sup>



Here  $\text{Ox}^{\bullet}$  is a one-electron oxidant, which could be an oxidizing radical generated from coreactants, dissolved oxygen, or  $\text{F}^+$ -centers existing in thin aluminum oxide film. The hydrated electrons generated by cathodic pulse polarization of an insulating film-coated electrode are strong reductants, capable of reacting even with benzene.<sup>163</sup> In fact, aromatic luminophores could undergo either one-electron reduction initiated oxidative excitation (25a-26b) or one-electron oxidation initiated reductive excitation (26a-26b), and finally relax to the ground state by emitting light (27). For efficient ECL generation, not only should the free energy change in step (25b) or (26b) step be large enough to raise Ar to its excited state, but the radical formed in the first step [(25a) or (26a)] should be stable.

### 6.2.1 Long-lived ECL of luminol

Great attention has been paid to the ECL of luminol, now a widely used label in bioaffinity assay.<sup>168-170</sup> Luminol, isoluminol, and their derivatives are electrochemiluminescent at oxide-covered aluminum electrodes, and the mechanism of cathodic ECL of luminol at oxide film coated aluminum electrode has been studied.<sup>171</sup> Luminol has been suggested to produce cathodic ECL by mechanisms in which luminol is disintegrated and the final emitter is considered to be 3-aminophthalate.<sup>171</sup>

Our recent study (paper I) focusing on the ECL of luminol offered an interesting finding: the ECL of luminol is exceptionally long-lived, not the short-lived emission assumed earlier. This makes time-resolved ECL (TR-ECL) detection available for luminol used as ECL label in bioaffinity assays. TR-ECL detection offers excellent sensitivity in determinations by effectively separating the background solid-state electroluminescence from the long-lived ECL of luminophores. This is done by measurement of ECL after a certain time-lag from the end of the excitation pulse.

The ECL lifetime of luminol is of the order of several milliseconds (Fig. 5). Many organic luminophores have very short ECL lifetimes; platinum coproporphyrin,<sup>62</sup> for example, has a lifetime 100 times shorter than luminol in the present study. The difference in lifetimes allows the simultaneous excitation of luminol with other molecules or chelates having short luminescence lifetime. Similar to simultaneous excitation of  $\text{Ru}(\text{bpy})_3^{2+}$  with a Tb(III) chelate,<sup>172</sup> TR-ECL detection of luminescent labels is possible for luminol and  $\text{Ru}(\text{bpy})_3^{2+}$  system (Fig. 6). In addition, the inset of Fig. 6 shows that luminescent labels can also be individually detected by wavelength discrimination (the maximum emission wavelength of luminol is 425 nm and that of  $\text{Ru}(\text{bpy})_3^{2+}$  610nm.)



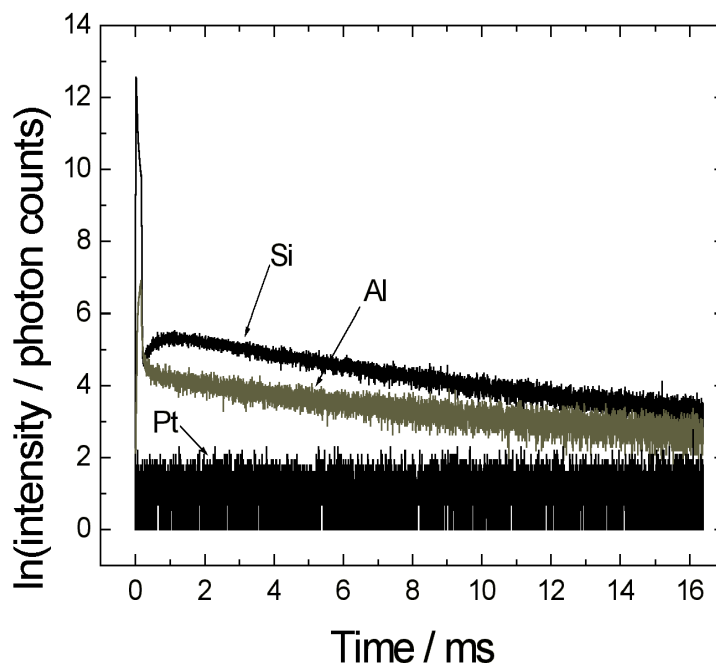


**Fig. 5** ECL intensity of 0.1  $\mu\text{M}$  luminol on three electrodes: Pt, Al with natural oxide film, and n-Si with 3.6 nm oxide film. The luminol solutions were made in 0.05M  $\text{Na}_2\text{B}_4\text{O}_7$  at pH 9.2. Analysis conditions: pulse charge 39  $\mu\text{C}$ , pulse voltage -50V and pulse frequency 20 Hz. The intensity was measured over 5000 excitation pulses.

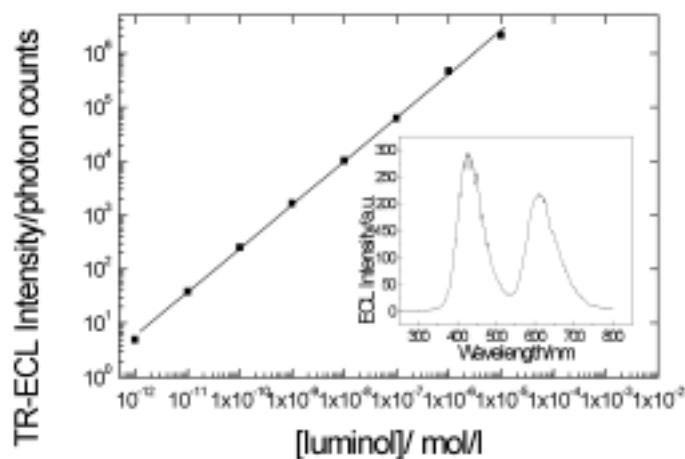


**Fig. 6** Time-resolved ECL intensity of luminol as a function of concentration; inset: ECL spectrum of a mixture of luminol and  $\text{Ru}(\text{bpy})_3^{2+}$ . Conditions: 420 nm interference filter with a band width of 40 nm. Pulse charge 120 $\mu\text{C}$ , pulse voltage -40V and pulse frequency 20 Hz, 0.05M  $\text{Na}_2\text{B}_4\text{O}_7$ , pH 9.2, 0.01M  $\text{NaN}_3$ , the intensity was integrated over 1000 excitation pulses. Inset conditions: otherwise as above, but  $1.0 \times 10^{-5}$  M luminol,  $2 \times 10^{-7}$  M  $\text{Ru}(\text{bpy})_3^{2+}$ ,  $5.0 \times 10^{-4}$  M  $\text{K}_2\text{S}_2\text{O}_8$ , and pulse frequency 100 Hz, measured with Perkin-Elmer LS 5 spectrometer.

The material of the working electrode affects the ECL decay of luminol in air-saturated solution (Fig. 5). On oxide-coated n-Si, the ECL decay was close to a single exponential process, with luminescence lifetime close to 7 ms. On oxide-covered aluminum, however, the corresponding decay curve could be fitted with two separate

luminescent processes, in which the shorter luminescence lifetime was similar to that produced on n-Si and the longer was of the order of 10 ms (Paper I). The dominating luminescence lifetime of luminol in borate buffer appears to be between 6 and 7 ms. Moreover, both the ECL lifetime and ECL intensity of luminol were affected in the presence of radical scavengers, such as ethanol, azide and peroxodisulfate. For example, after addition of 1.5 M ethanol to 0.05 M Na<sub>2</sub>B<sub>4</sub>O<sub>7</sub> solution (pH 9.2) (Paper I), the ECL lifetime increased from about 6 ms up to 35 ms, while the TR-ECL intensity of luminol decreased to 3 % of the original intensity. The effect of peroxodisulfate is different from that of ethanol. Evidently, the scavengers affect primary radicals in the ECL excitation pathway in different way.

### 6.2.2 Cathodic ECL of coumarin derivatives

Coumarin was first reported and isolated in the 1820s, recognized as the hay-like sweet aroma of the tonka bean.<sup>173,174</sup> Coumarin derivatives find use in fields as diverse as biology, medicine, polymer science, and industry in general.<sup>175</sup> They have also been used in analysis as labels for antigens in homogeneous and heterogeneous fluoroimmunoassays.<sup>176</sup> Coumarin derivatives have been applied as fluorogenic substrates for enzyme determinations in fluorometric enzyme immunoassays and as fluorogenic substrates coupled to antigens in substrate-labeled fluorescence immunoassays.<sup>177-180</sup>

Interestingly, ECL of coumarin derivatives can also be generated at pulse-polarized C/I/E junction cathodes. ECL of three differently substituted coumarins — 7-hydroxy-4-methylcoumarin (**HMC**), 6,7-dihydroxy-4-methylcoumarin (**DHMC**), and 7-amino-4-methylcoumarin (**AMC**) — is produced at thin insulating film-coated aluminum electrodes. The structures of the three studied coumarins are presented in Fig. 7. Amongst these compounds **HMC** and **DHMC** are promising labels for immunoassay applications based on ECL detection methods.

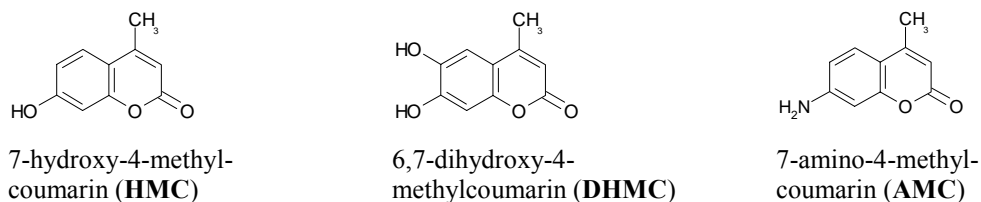


Fig. 7 Structures of coumarins studied.

Uncorrected ECL spectra of **HMC**, **DHMC**, **AMC** (Fig. 8) showed that all these coumarins emit ECL at the same 450 nm wavelength, which is also the same as the fluorescence emission wavelength of **DHMC**. Certain radical scavengers have a strong quenching effect on the ECL. Investigations of the effect of hydrated electron scavengers and sulfate radical scavengers on the ECL of coumarins again supported the generation of hydrated electrons at thin oxide film-coated aluminum electrodes as the first step in ECL excitation pathway (paper II).

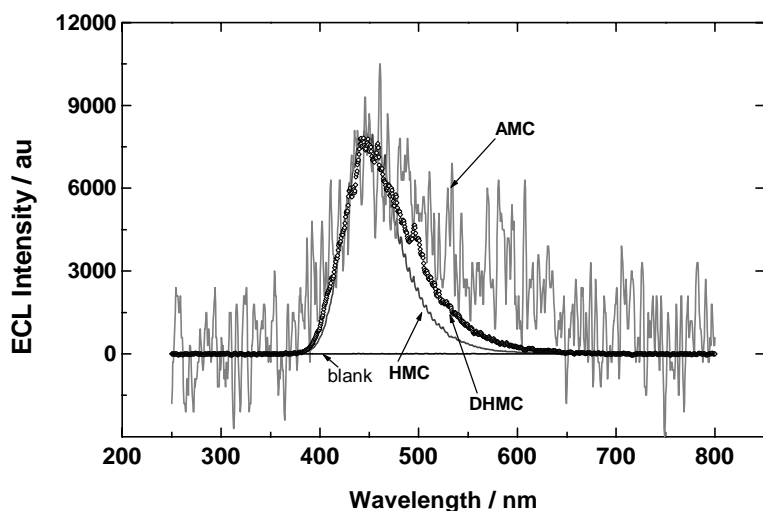
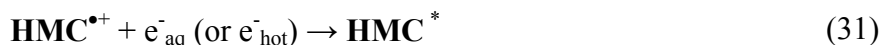


Fig. 8 Uncorrected ECL spectra of coumarins at the oxide-covered aluminum electrode. Spectra are normalized and thus the signal measured from  $1.0 \times 10^{-5}$  M solutions of **HMC**, **DHMC**, **AMC** and background (blank, measuring buffer) multiplied by factor 1.0, 8.0, 600 and 1.0, respectively. Conditions: 0.2 M boric acid-borate buffer pH 9.2,  $1 \times 10^{-3}$  M  $S_2O_8^{2-}$ , Perkin-Elmer LS-5 spectrofluorometer excitation slit closed and emission slit 20 nm, scan speed 240 nm/min, coulostatic pulse generator excitation pulse charge 120  $\mu$ C, frequency 80 Hz and voltage  $-50$  V.

The probable ECL excitation routes for coumarins are the luminophore-reduction-initiated oxidative-excitation pathway (red-ox pathway, reactions 28-29) and the luminophore-oxidation-initiated reductive-excitation pathway (ox-red pathway, reactions 30-31), where **HMC** is used as model coumarin and  $Ox^\cdot$  is a strong oxidant, e.g. sulfate or hydroxyl radical.





It is impossible to say which pathway is predominant before the rate constants of reactions of coumarins are known. In addition, it is necessary to take into account the stability of the radical ions of coumarin derivatives together with thermodynamic and kinetic issues. It seems, nevertheless, that the ox-red pathway (reactions 30-32) could be the predominant one, because oxidants like F-centers, and hydroxyl and sulfate radicals formed on cathodically pulse polarized thin insulating oxide film-covered aluminum electrodes are strong enough to oxidize these coumarins to their cation radicals, which further can react with hot or hydrated electrons to form the coumarin molecule in its excited state.

Comparison of ECL spectra (Fig. 8) of the three coumarin derivatives with their corresponding fluorescence emission spectra (Fig. 9) suggests that the final ECL emitting molecule in all ECL experiments is the same in all cases, i.e. excited **DHMC** molecule. In explanation of that, **HMC** and **AMC** molecules might be converted to **DHMC** during electrochemical excitation; this requires further study, however. Another explanation could be the considerable uncertainty in ECL emission maxima when Perkin-Elmer LS5 is used for ECL spectra measurements (it is only designed for PL measurements) because ECL signal from DHMC, and especially that from AMC is weak. Thus, it is probable that, for each coumarin, the ECL and fluorescence emission spectra are essentially the same (Fig. 8 and 9) and in each case the emissive species is the original coumarin compound in its singlet excitation state.

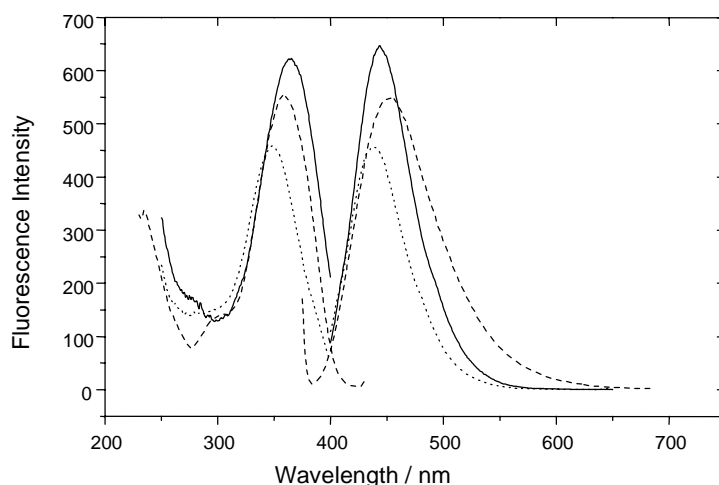


**Fig. 9** Fluorescence excitation and emission spectra of **HMC** (solid line;  $\lambda_{\text{ex}}=365$ ,  $\lambda_{\text{em}}=442$ ), **DHMC** (dashed line;  $\lambda_{\text{ex}}=356$ ,  $\lambda_{\text{em}}=451$ ) and **AMC** (dotted line;  $\lambda_{\text{ex}}=348$ ,  $\lambda_{\text{em}}=439$ ). Conditions: Spectrofluorometer Perkin-Elmer LS-5 excitation and emission slits 15 and 10 nm, respectively, scan speed 120 nm/min. Aqueous solutions of  $1.0 \times 10^{-7}$  M coumarins in 0.2 M boric acid-borate buffer pH 9.2.

While the long-lasting triplet-state emission is extremely weak and has no analytical applicability, the strong singlet-state ECL emission of coumarin derivatives provides calibration plots spanning four orders of magnitude of concentration. The low detection limit for **HMC** (strongest ECL signal), close to  $10^{-10}$  M (Fig. 10), makes the **HMC** especially promising. In summary, then, some coumarin derivatives manufactured for photoluminescence purposes can be regarded as potentially useful ECL labels in bioaffinity assays.

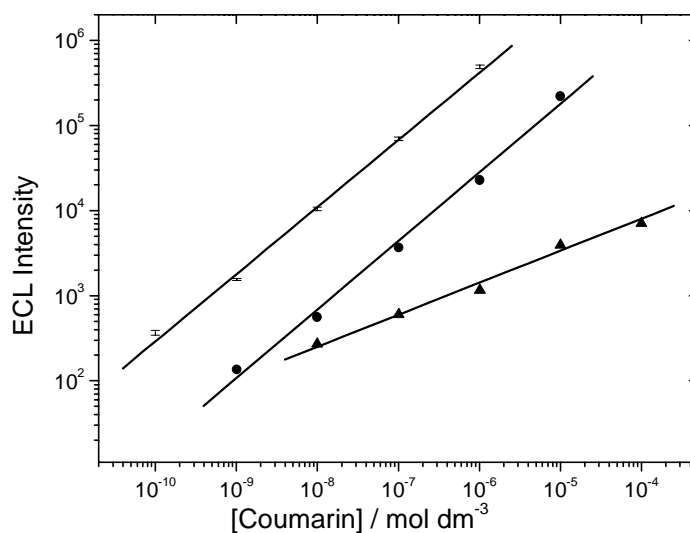


**Fig. 10** ECL calibration curves of **HMC** (■), **DHMC** (●), and **AMC** (▲) at the oxide-covered aluminum electrode. Conditions: 0.2 M boric acid-borate buffer pH 9.2,  $1 \times 10^{-3}$  M  $\text{S}_2\text{O}_8^{2-}$ . Potentiostatic pulse generator with 0.2 ms,  $-10$  V and 100 Hz cathodic excitation pulses. Interference filter 450 nm and presented ECL signals integrated as a sum of 1000 excitation pulses.

### 6.2.3 Hot electron-induced ECL of rhodamine B

Rhodamine compounds, due to their high PL efficiency, are extensively utilized as labels in bioaffinity assays based on photoluminescence. Amongst these compounds, rhodamine B (RhB) dye is excited in the visible part of the spectrum (ca. 560 nm), has a photoluminescence (PL) quantum yield approaching 1, and is fairly photostable (e.g., as compared with fluorescein).<sup>181</sup> In addition, RhB in aqueous solution has been observed to produce radiochemiluminescence (RCL) under steady X-ray irradiation<sup>182,183</sup> or pulse radiolysis with 2- $\mu$ s 4-MeV electron pulses<sup>184</sup>. One-electron reduced and oxidized radical forms of RhB ( $\text{RhB}_{\text{red}}^{\bullet}$  and  $\text{RhB}_{\text{ox}}^{\bullet}$ ) were found during and after the electron pulses, produced by the primary species of the radiolysis of water (i.e. hydrated electrons and hydroxyl radicals). The oxidation of  $\text{RhB}_{\text{red}}^{\bullet}$  by hydroxyl radical and the reduction of  $\text{RhB}_{\text{ox}}^{\bullet}$  by hydrated electron were assumed to be the sources of the excited  $\text{RhB}^*$ .<sup>184</sup>

Support or counter-evidence was sought for the generation of hydrated electrons and highly oxidizing species from suitable precursors in cathodic pulse polarization of thin insulating film-coated cathodes. Taking note of Pruetz's proposal,<sup>182,183</sup> the possibility of cathodic ECL of RhB at oxide-covered aluminum electrode was studied. If cathodic ECL exists, the scavenging of hydroxyl radicals and/or hydrated electrons should have a strong quenching effect on the ECL, and if hydrated electrons and hydroxyl radicals exist as redox mediators in the cell, the ECL should be observable also after the cathodic pulse.

Interestingly, we found the ECL spectrum of RhB produced at oxide-coated aluminum electrodes to be similar to its fluorescence spectrum with emission maximum at 575 nm (Fig. 11). It seems reasonable to conclude, therefore, that the emission occurs from the same excited species in the two cases. The ECL intensity of RhB was relatively constant in a wide pH range from 3 to 9, and the pH range of maximum ECL intensity of RhB coincides with the physiological pH range. Thus, the use of derivatives of RhB as ECL labels has potential in immunoassays.

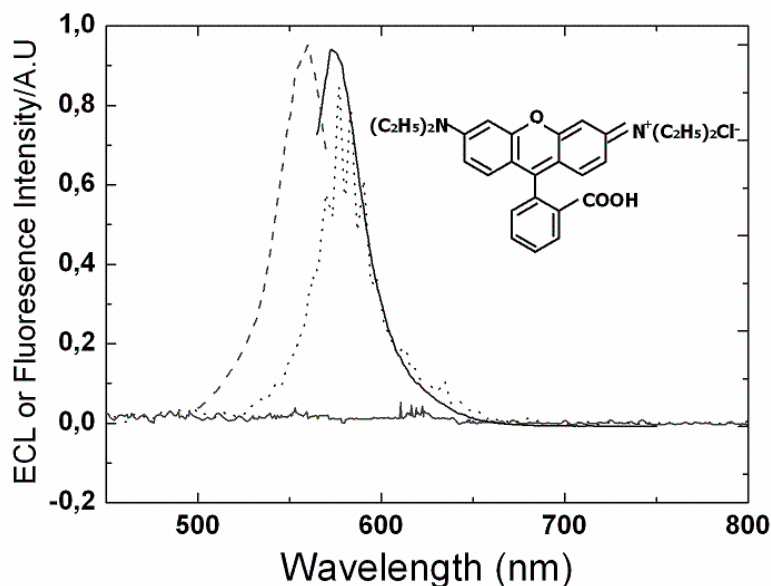


**Fig. 11** Uncorrected ECL(dot line) and fluorescence emission spectra(solid line) of rhodamine B. Conditions: scanning speed  $240 \text{ nm min}^{-1}$  with Perkin-Elmer LS-50B spectrometer, slit widths 10 nm, coulostatic pulse generator: pulse voltage  $-45\text{V}$ , 20Hz,  $120\mu\text{C}$ , aluminum strip cathode, platinum wire anode. Molecular structure of RhB is given in the inset.

The effects of oxide film thickness (Fig. 12) and free radical scavengers on ECL (Figs. 13 and 14) provide indirect support that hydrated electrons and hydroxyl radicals are the primary species exciting ECL from RhB in aqueous solution. The ECL is very strong only in cases of ultra-thin oxide films ( $< 4 \text{ nm}$  in Fig. 12), since in this case, the emission of hot electrons is in the regime of the direct field assisted tunneling. Therefore, electrons with energy above the conduction band edge of water can become hydrated and intense ECL is observed. In the case of oxide film thickness exceeding ca.  $4 \text{ nm}$ , the ECL decreases abruptly with the increase in oxide film thickness (Fig. 12), due to the Fowler-Nordheim (F-N) tunneling being the predominant tunneling mechanism<sup>54,159,160</sup>. Under this regime, less or none of the transferred electrons can become hydrated. Therefore, we suggest that hydrated electrons are important primary species in ECL excitation pathway of RhB. For free radical scavengers,  $\text{Co}(\text{NH}_3)_6^{3+}$ , for example, which is highly unreactive toward hydrogen atom ( $k(\text{H}^\bullet + \text{Co}(\text{NH}_3)_6^{3+}) < 9 \times 10^4 \text{ L mol}^{-1} \text{ s}^{-1}$ ),<sup>163</sup> is the fastest hydrated electron scavenger amongst all tested reagents and it very strongly quenches the present ECL (Fig. 13). Thus, hydrogen atom can be ruled out as being an important cathodically generated mediating species in the ECL mechanism of rhodamine B. The detailed explanation of the effect of scavengers on ECL of RhB was presented in paper III.

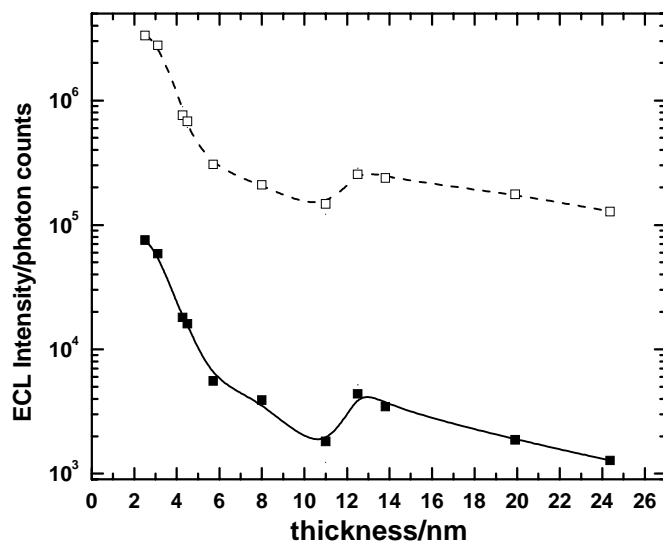


**Fig. 12** Effect of oxide film thickness on ECL of Rhodamine B. ( ) Cathodic ECL; (■) Time-resolved-ECL. Conditions:  $1.0 \times 10^{-6}$  M RhB in 0.05M  $\text{Na}_2\text{B}_4\text{O}_7$  buffer solutions. Aluminum electrodes with varied oxide thickness were used as disposable working electrodes. Pulse voltage  $-45$  V, pulse charge  $120 \mu\text{C}$ , pulse frequency 20 Hz. TR-ECL signals were measured by delay  $0 \mu\text{s}$ , gate time  $200 \mu\text{s}$ . ECL and TR-ECL intensities were integrated over 1000 excitation cycles. All signals were measured through a 600 nm interference filter with half-width of the transmission band ca. 40 nm.

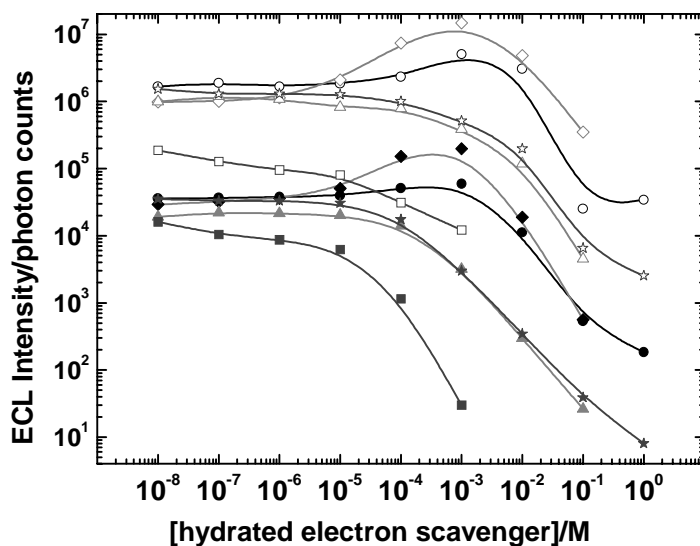


**Fig. 13** Effect of hydrated electron scavengers on the ECL of Rhodamine B. (◇) Effect of  $\text{K}_2\text{S}_2\text{O}_8$  on TR-ECL affected by (◆) Effect of  $\text{K}_2\text{S}_2\text{O}_8$  on cathodic ECL, (○) Effect of  $\text{H}_2\text{O}_2$  on TR-ECL, (●) Effect of  $\text{H}_2\text{O}_2$  on cathodic ECL, (◐) Effect of  $\text{Co}(\text{NH}_3)_6^{3+}$  on TR-ECL, (•) Effect of  $\text{Co}(\text{NH}_3)_6^{3+}$  on cathodic ECL, (Δ) Effect of  $\text{NaNO}_2$  on TR-ECL, (▲) Effect of  $\text{NaNO}_2$  on cathodic ECL, (☆) Effect of  $\text{NaNO}_3$  on TR-ECL, (★) Effect of  $\text{NaNO}_3$  on cathodic ECL. Conditions:  $1.0 \times 10^{-6}$  M RhB, 0.05 M  $\text{NaB}_4\text{O}_7$  at pH 9.2 buffer solution, otherwise the same as that in Fig. 12.



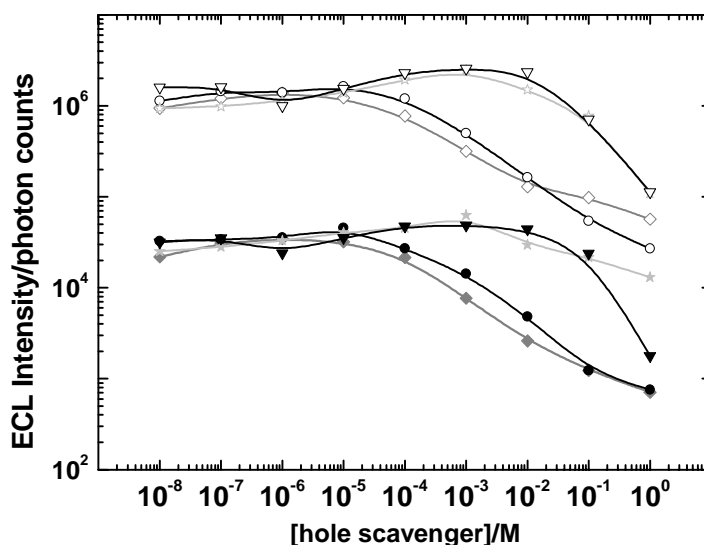


**Fig. 14** Effect of different hole scavengers on the ECL intensity of RhB ( $1 \times 10^{-6} \text{M}$ ). ( $\diamond$ ) TR-ECL, ethanol; ( $\blacklozenge$ ) Cathodic ECL, ethanol, ( $\circ$ ) TR-ECL, NaI; ( $\bullet$ ) Cathodic ECL, NaI; ( $\nabla$ ) TR-ECL,  $\text{NaN}_3$ ; ( $\blacktriangledown$ ) Cathodic ECL,  $\text{NaN}_3$ ; ( $\star$ ) TR-ECL, NaBr; ( $\blackstar$ ) Cathodic ECL, NaBr. Conditions: As in Fig. 12.

The formal reduction potential of RhB is reported to be ca.  $-0.52 \text{ V}$  vs. SHE in aqueous<sup>185</sup> and ca.  $-0.75 \text{ V}$  vs. SHE in alkaline aqueous solution<sup>186</sup>, and the oxidation potential in acidic conditions on  $\text{SnO}_2$  glass electrode is ca.  $1.24 \text{ V}$  vs. SHE.<sup>186</sup> However, since RhB is rapidly oxidized by azide radical having reduction potential  $1.3 \text{ V}$  vs. SHE<sup>187</sup>, the oxidation potential of solvated RhB must be somewhat lower, probably about  $1.0 \text{ V}$  vs. SHE. In principle, the ECL excitation route of RhB could be the reduction-initiated oxidative excitation (red-ox) pathway (reactions 33a-33b) or the oxidation-initiated reductive excitation (ox-red) pathway (reactions 34a-34b). The mechanisms are as follows:



where,  $\text{Ox}^{\bullet}$  is again a one-electron oxidant, normally a hydroxyl radical, or better an azide radical. The initial step in the red-ox pathway (33a) proceeds with rate constant  $k(\text{RhB} + e^-_{\text{aq}}) = 3.0 \times 10^{10} \text{ L mol}^{-1} \text{ s}^{-1}$ <sup>188</sup> in aqueous solution. The ox-red pathway, in turn,

can be initiated by a hydroxyl radical (34a) ( $k(\text{OH}^\bullet + \text{RhB}) = 9 \times 10^9 \text{ L mol}^{-1} \text{ s}^{-1}$ ),<sup>188</sup> or by secondary radicals produced from a coreactant such as azide ion [ $k(\text{N}_3^\bullet + \text{RhB}) = 5.0 \times 10^9 \text{ L mol}^{-1} \text{ s}^{-1}$ ].<sup>189</sup>

Taking into the consideration the enthalpies of the excitation steps of each pathway, we get

$$\Delta H^\circ = \Delta G^\circ + T\Delta S^\circ = nF(E^\circ(\text{R}_2^{+\bullet}/\text{R}_2) - E^\circ(\text{R}_1/\text{R}_1^\bullet)) - 0.16 \text{ eV} \quad (9)$$

Considering above mentioned redox potentials of RhB and the fact that the 0-0 transition of RhB is at 567 nm (Fig. 11), i.e, at about 2.18 eV, the excited state of RhB can be reached via red-ox pathway by any oxidants having their formal reduction potential higher than about 1.59 V vs. SHE in basic solution. In the ox-red pathway, any reductants having formal reduction potential clearly below ca. -1.33 V vs. SHE should be able to carry out the final excitation step. Since hydrated electron does not follow Marcus's electron transfer theory (it rapidly reduces even extremely strongly oxidizing species),<sup>163</sup> it is inferred that the ECL in the present systems is mainly generated by the ox-red pathway. On thermodynamic basis the red-ox pathway is also possible in the absence of added azide ions.

For the existence of weak ECL in the case of oxide films thicker than about 10 nm, we propose that less energetic electrons replace hydrated electrons in the above pathways (33-35). Since RhB is readily reduced ( $E^\circ(\text{RhB}/\text{RhB}_{\text{red}}) = -0.75 \text{ V vs. SHE}$ ),<sup>185</sup> the less energetic heterogeneously transferred electrons from the bottom of the conduction band of aluminum oxide at the electrolyte/oxide film interface under F-N tunneling regime may be sufficiently strong reductants for the system.

The ECL lifetime of RhB (i.e, the reciprocal of the slope of the ln ECL Intensity vs. Time) is 12.3  $\mu\text{s}$  in the presence of peroxodisulfate ions, and 19.4  $\mu\text{s}$  in the presence of azide ions. In both cases, lifetimes are longer than that of the background solid-state electroluminescence (ca. 5  $\mu\text{s}$ ), making possible the discrimination of ECL signals from the background signals. The time-resolved ECL signal shows linear response from  $10^{-10}$  to  $10^{-5} \text{ M}$  in the presence of 0.01 M  $\text{NaN}_3$  (Fig. 15). Thus, RhB-based labels can be combined with other electrochemiluminescent labels, such as Tb

chelates with longer ECL lifetime or coumarins with shorter ECL lifetime to provide multicomponent assays based on time discrimination.

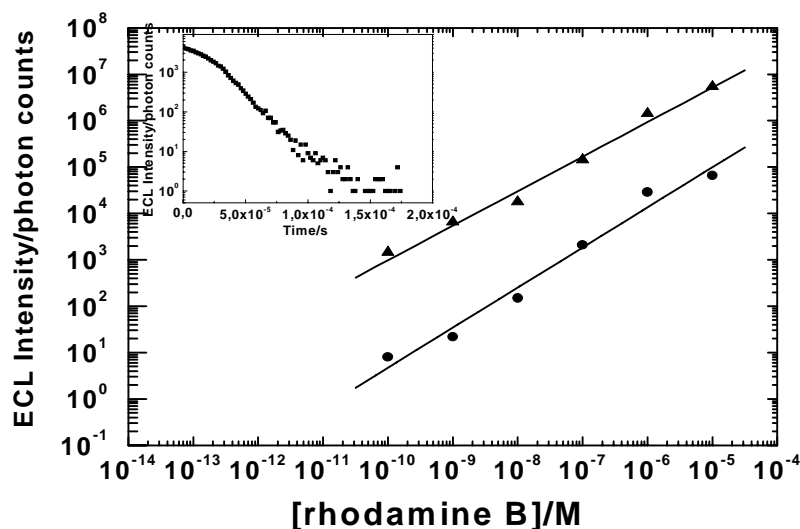


**Fig. 15** Calibration plot of RhB using disposable aluminum electrodes. (▲) Cathodic ECL during pulse, (●) Time-resolved ECL. Conditions: all measurements were made in 0.05 M  $\text{Na}_2\text{B}_4\text{O}_7$  at pH 9.2 buffer solution containing 0.01 mol/L  $\text{NaN}_3$ . Otherwise the same as that in Fig. 12. Inset: ECL decay curve of RhB after the cathodic pulse.

The well-known radiochemiluminescent compound rhodamine B shows strong and relatively long-lived ECL during cathodic pulse polarization of oxide-coated aluminum electrode in fully aqueous solution. It should be possible, therefore, to use derivatives of RhB with suitable linking side groups in multilabel assays based on time-discrimination, together with some shorter-lived ECL-displaying labels such as coumarins (Paper II).

#### 6.2.4 Hot electron-induced ECL of lucigenin

Lucigenin (N, N'-dimethyl-9-9'-biacridinium dinitrate) and acridinium esters have been studied as a class of aromatic luminophores.<sup>190</sup> Lucigenin (Luc) produces strong chemiluminescence in the presence of hydrogen peroxide or reducing agents in alkaline solution. Luc has also been found to be cathodically excitable at about - 0.5 V vs. Ag/AgCl at glassy carbon electrodes<sup>191</sup> and at ca. - 0.65 V vs. Ag/AgCl at platinum electrode<sup>192</sup>. The luminescence of Luc is of interest, and has been extensively exploited in determinations of substances generated from biological tissues, for example, peroxide ion ( $\text{O}_2^{\bullet-}$ ), hydrogen peroxide and epinephrine.<sup>193-197</sup> ECL of Luc has also been used to detect riboflavin,<sup>192</sup> human chorionic gonadotropin,<sup>198</sup> and hemin.<sup>199</sup>

The mechanism for ECL of Luc induced by conventional electrochemistry is similar to that for CL of Luc.<sup>190, 200, 201</sup> Although the reactions undergone by lucigenin are complex, a common CL mechanism with three steps has been proposed:<sup>190,200,201</sup> (1) a one-electron transfer to  $\text{Luc}^{2+}$  producing radical  $\text{Luc}^{\bullet+}$ ; (2) reaction of  $\text{Luc}^{\bullet+}$  with molecular oxygen or a superoxide radical ( $\text{O}_2^{\bullet-}$ ) yielding an extremely unstable dioxetane-type intermediate; (3) decomposition of this intermediate providing an excited state of N-methyl-acridone ( $\text{NMA}^*$ ).  $\text{NMA}^*$  is the primary emitter, emitting at ca. 452 nm.

$\text{Luc}^{2+}$  and dimethylbiacridene (DBA), a product of lucigenin two-electron reduction, have been proposed as secondary emitters. Both  $\text{Luc}^{2+}$  and DBA could act as energy acceptors from excited  $\text{NMA}^*$  by singlet-singlet energy transfer, finally emitting at 510 nm and 505 nm, respectively. It is generally accepted that the observed CL is mainly due to the emission of both excited  $\text{NMA}^*$ , and secondary emitters ( $\text{Luc}^{2+*}$  and/or  $\text{DBA}^*$ ), resulting a mixed broad band light emission.<sup>190,191,200-202</sup>

Papadopoulos et al.<sup>203</sup> observed that when irradiated oxygen-saturated solutions of amines or amides were added to aqueous solutions of lucigenin,<sup>203</sup> intense CL was induced, with  $\text{DBA}^*$  as the major emitting species.

In earlier studies in our laboratory,<sup>48,49,60,171,204</sup> reduction-initiated oxidative excitation (red-ox) and oxidation-initiated reductive excitation (ox-red) were proposed as the general ECL excitation routes for luminophores in our cathodic pulse polarization method. The luminophores are excited to singlet or triplet state by species cathodically generated at conductor/insulator/electrolyte (C/I/E) tunnel junction electrodes by successive one-electron transfer steps.<sup>48,49,60,171,204</sup> Sometimes, however, the ECL mechanism involves the decomposition of the luminophore.<sup>171</sup> In the present work, the possibility of generation of cathodic ECL of lucigenin at thin oxide film-coated aluminum electrodes was studied.

The cathodic ECL spectrum of lucigenin produced at an oxide-coated aluminum electrode is different from its fluorescence emission spectrum (Fig. 16). The ECL spectrum has a broad band with maximum at 510 nm and is asymmetrical, also

including a weaker emission at longer wavelengths (Fig. 16). The ECL emission is not due to  $\text{NMA}^*$ , which emits at about 450 nm. It was assumed that the main emitter could be excited  $\text{Luc}^{2+*}$  or excited  $\text{DBA}^*$ , or a mixture of these. Possibly, the weak emission at longer wavelengths originates from the excited triplet state  $^3\text{Luc}^{2+*}$ .

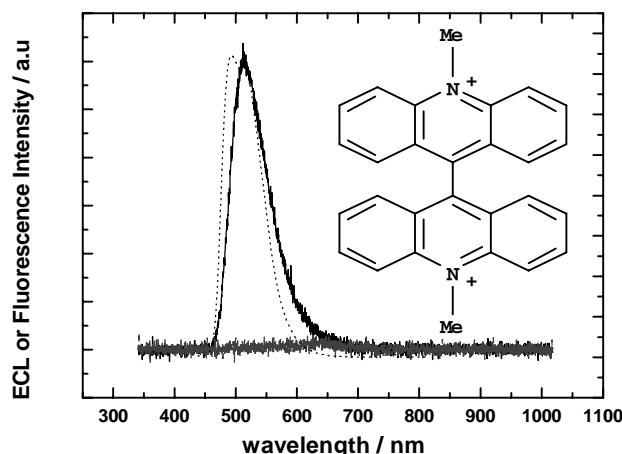


**Fig. 16** ECL spectrum and fluorescence emission spectrum of lucigenin. Conditions: fluorescence emission spectrum (dot line) was measured by Perkin-Elmer LS-50B spectrometer with scan speed  $240 \text{ nm min}^{-1}$ ,  $\lambda_{\text{ex}}$  369 nm; ECL spectrum (solid line) was measured by Ocean Optics USBFL-2000 spectrometer integrated for 1000 ms; Solution for ECL spectrum was  $1 \times 10^{-3} \text{ M}$  lucigenin in  $3 \times 10^{-3} \text{ M}$   $\text{K}_2\text{S}_2\text{O}_8$ ,  $0.05 \text{ M}$   $\text{Na}_2\text{B}_4\text{O}_7$  buffer at pH 7.8; Solution for fluorescence spectrum is  $1 \times 10^{-5} \text{ M}$  lucigenin,  $0.05 \text{ M}$   $\text{Na}_2\text{B}_4\text{O}_7$  buffer at pH 7.8. Coulostatic pulse generator: pulse voltage  $-45 \text{ V}$ , pulse frequency  $20 \text{ Hz}$ , pulse charge  $120 \mu\text{C}$ , aluminum strip cathode, platinum wire anode. Molecular structure of lucigenin is given in the inset.

The ECL intensity was relatively constant in pH range 4 to 11, which is close to the pH range of stability of  $\text{Al}_2\text{O}_3$  film (Fig. 17).<sup>172</sup> The effect of oxide film thickness on the ECL intensity (Fig. 18) is analogous to that observed with metal chelates and organic luminophores.<sup>45,48,160</sup>

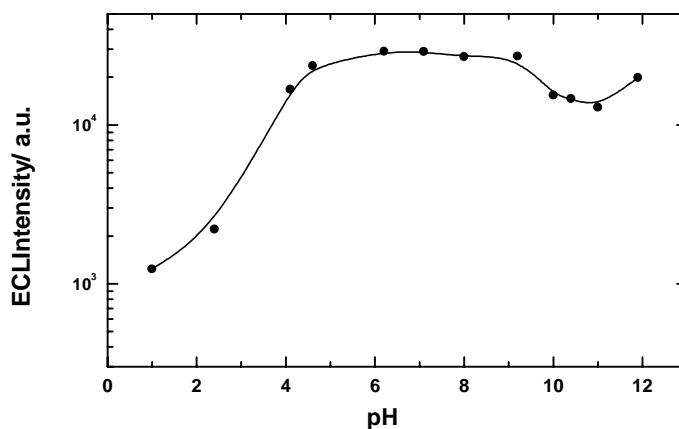


**Fig. 17** Effect of pH on the lucigenin ECL. Conditions:  $1.0 \times 10^{-5} \text{ M}$  lucigenin in  $0.1 \text{ M}$   $\text{Na}_2\text{SO}_4$  supporting electrolyte solutions. Solutions were adjusted to the desired pH with sulfuric acid or sodium hydroxide; pulse voltage  $-50 \text{ V}$ , pulse frequency  $80 \text{ Hz}$ , pulse charge  $100 \mu\text{C}$ . ECL was measured by Perkin-Elmer LS-5 spectrometer in Phosphorescence mode with excitation light path closed, scan speed  $240 \text{ nm min}^{-1}$ , delay time  $0.1 \text{ ms}$ , gate time  $13 \text{ ms}$ .

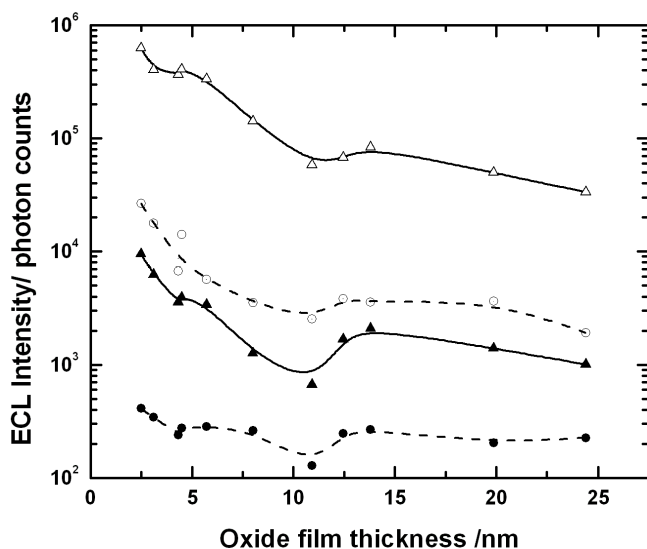


**Fig. 18** Effect of oxide film thickness on the ECL intensity of lucigenin. (□) Cathodic ECL and (▲) TR-ECL of  $1.0 \times 10^{-6}$  M lucigenin in 0.05 M  $\text{Na}_2\text{B}_4\text{O}_7$  buffer solution at pH 7.8. (○) Cathodic ECL and (●) TR-ECL of 0.05 M  $\text{Na}_2\text{B}_4\text{O}_7$  buffer solution at pH 7.8. Aluminum electrodes with varied oxide thickness were used as disposable working electrodes. TR-ECL: delay time 5  $\mu\text{s}$ , gate time 1.00 ms. ECL and TR-ECL intensities were integrated over 1000 excitation cycles. All signals were measured through a 500-nm interference filter with half-width of the transmission band ca. 10 nm. Pulse voltage  $-45$  V, pulse frequency 20 Hz, pulse charge 120  $\mu\text{C}$ .

Therefore, it is again proposed that direct field-assisted tunneling is predominating in case of ultra-thin insulating films (thickness  $<$  ca. 4 nm). The ECL intensity began to increase slightly when the oxide film thickness exceeded 12 nm. Considering that lucigenin is easily reduced ( $E^\circ(\text{Luc}^{2+}/\text{Luc}^{\bullet+}) = -0.13$  V vs. SHE)<sup>202</sup> compared with the other luminophores studied previously.<sup>54,57,60</sup> We assumed that considerable ECL also could be induced by less energetic electrons transferred from the bottom of the conduction band of oxide film at the electrolyte/ oxide film interface under F-N tunneling regime.

The effects of hydroxyl radical and hydrated electron scavengers on ECL of lucigenin (Figs. 19 and 20) support the assumption that hydrated electrons and hydroxyl radicals (or other oxidizing species with properties similar to those of the hydroxyl radical) play important roles in the excitation ECL pathway.

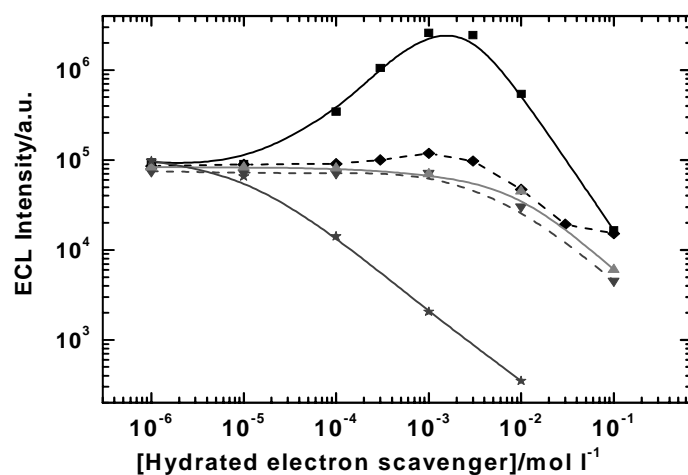


**Fig. 19** Effect of several hydrated electron scavengers on the ECL intensity of lucigenin ( $1 \times 10^{-5}$  M). (■) Cathodic ECL,  $K_2S_2O_8$ ; (□) Cathodic ECL,  $H_2O_2$ ; (▼) Cathodic ECL,  $NaNO_2$ ; (▲) Cathodic ECL,  $NaNO_3$ ; (□) Cathodic ECL,  $Co(NH_3)_6^{3+}$ . Conditions: measurements were made in 0.05 M  $Na_2B_4O_7$  buffer solution at pH 7.8, otherwise the same as in Fig. 17.

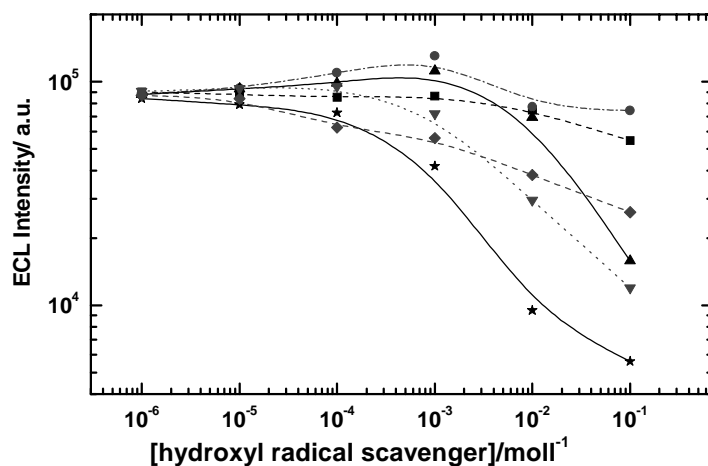


**Fig. 20** Effect of different hydroxyl radical scavengers on the ECL intensity of lucigenin ( $1 \times 10^{-5}$  M). (●) NaBr, (▲)  $NaN_3$ , (■) NaCl, (□) ethanol, (▼) NaSCN, (□) NaI; Conditions: measurements were made in 0.05 M  $Na_2B_4O_7$  solution at pH 7.8, otherwise the same as in Fig. 17.

Taking into consideration the redox potential values of lucigenin,<sup>200, 202</sup> the ECL excitation route could be the reduction-initiated oxidative excitation (red-ox) pathway (36a-c). The mechanism is as follows:



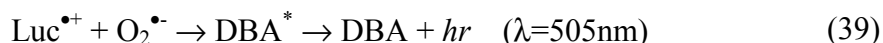
In this case, the enthalpy of the excitation step equals the energy of emission light at wavelength 510 nm, i.e, 2.43 eV. On thermodynamic grounds,<sup>33</sup> the excited state can be achieved by oxidants having a redox potential higher than about 2.46 V vs. SHE. This can be demonstrated by the large enhancement of ECL in the presence of peroxodisulfate ions (Fig. 19).

In view of the weak enhancement of lucigenin ECL in the presence of a suitable concentration of azide ions (Fig. 20), it is not considered impossible that lucigenin could be oxidized by azide radical ( $E^\circ(\text{N}_3^\bullet/\text{N}_3^-)=1.33 \text{ V vs. SHE}$ )<sup>163</sup>. This would mean that  $\text{Luc}^{3+}$  has a formal reduction potential perhaps at around 1 V vs. SHE, and the whole excitation sequence would be:



The highly negative reduction potential of hydrated electron (-2.9 V vs. SHE)<sup>163</sup> means that the ox-red excitation pathway is easily possible on thermodynamic grounds.

Because CL of lucigenin is a very complex process, with several reactions proceeding in parallel, it is quite possible that also  $\text{DBA}^*$  is produced, as described by Papadopoulos.<sup>203</sup> In air-saturated solution, a parallel reductive excitation pathway is plausible:



In principle, all CL pathways involving formation of a dioxetane-type intermediate by reaction with superoxide radical or hydrogen peroxide are possible.



The ECL lifetime of lucigenin at oxide-covered aluminum electrode is 18.4  $\mu\text{s}$  (Fig. 21) and the linear response range is from  $10^{-10}$  to  $10^{-6}$  M in the presence of  $10^{-3}$  M  $\text{K}_2\text{S}_2\text{O}_8$ . Suitable derivatives of lucigenin can thus be proposed as labels in bioaffinity assays. Lucigenin derivatives (e.g. BADE and SPBA) having conjugation groups to link them to biological molecules of interest could also be used as a labels in bioaffinity assays based on our cathodic pulse polarization method.

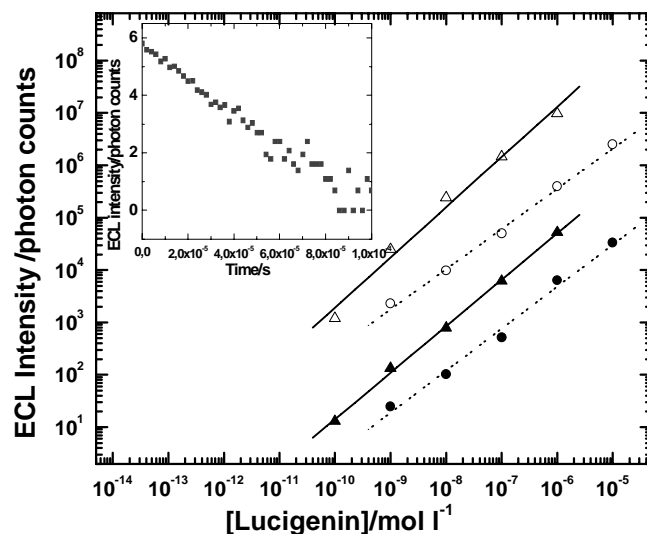


Fig. 21 Calibration plot of lucigenin using disposable oxide-covered aluminum electrodes. ( $\Delta$ ) ECL in the presence of 1 mM  $\text{K}_2\text{S}_2\text{O}_8$ , ( $\blacktriangle$ ) TR-ECL in the presence of 1 mM  $\text{K}_2\text{S}_2\text{O}_8$ , ( $\circ$ ) ECL in the absence of  $\text{K}_2\text{S}_2\text{O}_8$ , ( $\bullet$ ) TR-ECL in the absence of  $\text{K}_2\text{S}_2\text{O}_8$ . Conditions: all measurements were made in 0.05M  $\text{Na}_2\text{B}_4\text{O}_7$  buffer solutions at pH 7.8. Otherwise the same as that in Fig.18. ECL decay curve of lucigenin is shown in the inset.

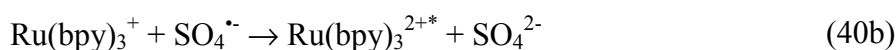
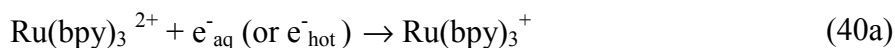
### 6.3 Transition metal chelates

#### 6.3.1 ECL of $\text{Ru}(\text{bpy})_3^{2+}$ induced at oxide film-coated silicon electrodes and CL of $\text{Ru}(\text{bpy})_3^{2+}$

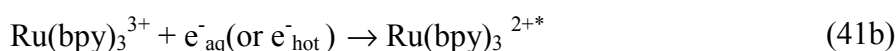
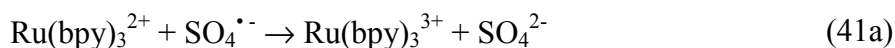
As mentioned above,  $\text{Ru}(\text{bpy})_3^{2+}$  is one of the most widely studied ECL-producing compounds, and it is in wide use as a label chelate in bioaffinity assays<sup>11,68,205</sup>. In previous work our group has shown briefly that  $\text{Ru}(\text{bpy})_3^{2+}$  chelates display strong ECL in aqueous solutions at both oxide film-covered aluminum electrodes and at n-silicon electrodes oxidized *in situ* by anodic pulses during the measurement.<sup>49,172</sup> In the present research, silicon chips oxidized by rigorously controlled dry thermal oxidation were applied as working electrodes for ECL applications (Paper V). The ECL of  $\text{Ru}(\text{bpy})_3^{2+}$  chelate produced at silicon dioxide film-coated n- and p-type

planar silicon electrodes was studied in detail and comparison was made with the ECL produced at oxide film-covered aluminum electrodes.

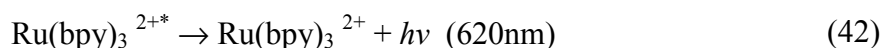
$\text{Ru}(\text{bpy})_3^{2+}$  shows a typical  $^3\text{MLCT}$  emission spectrum during cathodic pulse polarization at oxide-coated silicon or aluminum electrodes, with emission maximum at 620 nm.<sup>49,68,172</sup> The mechanism of  $\text{Ru}(\text{bpy})_3^{2+}$  ECL induced on the oxide film-coated silicon electrode was proposed to be identical to that induced on the oxide film-covered aluminum electrode.<sup>172</sup> The ECL excitation of  $\text{Ru}(\text{bpy})_3^{2+}$  can occur by reduction-initiated oxidative excitation (red-ox) pathway (reaction 40a and 40b) or oxidation-initiated reductive excitation (ox-red) pathway (reactions 41a and 41b), as follows:



or:



After these excitation steps,  $\text{Ru}(\text{bpy})_3^{2+*}$  relaxes (reaction 42) to the ground state producing the peak emission at 620 nm.



As an excellent one-electron oxidant, sulfate radical ( $E^0(\text{SO}_4^{\bullet-}/\text{SO}_4^{2-}) = 3.4 \text{ V vs. SHE}^{206}$ ) is even capable of rapidly oxidizing benzene and reacts very sluggishly with water [ $k(\text{SO}_4^{\bullet-} + \text{H}_2\text{O}) = 60 \text{ dm}^3 \text{ mol}^{-1} \text{ s}^{-1}$ ].<sup>207</sup> Sulfate radical is thus often used in generating or enhancing redox luminescence of chemiluminophores at thin insulating film-covered electrodes in aqueous solutions.<sup>48,68</sup> The dependence of the ECL intensity of  $\text{Ru}(\text{bpy})_3^{2+}$  on the concentration of peroxodisulfate ion was presented in Fig. 22, for the cases of n- and p-type silicon electrodes coated with ca. 4 nm thermal oxide film. The results were similar to earlier results for oxide film-covered aluminum electrodes,<sup>172</sup> and the optimal concentration of peroxodisulfate ion as coreactant was ca.  $3 \times 10^{-3} \text{ mol/l}$  for oxide film-coated silicon used as working electrodes.

Furthermore, the effect of buffer solution pH on thermal oxide film-coated silicon working electrode was similar to that for oxide film-covered aluminum electrodes (Fig. 23). This finding suggests that the present ultra-thin silicon dioxide films may be dissolved and damaged in strongly basic solutions, and these solutions possibly should not be used.

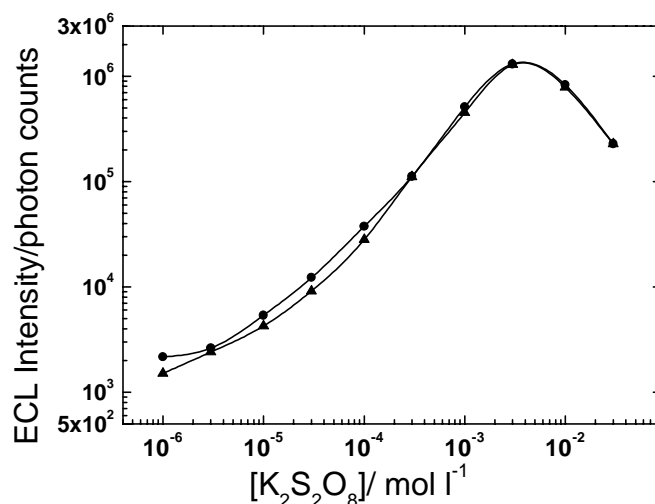


**Fig. 22** Effect of  $\text{K}_2\text{S}_2\text{O}_8$  concentration on  $\text{Ru}(\text{bpy})_3^{2+}$  chelate ECL. Conditions:  $1.0 \times 10^{-6}$  M  $\text{Ru}(\text{bpy})_3^{2+}$  in 0.05M  $\text{Na}_2\text{B}_4\text{O}_7$  at pH 9.2, coulostatic pulse generator, pulse charge 300  $\mu\text{C}$ , -25V, frequency 50 Hz, (●)  $\text{n}^+\text{-Si}$  (thickness of oxide film 3.6 nm) and (▲)  $\text{p}^+\text{-Si}$  (thickness of oxide film 3.9 nm) as working electrodes, respectively. ECL intensity was integrated over 1000 excitation cycles.

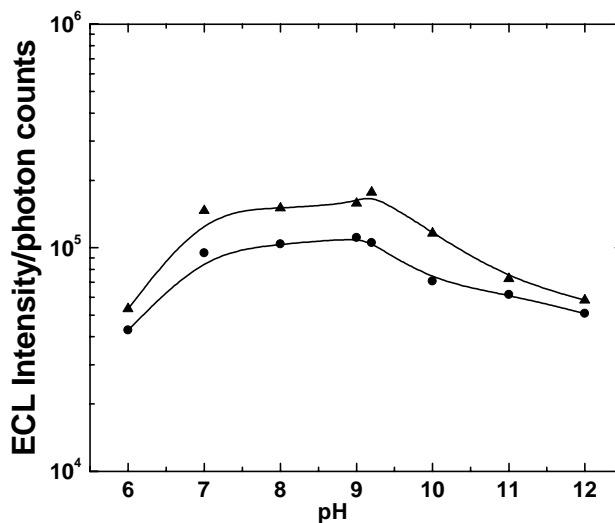


**Fig. 23** Effect of pH on  $\text{Ru}(\text{bpy})_3^{2+}$  chelate ECL: (●)  $\text{n}^+\text{-Si}$  and (▲)  $\text{p}^+\text{-Si}$ . Conditions:  $1.0 \times 10^{-6}$  M  $\text{Ru}(\text{bpy})_3^{2+}$  in 0.1M  $\text{Na}_2\text{SO}_4$  and 30 mM  $\text{Na}_2\text{B}_4\text{O}_7$  supporting electrolyte solution,  $1.0 \times 10^{-3}$  M  $\text{K}_2\text{S}_2\text{O}_8$ , solution was adjusted to the desired pH with sulfuric acid or sodium hydroxide, pulse charge 300  $\mu\text{C}$ , -25V and pulse frequency 50 Hz. ECL intensity was integrated over 1000 excitation cycles. Oxide film thicknesses as that in Fig. 22.

For long-lasting cathodic pulses of the order of 2.2 ms, the ECL intensity of  $\text{Ru}(\text{bpy})_3^{2+}$  at oxide-coated silicon electrodes was found to be considerably higher than that at natural oxide film-covered aluminum. With shorter pulse times, the difference in ECL intensity between these silicon and aluminum electrodes was smaller. The ECL intensity of p-type silicon electrodes also seems to be higher than that of n-type electrodes (Paper V). However, the calibration plot of  $\text{Ru}(\text{bpy})_3^{2+}$  at n-silicon was still very nice (Fig. 24). The reason for this may be that thermal oxidation of heavily doped p-type silicon gives a bit better quality oxide film. Oxide-covered aluminum electrodes also gave much higher blank emission in ECL wavelength range of  $\text{Ru}(\text{bpy})_3^{2+}$ , and thermal silicon oxide film formed on n-type silicon showed the lowest blank emission amongst all the electrode types tested (Fig. 25). Thus it is suggested that oxide films formed on n-type substrate have fewer defects or impurities able to act as solid-state electroluminescence emission centers under high field conditions.

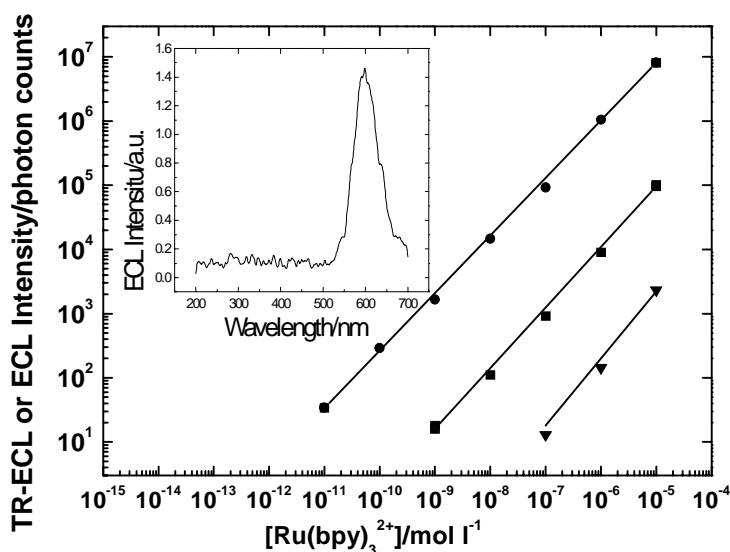


**Fig. 24** Calibration curve for  $\text{Ru}(\text{bpy})_3^{2+}$  using disposable electrodes and either cathodic signal or time-resolved signal after the excitation pulse: (●) cathodic ECL at disposable n-silicon electrodes with 3.6 nm thermal oxide film coating, (▼) time-resolved signal at oxide-coated n-silicon electrodes and (■) time-resolved signal using disposable oxide-covered aluminium electrodes. Conditions: electrode area 63.6mm<sup>2</sup>, 0.05M  $\text{Na}_2\text{B}_4\text{O}_7$  buffer at pH 9.2,  $3.0 \times 10^{-3}\text{M}$   $\text{K}_2\text{S}_2\text{O}_8$ , pulse charge 120  $\mu\text{C}$ , pulse length ca. 560  $\mu\text{s}$ , pulse voltage  $-45\text{V}$  and pulse frequency 20 Hz. Time-resolved measurements: delay time 0  $\mu\text{s}$  and gate time 200 $\mu\text{s}$ . ECL intensity was integrated over 1000 excitation cycles. Inset: Uncorrected ECL spectrum of  $\text{Ru}(\text{bpy})_3^{2+}$  measured by Pekin-Elmer LS-5 spectrometer.

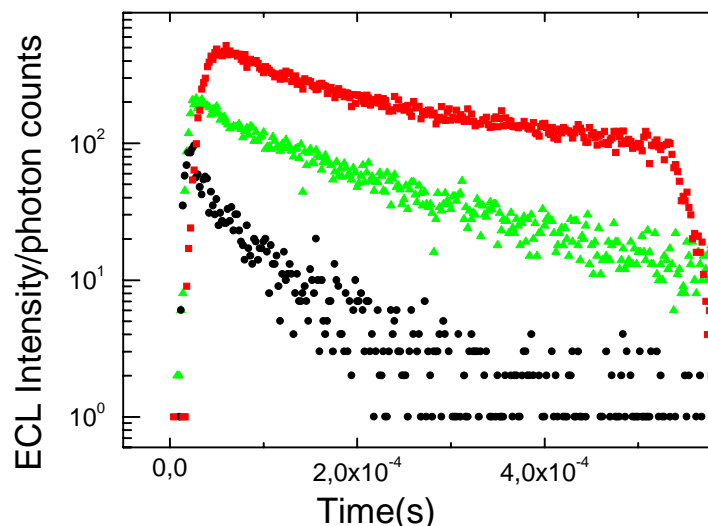


**Fig. 25** ECL blank emission pulses at 620 nm: (●) n<sup>+</sup>-Si with 3.6 nm oxide film, (▲) p<sup>+</sup>-Si with 3.7 nm oxide film and (■) aluminum with natural oxide film. Conditions: pulse voltage -25V, pulse charge 300μC, pulse frequency 50 Hz, pulse length ca. 850 μs, otherwise as in Fig. 24.

In a study of the decay of Ru(bpy)<sub>3</sub><sup>2+</sup> ECL, it was observed that the ECL emission at oxide film-coated n- and p-type silicon were identical and the decay was much faster than that at oxide-covered aluminum. It is proposed that the ECL of Ru(bpy)<sub>3</sub><sup>2+</sup> might be also induced by the relatively strong intrinsic ECL of oxide film-covered aluminum electrodes through energy transfer mechanism. Such it would not occur in the case of oxide film-coated silicon electrode because of the weak intrinsic ECL of this electrode. Other relevant factors could be changes in the surface of the aluminum electrode, such as alkalization due to hydrogen evolution, or dissolution of oxide film during cathodic pulse polarization.<sup>48</sup>

Moreover, the rise stage of the ECL signal induced on oxide-covered aluminum electrodes was observed to differ from that on oxide-coated silicon electrodes under the same conditions (Fig. 26). The thermally oxidized ultra-thin oxide-coated n- and p-type silicon electrodes exhibited a lag time of about 8 μs from the onset of voltage before luminescence is observed, while the lag time for aluminum oxide film was about 14 μs. However, in all cases the rise time from the moment of zero intensity to 90 % intensity was about 30 μs. The reason for the different lag times between silicon dioxide and aluminum oxide film yet is not clear.

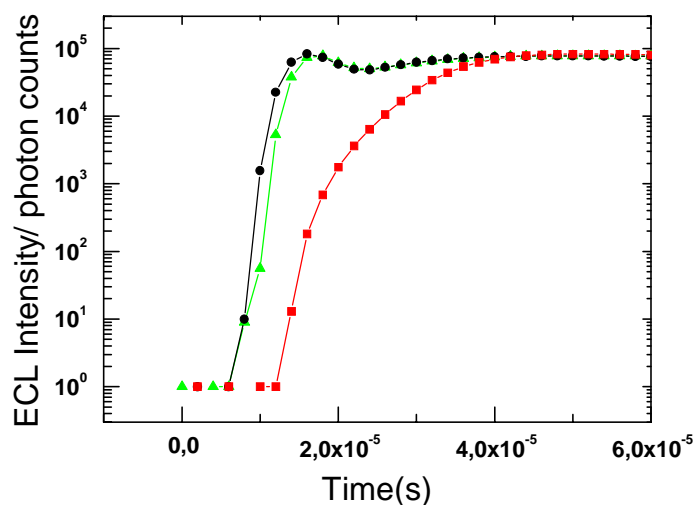


**Fig. 26** The rise of the ECL pulse at different electrode types: (●) n-silicon with 3.6 nm oxide film, (▲) p-silicon with 3.7 nm oxide film and (■) aluminum covered with a natural oxide film. Conditions: electrode area 63.6 mm<sup>2</sup>, 0.05M Na<sub>2</sub>B<sub>4</sub>O<sub>7</sub> buffer at pH 9.2, 3.0×10<sup>-3</sup> M K<sub>2</sub>S<sub>2</sub>O<sub>8</sub>, pulse charge 120 μC, pulse length ca. 560μs, -45V, 20 Hz. ECL integrated over 5000 excitation cycles.

Chemiluminescence can also be generated from Ru(bpy)<sub>3</sub><sup>2+</sup> through chemical reactions in the presence of suitable oxidants and reductants, such as sulfate radicals and hydrated electrons.<sup>59,172,205</sup> CL of Ru(bpy)<sub>3</sub><sup>2+</sup> chelates generated during dissolution of aluminum metal in alkaline aqueous solution and during dissolution of magnesium in acidic conditions was studied. (Paper VI)

The dissolution of aluminum can result in the action of metallic aluminum as a reductant, but also short-lived Al<sup>+</sup> and Al<sup>2+</sup> species, hydrogen atom and its conjugated base, hydrated electron, can act as strong reductants<sup>208</sup>. It has been reported that tetrahydroxylaluminate(III) ion (Al<sup>3+</sup> is four-coordinated) is not reduced by e<sup>-</sup><sub>aq</sub> (k(e<sup>-</sup><sub>aq</sub> + Al(OH)<sub>4</sub><sup>-</sup>) = 5.5 × 10<sup>6</sup> M<sup>-1</sup> s<sup>-1</sup>)<sup>209</sup>, which implies that aluminate(II) ion is a stronger reductant than the hydrated electron. Approximation of one-electron reduction potentials of metal ions in aqueous solutions within each group can be calculated by equation (43) according to Jørgensen.<sup>210</sup>

$$E^{\circ}M(z/z-1) = I_z - (2z - 1) \kappa - 4.5 \text{ eV} \quad (43)$$

Here  $z$  is the oxidation state,  $I_z$  is the  $z$ th ionization energy of the element and  $\kappa$  is a parameter of hydration energy difference, which is 5.3 eV for the 3d series, and reported values for Al and Mg are 5.37 and 4.98 eV, respectively<sup>210</sup>. Thus, for the couple  $\text{Al}^{3+}/\text{Al}^{2+}$ ,  $E^\circ(\text{Al}^{3+}/\text{Al}^{2+})$  is estimated to be - 2.9 eV vs SHE.

It is proposed that  $\text{Al}^0$  and  $\text{Al}^{2+}$ , as solvated species in water, are one-electron reductants comparable to  $e^-_{\text{aq}}$ , alkali metal colloids, and  $\text{Mg}^+$ .  $\text{Al}^{2+}$  is assumed to disproportionate in aqueous solutions to oxidation states (I) and (III), similarly to  $\text{In}^{2+}$  and  $\text{Tl}^{2+}$ .<sup>187</sup>  $\text{Al}^+$  has never been reliably demonstrated, however, owing to its poor stability in aqueous solutions. In the presence of the above reductants and suitable oxidizing agent (e.g., peroxodisulfate ions), extrinsic lyoluminescence of aluminum was induced by  $\text{Ru}(\text{bpy})_3^{2+}$  (Fig. 27), where the 620 nm emission peak can be assigned to the well-known relaxation of the metal-to-ligand charge transfer excited triplet state  $^3\text{Ru}(\text{bpy})_3^{2+*}$ . Magnesium induced analogous extrinsic lyoluminescence under similar conditions but in the acidic aqueous solution, suggesting that one-electron reductions might be produced during the dissolution of magnesium metal into aqueous solution.

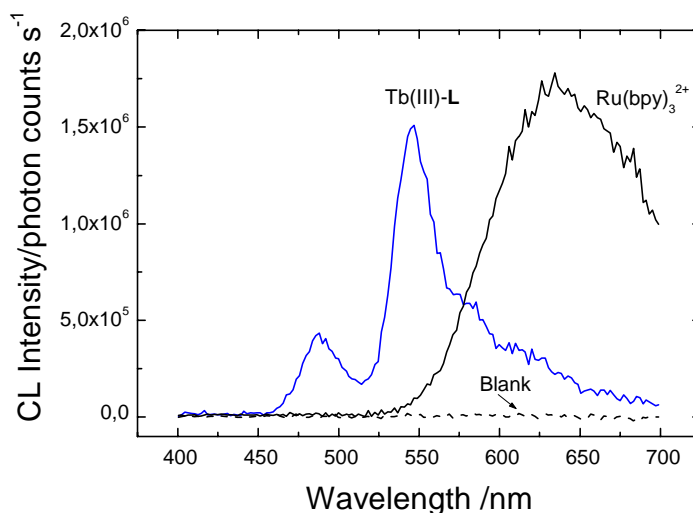
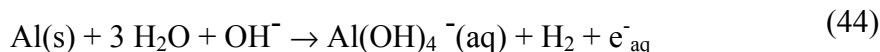


**Fig. 27** CL emission spectra of  $\text{Ru}(\text{bpy})_3^{2+}$  and  $\text{Tb}(\text{III})\text{-L}$  induced by dissolution of aluminum in alkaline peroxodisulfate solutions. Conditions: 1.0 M NaOH, peroxodisulfate concentration  $1.0 \times 10^{-3}$  M, luminophore concentrations  $5 \times 10^{-5}$  M.  $\text{Tb}(\text{III})\text{-L}$  = Terbium(III)-{2,6-bis[*N,N*-bis(carboxymethyl)aminomethyl]-4-benzoylphenol}.

Even though the dissolution of aluminum involves many reactions, which results in various mediators, the following overall reaction is suggested as a source of hydrated electron useful in generating chemiluminescence from luminophores tolerating highly alkaline conditions:



Hydrated electron reacts slowly with water,  $k(\text{e}^-_{\text{aq}} + \text{H}_2\text{O}) = 19 \text{ l mol}^{-1}\text{s}^{-1}$ .<sup>163</sup> If peroxodisulfate ions are added to the solution, highly oxidizing  $\text{SO}_4^{\bullet-}$  radicals are formed, by a one-electron reduction, with the rate constant  $k_{46} = 1.2 \times 10^{10} \text{ l mol}^{-1}\text{s}^{-1}$ .<sup>163</sup>



Thus the aluminum/( $\text{Al}_2\text{O}_3$ ,  $\text{Al(OH)}_3$ ,  $\text{OH}^-$ ,  $\text{Al(OH)}_4^-$ ,  $\text{Al}^+$ ,  $\text{Al}^{2+}$ ,  $\text{H}^{\bullet}$ ,  $\text{e}^-_{\text{aq}}$ ,  $\text{SO}_4^{\bullet-}$ ) interface provides various routes to produce the observed 2.1 eV <sup>3</sup>MLCT excited state through an oxidation-initiated reductive (ox-red) pathway or an alternative reduction-initiated oxidative pathway (red-ox) described above as equations (40)–(41).

Alternatively, this excited triplet state can be directly formed by reactions analogous to (40b) and (41b) in which other species with suitable energy replace  $\text{e}^-_{\text{aq}}$  or sulfate radical. In principle, species with energy above that of  $\text{Ru(bpy)}_3^{2+}/\text{Ru(bpy)}_3^+$  in the energy diagram (Fig. 28) are thermodynamically able to reduce  $\text{Ru(bpy)}_3^{2+}$  and initiate the red-ox excitation pathway. This is energetically possible for bulk aluminum,  $\text{Al}^{2+}$ ,  $\text{Al}^+$ , and atomic hydrogen, as well as hydrated electron. The ox-red excitation pathway, in turn, can only be initiated by oxidants with energy below that of the couple  $\text{Ru(bpy)}_3^{3+}/\text{Ru(bpy)}_3^{2+}$  in the energy diagram. Thus, only  $\text{SO}_4^{\bullet-}$  and  $\text{O}^{\bullet-}$  are energetically capable of the initiation. However, oxide radical ions, which could be generated in air-equilibrated solution by reactions analogous to equations (19)–(22), have a strong tendency for addition reaction to pyridine rings rather than the preferable one-electron oxidation,<sup>211,212</sup> and it is highly likely that only sulfate radical can efficiently initiate the ox-red excitation pathway. Thus, the ox-red excitation pathway is almost certainly the more favorable pathway in the presence of relatively concentrated peroxodisulfate ion solution.



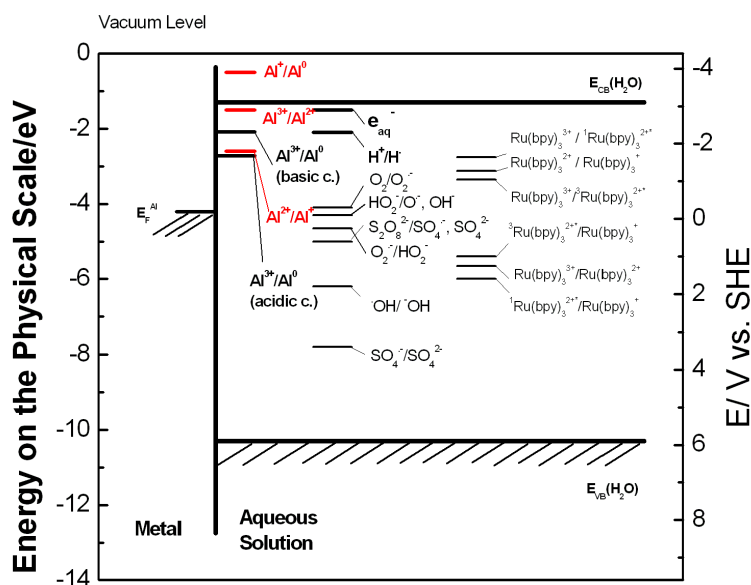


**Fig. 28** Energy diagram of  $\text{Al}/\text{OH}^- - \text{S}_2\text{O}_8^{2-} - \text{Ru}(\text{bpy})_3^{2+}$ -system. The diagram is sketched on the grounds discussed in detail<sup>53</sup> and using values for oxyradicals given by Koppenol<sup>44</sup> and calculated one-electron reduction potentials of Al-species according to Jørgensen<sup>210</sup>.

As a comparison, the possibility of using  $\text{Ru}(\text{bpy})_3^{2+}$  in acid solutions to produce extrinsic CL of aluminum was studied. However, no extrinsic CL of aluminum was induced by  $\text{Ru}(\text{bpy})_3^{2+}$  chelate in either hydrochloric or sulfuric acid medium, nor in the absence or presence of peroxodisulfate ions.

From the open circuit potentials of Al measured in hydrochloric acid, we assume that an Al electrode originally covered with passive oxide layer never loses its passivity during dissolution in hydrochloric acid, i.e., aluminum is at all times covered with a thin (though possibly partly hydrous) aluminum oxide film even in concentrated HCl. During the dissolution of oxide film in acid solution, the electron transfer from metal occurs in part by tunneling through the dissolution-thinned oxide layer and possibly also inside the oxide layer.

Atomic hydrogen can act as an oxidant in acidic solutions because the formal reduction potential of the couple  $\text{H}^+/\text{H}^-$  is under strongly acidic conditions is about 1.6 V vs. SHE.<sup>187, 207</sup> Thus, hydrogen atoms may be able to oxidize aluminum metal and low-valent aluminum species. This being the case, the oxidation of aluminum would occur at the metal/oxide interface mainly by in-diffused hydrogen atom, and the dissolution of aluminum would be almost solely occur through the dissolution of aluminum oxide in acids. The trapped charges liberated by dissolution<sup>59,213</sup> would

seem to be unable to generate any observable luminescence from the studied luminophores under acidic conditions.

In contrast to this, CL has been observed from  $\text{Mg}/\text{H}^+ - \text{S}_2\text{O}_8^{2-} - \text{Ru}(\text{bpy})_3^{2+}$  system. This system seems to be more effective than the  $\text{Al}/\text{OH}^- - \text{S}_2\text{O}_8^{2-} - \text{Ru}(\text{bpy})_3^{2+}$  system discussed above, and both  $\text{Ru}(\text{bpy})_3^{2+}$  and  $\text{K}_2\text{S}_2\text{O}_8$  can be detected down to very low concentration levels at pH 0 (Fig. 29).

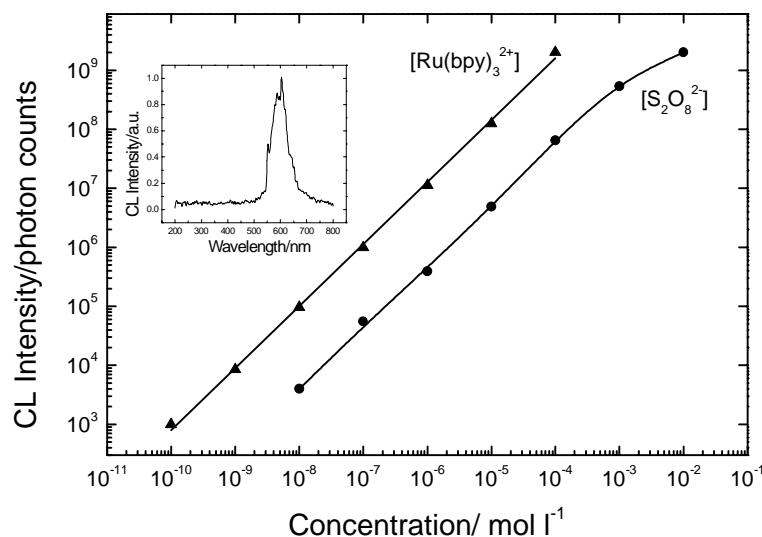


**Fig. 29** Calibration curves for  $\text{Ru}(\text{bpy})_3^{2+}$  and  $\text{K}_2\text{S}_2\text{O}_8$  using  $\text{Mg}/\text{H}^+ - \text{S}_2\text{O}_8^{2-}$  system for generation of CL. ( $\blacktriangle$ )  $1 \times 10^{-4}$  M  $\text{Ru}(\text{bpy})_3^{2+}$  and ( $\bullet$ ) 0.01M  $\text{K}_2\text{S}_2\text{O}_8$ . Photon counting lyoluminometer, 620 nm interference filter. Integration time 500 s. Inset displays an uncorrected emission spectrum of the present CL system as measured by LS 50B equipped with blue sensitive PMT ( $1 \times 10^{-4}$  M  $\text{Ru}(\text{bpy})_3^{2+}$ , 0.01M  $\text{K}_2\text{S}_2\text{O}_8$ , 0.1M HCl, emission slit 15 nm).

Magnesium is a more electropositive element than aluminum and its two-electron standard reduction potential is  $-2.356$  vs. SHE in acidic conditions<sup>214</sup>. In principle, the  $\text{Mg}/\text{H}^+ - \text{S}_2\text{O}_8^{2-} - \text{Ru}(\text{bpy})_3^{2+}$  system is closely similar to the  $\text{Al}/\text{OH}^- - \text{S}_2\text{O}_8^{2-} - \text{Ru}(\text{bpy})_3^{2+}$  system. When metallic magnesium is in direct contact with strongly acidic aqueous solution, magnesium is dissolved in reaction with protons:



It is probable that not all hydrogen atoms produced according to eq. (46) are lost in evolution of molecular hydrogen; part of them are available to act as reductants or oxidants. The short-lived low-valent  $\text{Be}^+$ , which belongs to the same group as magnesium, has been observed at lower concentration than 5 mM of water in ethanol solutions of lithium perchlorate electrolyte.<sup>215</sup> Thus, the present system was assumed

to include  $\text{Mg}^+$  as an extremely strong one-electron reductant, but its lifetime must be very short.

The most significant differences between the  $\text{Mg}/\text{H}^+-\text{S}_2\text{O}_8^{2-}-\text{Ru}(\text{bpy})_3^{2+}$  and  $\text{Al}/\text{OH}^--\text{S}_2\text{O}_8^{2-}-\text{Ru}(\text{bpy})_3^{2+}$  systems are that: in the Mg system, under highly acidic conditions, (i) there is no generation of hydrated electron, and even if it were somehow generated it would be rapidly converted to its conjugated acid ( $k(\text{e}^-_{\text{aq}} + \text{H}^+) = 2.3 \times 10^{10} \text{ l mol}^{-1} \text{ s}^{-1}$ );<sup>163</sup> (ii) in addition to  $\cdot\text{OH}$  and  $\text{SO}_4^{\cdot-}$  radicals, atomic hydrogen, and also  $\text{HO}_2^-$ , are able to initiate the ox-red excitation pathway, and also able to terminate the red-ox excitation pathway. This means that part of the atomic hydrogen may also act as a moderately strong oxidant, as discussed above. However, CL is weak in the absence of sulfate radicals, but on thermodynamic basis it is clear that  $\text{Mg}^+/\text{Mg}$  and  $\text{Mg}^{2+}/\text{Mg}^+$  couples can easily serve as the reductants of the system.

It is proposed that the ox-red pathway is the prevailing excitation route due to the very long lifetime of  $\text{Ru}(\text{bpy})_3^{3+}$ . In this route, electron is donated from a metal-centered orbital (a true Ru(III) oxidation state), and fast decomposition of the ligand centered radical of  $\text{Ru}(\text{bpy})_3^+$  (i.e. central ion is actually in oxidation state II) occurs in aqueous solution.<sup>68,216,217</sup>

In short, dissolution of aluminum in alkaline aqueous solution and dissolution of magnesium in acidic aqueous solution appear to create interesting metal/aqueous solution interfaces, which provide the possibility to generate CL from a wide variety of luminophores excitable by redox reactions. The  $\text{Mg}/\text{H}^+-\text{S}_2\text{O}_8^{2-}$  system in particular offers good analytical behavior for the detection of  $\text{Ru}(\text{bpy})_3^{2+}$ -based labels known to be useful in bioaffinity assays.<sup>68</sup> Thus, it is proposed that immunoassays and other bioaffinity assays can be carried out on the surface of oxide-covered magnesium slides or in miniature vessels under basic conditions, and then the detection of the label is carried out in a very simple way in acidic  $\text{S}_2\text{O}_8^{2-}$  solution. The  $\text{Al}/\text{OH}^--\text{S}_2\text{O}_8^{2-}$  system is more useful with derivatives of luminol and probably also with aromatic Tb(III) chelates as labels than with  $\text{Ru}(\text{bpy})_3^{2+}$ -based labels.

### 6.3.2 ECL of carboxylate derivative of $\text{Ru}(\text{bpy})_3^{2+}$

Modified  $\text{Ru}(\text{bpy})_3^{2+}$  chelates and commercially available instrumentation for immunoassay and DNA-probe applications have appeared in recent years.<sup>111,112,218,219</sup> Two derivatives of  $\text{Ru}(\text{bpy})_3^{2+}$ , i.e. [4-ethoxycarbonyl-4'-carboxy-2,2'-bipyridine]bis(2,2'-bipyridine) ruthenium(II) hexafluorophosphate complex ( $\text{Ru}(\text{bpy})_2\text{L}_a \cdot 2\text{PF}_6$ ,  $\text{L}_a = 4\text{-ethoxycarbonyl-4'-carboxy-2,2'-bipyridine}$ ) and [4,4'-diethoxycarbonyl-2,2'-bipyridine]bis(2,2'-bipyridine) ruthenium(II) hexafluorophosphate complex ( $\text{Ru}(\text{bpy})_2\text{L}_b \cdot 2\text{PF}_6$ ,  $\text{L}_b = 4,4'\text{-ethoxycarbonyl-2,2'-bipyridine}$ ) were synthesized and characterized as reported in detail in paper VII. The former complex can be linked with primary amino groups through carboxyl functional group linked with NHS ester as acylating agent, which enables labeling of proteins, peptides and DNA to be labeled.<sup>220</sup>

Photoluminescence, ECL, and CL of the two derivatives of  $\text{Ru}(\text{bpy})_3^{2+}$  were measured. Aluminum strips were the working electrodes, for the ECL spectrum; and chemiluminescence was measured under acidic conditions with using magnesium metal as a strong reductant and potassium peroxydisulfate as a strong oxidant.  $\text{Ru}(\text{bpy})_2\text{L}_a^{2+}$  displays weaker PL than  $\text{Ru}(\text{bpy})_3^{2+}$  and the  $^3\text{MLCT}$  excitation maximum as well as the emission maximum are somewhat red shifted relative to the PL spectra of unaltered  $\text{Ru}(\text{bpy})_3^{2+}$  (Fig. 30). These findings are consistent with the observations of other researchers.<sup>221</sup>  $\text{Ru}(\text{bpy})_2\text{L}_b^{2+}$  has the lower excited state excitation maximum at even longer wavelengths. Thus, ethoxycarbonyl substituents have a stronger bathchromic effect in aqueous solution than does the carboxylate substituent.

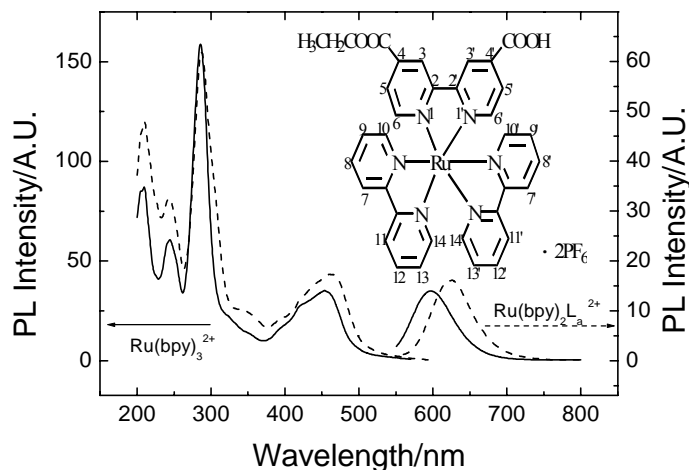


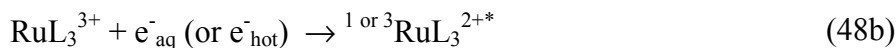
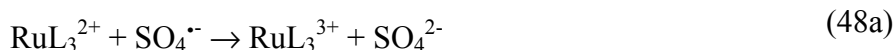
**Fig. 30** Uncorrected PL excitation and emission spectra of (a)  $\text{Ru}(\text{bpy})_3^{2+}$  (solid line) and (b)  $\text{Ru}(\text{bpy})_2\text{L}_a^{2+}$  (dashed line) complexes. Conditions: 0.05 M  $\text{Na}_2\text{B}_4\text{O}_7$ , pH 9.2,  $1 \times 10^{-5}$  M complexes, both slits 10 nm, (a) Excitation wavelength 455 nm and emission wavelength 597 nm. (b) Excitation wavelength 465 nm and emission wavelength 626 nm. Inset: the structure of the complex  $\text{Ru}(\text{bpy})_2\text{L}_a^{2+}$

Previous studies revealed that the redox properties of  $\text{RuL}_3^{2+}$  ( $\text{L} = 2,2'$ -bipyridine or substituted  $2,2'$ -bipyridine and the ligands can be identical or different) are affected by the molecular structure of the ligand.<sup>222</sup> The existence of polyethoxycarbonyl substituents at 4 and 4' positions of bipyridine moves the oxidation potential in a more positive direction and the first one-electron reduction potential in a less negative direction in comparison with unsubstituted  $\text{Ru}(\text{bpy})_3^{2+}$ .<sup>221</sup>  $\text{Ru}(\text{bpy})_2\text{L}_b^{2+}$  is oxidized at 0.14 V more positive potential (i.e. 1.38 vs. SCE) than  $\text{Ru}(\text{bpy})_3^{2+}$ , and the first one-electron reduction occurs at 0.34 V less negative potential (i.e., -0.93 V vs. SCE) in DMF.<sup>221</sup>

Since ligand structures of  $\text{L}_a$  and  $\text{L}_b$  are quite similar to that of  $\text{Ru}(\text{bpy})_3^{2+}$ , we assume that their redox potentials are close to that of  $\text{Ru}(\text{bpy})_3^{2+}$ . Thus,  $\text{Ru}(\text{bpy})_2\text{L}_a^{2+}$  and  $\text{Ru}(\text{bpy})_2\text{L}_b^{2+}$  are a bit easier to one-electron reduce and only slightly more difficult to one-electron oxidize than the unsubstituted  $\text{Ru}(\text{bpy})_3^{2+}$ . On the basis of a previous study<sup>172</sup>, a possible excitation pathway for  $\text{Ru}(\text{bpy})_2\text{L}_a^{2+}$  and  $\text{Ru}(\text{bpy})_2\text{L}_b^{2+}$  is a red-ox pathway:



Another possible excitation pathway, when peroxodisulfate ions are utilized as coreactant, is an ox-red excitation pathway.



Finally, an intersystem crossing takes place (49) followed by a radiative transition (50), or, if the  ${}^3\text{RuL}_3^{2+*}$  has earlier been directly formed, emission from  ${}^3\text{MLCT}$  excited state occurs without the need for an excited singlet state intermediate (50):



In addition, the cathodic ECL spectra of  $\text{Ru}(\text{bpy})_3^{2+}$  and  $\text{Ru}(\text{bpy})_2\text{L}_a^{2+}$  are similar to the corresponding PL spectra (Figs. 30 and 31). This suggests that the same excited states are induced by photo and the present electrochemical excitation methods.

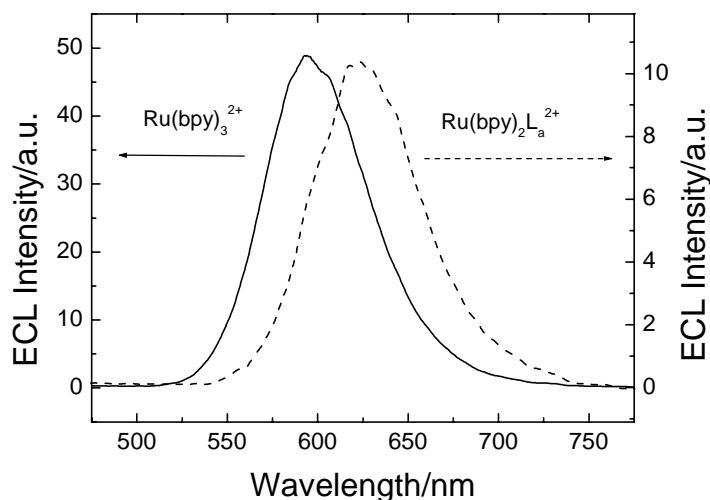


**Fig. 31** Uncorrected ECL spectra of  $1 \times 10^{-5}$  M  $\text{Ru}(\text{bpy})_3^{2+}$  (solid line) and  $1 \times 10^{-5}$  M  $\text{Ru}(\text{bpy})_2\text{L}_a^{2+}$  (dashed line) complexes measured with the same instrument. Conditions: as in Fig. 30 except solution contained 1.0 mmol/l  $\text{K}_2\text{S}_2\text{O}_8$  and emission slit 20 nm. Measured in bioluminescence mode, pulse charge 120  $\mu\text{C}$ , pulse frequency 100 Hz, pulse voltage  $-45$  V.

ECL of both  $\text{Ru}(\text{bpy})_2\text{L}_a^{2+}$  and  $\text{Ru}(\text{bpy})_2\text{L}_b^{2+}$  could be detected at oxide-covered aluminum with linear calibration curves spanning many orders of magnitude of concentration ( Fig. 32). At least  $\text{Ru}(\text{bpy})_2\text{L}_a^{2+}$  should be applicable as an ECL label. The red shift of the emission spectrum was relatively great for  $\text{Ru}(\text{bpy})_2\text{L}_b^{2+}$ , and  $\text{Ru}(\text{bpy})_2\text{L}_a^{2+}$  has a single exponential decay at oxide-coated n-silicon electrode with a long luminescence lifetime of 40.0  $\mu\text{s}$  (Fig. 33). The results of  $\text{Ru}(\text{bpy})_2\text{L}_b^{2+}$  would

have been much better if a red-sensitive detector and an appropriate optical filter had been available. Thus, it can also be detected with time-resolved ECL techniques when pulse excitation is applied.

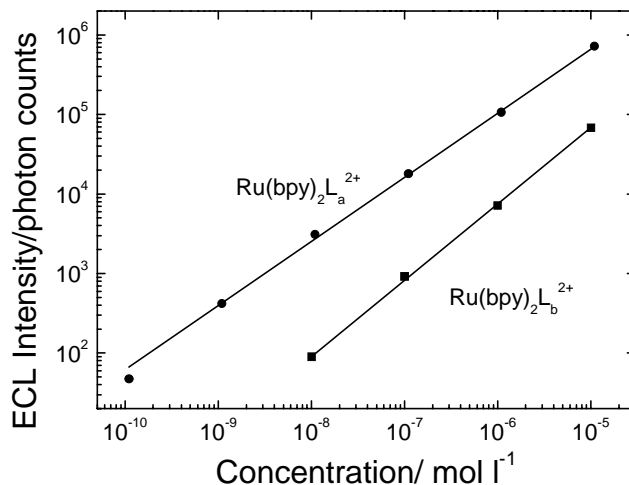


**Fig. 32** Calibration curves of  $\text{Ru}(\text{bpy})_2\text{L}_a^{2+}$  (●) and  $\text{Ru}(\text{bpy})_2\text{L}_b^{2+}$  (■) complexes. Conditions: as in Fig. 31 except pulse frequency was 20 Hz and measurements were carried out with photon counting electrochemiluminometer equipped with 620 nm interference filter. ECL was integrated over 500 excitation cycles.

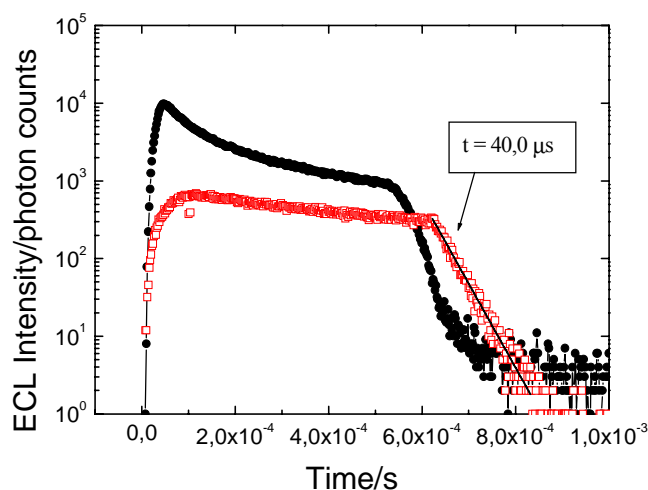


**Fig. 33** Rise and decay of  $1 \times 10^{-5}$  M  $\text{Ru}(\text{bpy})_2\text{L}_a^{2+}$  ECL pulse at oxide-coated aluminum and n-Si electrodes. Conditions: as in Fig. 32. Silicon dioxide film thickness 3.9 nm (□) and aluminum oxide film thickness about 2 nm (●).

According to previous studies,<sup>208, 213</sup> and analogously to aluminum, dissolution of magnesium in aqueous solution could be considered to lead to a highly reactive Mg/aqueous solution interface at which at least Mg,  $\text{Mg}^+$ , and atomic hydrogen might act as very strong reductants. Interestingly,  $\text{Ru}(\text{bpy})_2\text{L}_a^{2+}$  chelate exhibits strong CL (Fig. 34) at dissolving Mg/aqueous solution interface in the presence of peroxodisulfate ions under strongly acidic condition regardless of the type of acid

used. Peroxodisulfate ion appears to be a better oxidant than peroxodiphosphate in light generating pathways under these conditions.

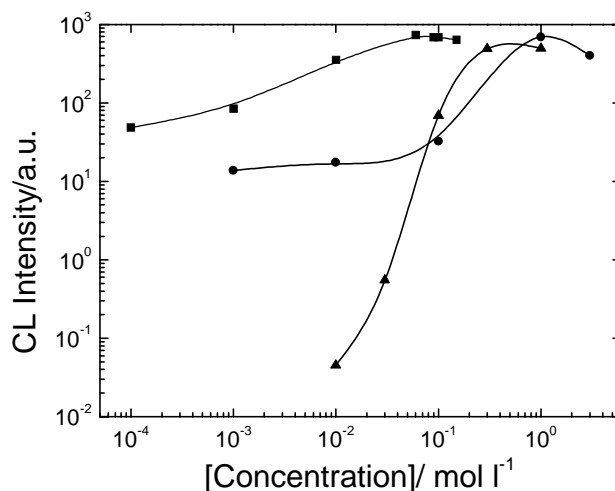


**Fig. 34** Chemiluminescence intensity of  $\text{Ru}(\text{bpy})_2\text{L}_a^{2+}$  as a function concentration of sulphuric acid ( $\blacktriangle$ ), hydrochloric acid ( $\bullet$ ) and potassium peroxodisulfate ( $\blacksquare$ ). Conditions:  $1 \times 10^{-6}$  M  $\text{Ru}(\text{bpy})_2\text{L}_a^{2+}$ , slit width 20 nm, emission monochromator at 600 nm (blue sensitive PMT), Perkin-Elmer LS 50B, integration time 200 s.

$\text{Ru}(\text{bpy})_2\text{L}_a^{2+}$  and  $\text{Ru}(\text{bpy})_2\text{L}_b^{2+}$  were cathodically electrochemiluminescent under the same experimental conditions as a simple  $\text{Ru}(\text{bpy})_3^{2+}$  chelate<sup>172</sup>. This observation suggests that immunoassays could be developed in which  $\text{Ru}(\text{bpy})_2\text{L}_a^{2+}$  is used as an electrochemiluminescent label, because it is not only electrochemiluminescent but also linkable with biomolecules. An immunoassay carried out on the surface of oxide-coated magnesium in basic conditions, followed by detection in highly acidic peroxodisulfate solutions, should also be possible.

## 6.4 Lanthanide chelates and their aromatic moieties

### 6.4.1 ECL of lanthanide chelates and their aromatic moieties

Cathodic time-resolved electrogenerated chemiluminescence (TR-ECL) of aromatic Tb(III) chelates at thin insulating film-coated electrodes can be exploited for the extremely sensitive detection of biologically or clinically interesting compounds in bioaffinity assays.<sup>49,51, 63,151,152,225</sup>

Eu(III) is another lanthanide(III) ion that after suitable chelation has sufficiently long luminescence lifetime for time-resolved detection based on photoluminescence<sup>176,224</sup>.



ECL of Eu(III) chelates has been studied and Eu(III) chelates have been used in binding assays.<sup>225</sup> The main drawback of these Eu(III) labels in practical analysis based on traditional electrochemical excitation methods is that fully aqueous solutions cannot be used, and the luminescence quantum yields of Eu(III) labels are very poor even in nonaqueous solutions.<sup>225</sup>

Both Tb(III) and Eu(III) ions have excellent luminescence properties, but their redox properties are quite different. Tb(III) ion is extremely difficult to one-electron reduce or oxidize ( $E^{\circ}(\text{Tb}^{3+}/\text{Tb}^{2+}) = -3.7 \text{ V vs. SHE}$ ,  $E^{\circ}(\text{Tb}^{4+}/\text{Tb}^{3+}) = 3.1 \text{ V vs. SHE}$ )<sup>226</sup>. Eu(III) ion, in turn, is one of the most difficult ions in the lanthanide series ( $E^{\circ}(\text{Eu}^{4+}/\text{Eu}^{3+}) = 6.4 \text{ V vs. SHE}$ ) to oxidize,<sup>226</sup> but it is easiest to reduce ( $E^{\circ}(\text{Eu}^{3+}/\text{Eu}^{2+}) = -0.35 \text{ V vs. SHE}$ ).<sup>226</sup>

Analogously, aromatic Tb(III) chelates show CL and ECL in aqueous solution via a “ligand-sensitization” route.<sup>54,58</sup> After redox excitation, the ligand transfers its excitation energy intramolecularly to the central ion,<sup>176,224</sup> and finally the central ion emits light by transitions from the lowest excited state multiplet to the ground state multiplet.<sup>176,224</sup> The whole process requires that (i) the triplet state of the ligand is somewhat higher in energy than the resonance level of the lanthanide(III) ion, (ii) the triplet state of the ligand does not react with the central ion by a rapid redox reaction, and (iii) the emitting central ion does not react with the ligand.<sup>176,224,164</sup> These prerequisites are often easily fulfilled for redox-inert Tb(III) ion, but not necessarily for Eu(III) ion. The optimal conditions for the Eu(III) centered ECL were studied in paper VIII. The molecular structures for ligand **1** and ligand **2** are shown in Fig. 35.

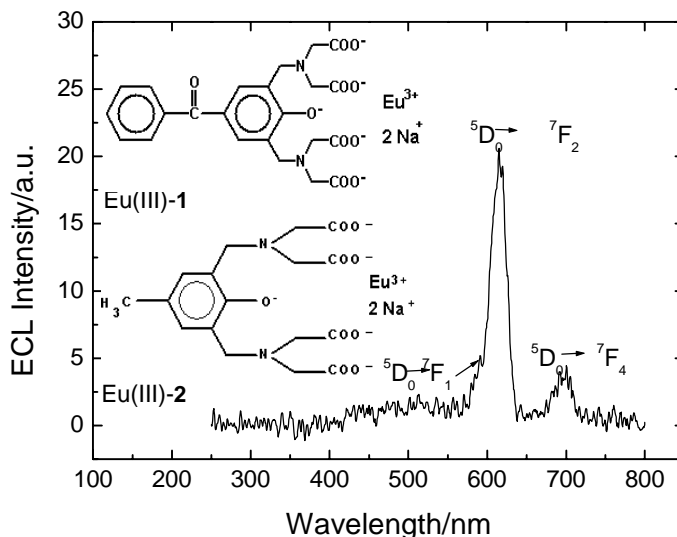


**Fig. 35** The structures of the ligands used and the ECL spectra of Eu(III)-1. Conditions: oxide-covered Al-plate working electrode, Pt-wire counter electrode, coulostatic pulse generator, applied pulse voltage  $-40$  V, pulse frequency 80 Hz, pulse charge  $200 \mu\text{C}$ ,  $0.2$  M boric acid buffer at pH 9.2,  $1.0 \times 10^{-3}$  M Eu(III)-1,  $3.0 \times 10^{-3}$  M  $\text{K}_2\text{S}_2\text{O}_8$ , Perkin-Elmer LS-5, emission slit 20 nm.

Comparing of the ECL signals of Eu(III)-1 and Eu(III)-2 with those of the corresponding Tb(III) and Gd(III) chelates showed that Eu(III)-1 cannot emit as intensely as Tb(III)-1 and Gd(III)-1 in the absence of peroxydisulfate, and Eu(III)-2 does not give any measurable ECL, although Gd(III)-2 and Tb(III)-2 show strong emission<sup>225</sup> under similar conditions. Eu(III)-2 is not photoluminescent either. Thus, it seems that the gap between the triplet state energy level of ligand 2 and the energy-accepting level of Eu(III) is too great for Eu(III)-2 to be used as either a photoluminescent or an electrochemiluminescent label.

The addition of peroxydisulfate ions as cathodic coreactants to the solution of Eu(III)-1 resulted in a strong enhancement of ECL, and a clear Eu(III) emission could be measured (Fig. 35). In addition, peroxydisulfate concentration affects the luminescence lifetime (Fig. 36). An appropriate concentration of peroxydisulfate ion increased the luminescence lifetime considerably, causing the decay to be dominated by a single long-lived component with luminescence lifetime of ca. 0.94 ms.

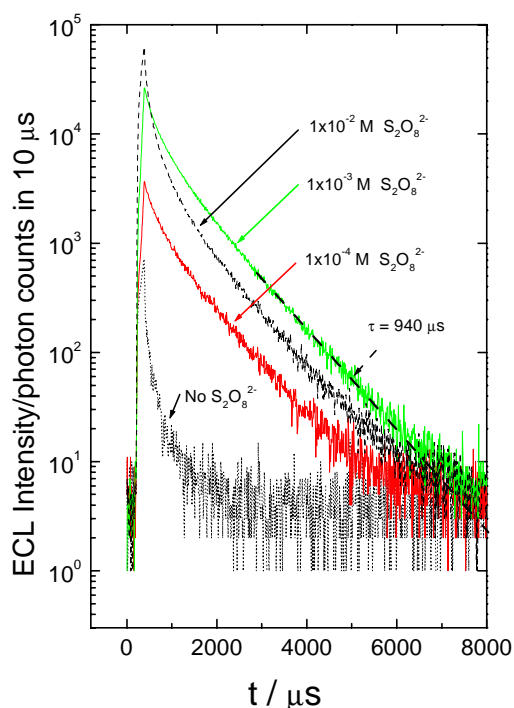


**Fig. 36** ECL time spectra of Eu(III)-1 in the presence of varied concentrations of peroxodisulfate ions. Conditions: oxide-covered Al-cup working electrode, Pt-wire counter electrode, Pine Instruments RD4 potentiostat, applied pulse voltage  $-10$  V, pulse frequency 100 Hz, pulse time 200  $\mu$ s, 10000 excitation pulses, 0.05 M sodium tetraborate buffer adjusted to pH 7.8 with sulfuric acid,  $1.0 \times 10^{-4}$  M Eu(III)-1. The light emission was registered by a MCS-II scaler card attached to a PC computer, with 600-nm long pass filter.

Study of the effects of hydrated electron and sulfate radical scavengers provided indirect support for the existence of hydrated electron as a cathodic mediator in the Eu(III) system (Fig. 37). Fast hydrated electron scavengers, such as  $\text{Co}(\text{NH}_3)_6^{3+}$  complexes, strongly quenched the ECL of the Eu(III)-1- $\text{S}_2\text{O}_8^{2-}$  system. And so did, fast sulfate radical scavengers (which are unreactive towards hydrated electrons), azide ions, for example. None of the oxidizing secondary radicals formed was observed to be a significantly better oxidant for the Eu(III) chelate system than sulfate radical. An efficient oxidant for the present system must have standard reduction potential, preferably at least 1.9 V vs. SHE.

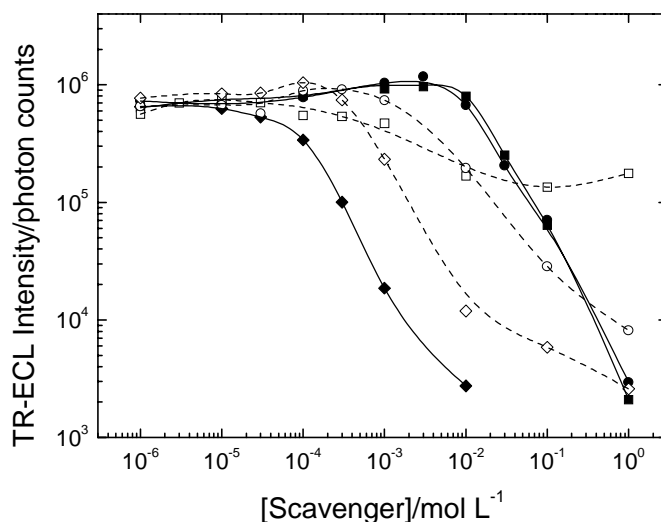
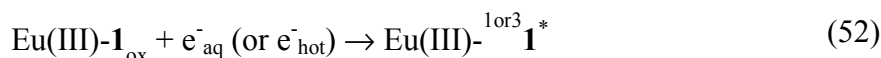
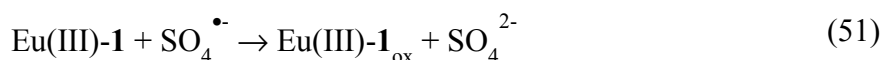
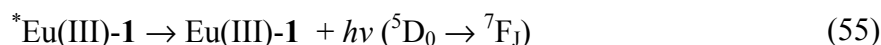


**Fig. 37** Quenching effects of added hydrated electron scavengers ( $\text{NO}_3^-$ , ■), ( $\text{H}_2\text{O}_2$ , ●), ( $\text{Co}(\text{NH}_3)_6^{3+}$ , ◆) and sulfate radical scavengers ( $\text{Cl}^-$ , □), ( $\text{Br}^-$ , ○), ( $\text{N}_3^-$ , ◇). Conditions: oxide-covered Al-cup working electrode, Pt-wire counter electrode, coulometric pulse generator, applied pulse voltage  $-40$  V, pulse frequency 20 Hz, pulse charge  $120 \mu\text{C}$ ,  $0.2$  M boric acid buffer at pH 9.2, long-pass filter with 600-nm cut off wavelength, delay and gate times were  $50 \mu\text{s}$  and  $2$  ms, (c) 12-spike Al-rake electrode, pulse time  $240 \mu\text{s}$ , pulse voltage  $-10$  V, delay time  $10 \mu\text{s}$  and gate time  $2.5$  ms,  $0.05$  M  $\text{Na}_2\text{B}_4\text{O}_7$  buffer adjusted to pH 7.8 with sulphuric acid, the concentrations of Eu(III)-1 and peroxodisulfate ion were  $1 \times 10^{-4}$  and  $1 \times 10^{-3}$  mol/L, respectively.

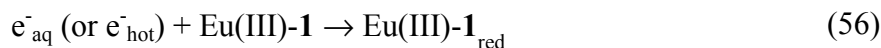
Eu(III) cannot be oxidized in aqueous solutions,<sup>226</sup> not even by sulfate radical, but sulfate radical can oxidize e.g. phenoxides at near diffusion-controlled rate.<sup>207</sup> Drawing from previous study of Tb(III) chelates,<sup>48,54,160,225</sup> we propose the ox-red excitation pathway<sup>54,225</sup> for Eu(III)-1 by taking account of the property of the ligand **1**<sup>164</sup>. Thus, ligand **1** containing the phenoxide moiety is rapidly oxidized by sulfate radical (eq. 51);<sup>45,58,160</sup> which is followed by a rapid reduction of the oxidized ligand radical  $\mathbf{1}_{\text{ox}}$  by either a hydrated or hot electron (eq. 52).



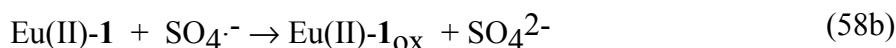
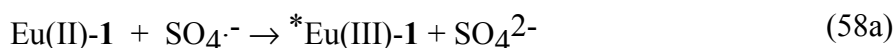
Finally the energy is transferred from the triplet state of the ligand to the resonance level  $^5\text{D}_0$  of Eu(III) at 2.1 eV (54), which emits light according to eq. 55:



In view of the easy reducibility of Eu(III) ion,<sup>226</sup> a direct reduction of Eu(III) should be considered. It is highly probable, moreover, that the one-electron reduced ligand **1**<sub>red</sub> formed by hydrated electrons<sup>54,225</sup> can reduce the central ion in the case of Eu(III). The following reactions are then possible:



After step (57), cathodically generated sulfate radical may directly oxidize Eu(II) ion to Eu(III) in its excited state (58a), which then emits according to (55), or it may one-electron oxidize the ligand (58b). The former possibility requires the electron transfer over a rather high energy gap, however, which, might mean a fairly slow reaction if Marcus's electron transfer theory is obeyed and the inverted region exists.



During the cathodic pulse, F-center luminescence emission peaks at 420 nm (2.95 eV)<sup>53,227</sup>, and possibly transfers energy to Eu(III) at close proximity to the surface, and the high-energy tail of the emission band may induce even weak Eu(III)-**1** excitation via the ligand. However, we suggest that the ox-red excitation pathway is the predominant pathway for generation of excited chelates in the Eu(III)-**1**-S<sub>2</sub>O<sub>8</sub><sup>2-</sup> system.

Eu(III)-**1** can be linked with antibodies and other proteins, e.g., via a thioureido group, as described elsewhere.<sup>51,228</sup> Eu(III)-**1** is the second choice for ECL labels with long luminescence lifetime at tunnel emission electrodes, together with some metalloporphyrins<sup>62</sup>, and various short-lived ECL-emitting organic luminophores, which can be efficiently excited under similar conditions.<sup>60,171,172</sup> In all these systems it is possible to obtain inner standardization or multiparameter analysis with multiple labels, not only on the basis of wavelength discrimination but also on the basis of time-resolution. These discrimination methods can be combined. An experiment, in

which the well-known luminescent label fluorescein isothiocyanate (FITC) and Eu(III)-1 isothiocyanate are excited simultaneously, is shown in Fig. 38.

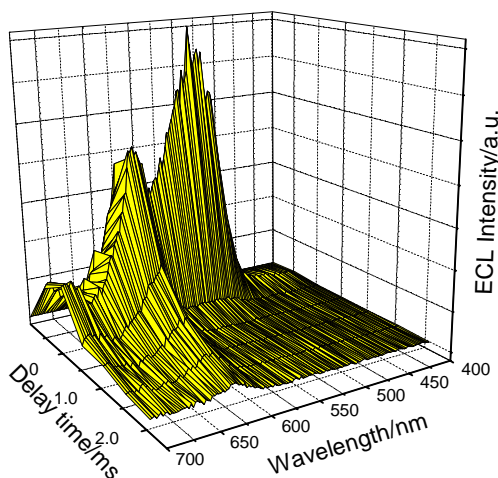
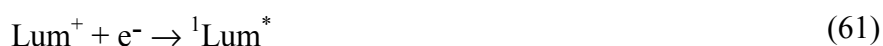


**Fig. 38** Simultaneous excitation of FITC and Eu(III)-1-NCS. Conditions: as in Fig.37. Time-resolved spectra were measured with an instrument having relatively good sensitivity but poor resolution.

For ECL of aromatic lanthanide chelate systems induced by cathodic pulse polarization of C/I/E junction electrodes, the excitation is initiated by intramolecular energy transfer from the excited aromatic ligands, followed by the emission of light from the central lanthanide ions.<sup>45</sup> Since the excited aromatic ligands play a crucial role, we studied features of ECL of typical aromatic moieties of our ECL-active Tb(III) chelates at cathodically pulse-polarized C/I/E junction electrodes (paper IX).

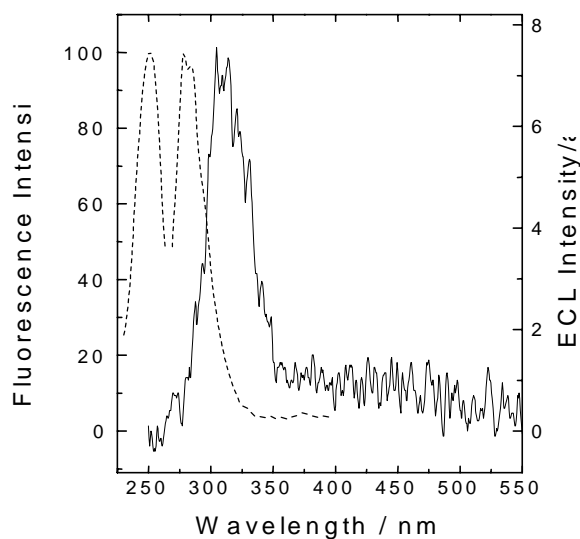
It has long been known that solid solutions of simple benzenoids produce recombination fluorescence and recombination phosphorescence during and after high energy irradiation via the following excitation pathway:<sup>229</sup>



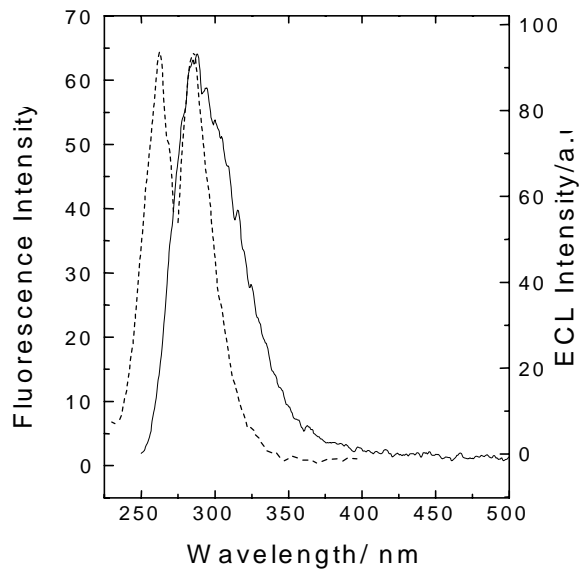
Generally, the  ${}^3\text{Lum}^* / {}^1\text{Lum}^*$  ratio is roughly 3:1.<sup>229</sup> Analogous processes can be observed by generating luminophore cation radicals from simple aromatics with

reductively produced sulfate radicals during injection of hot electrons into aqueous electrolyte solutions.

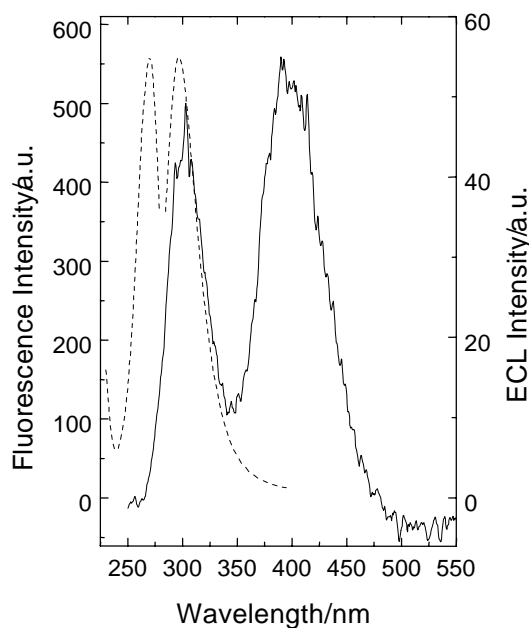
In measurements of fluorescence and ECL spectra of benzene, toluene, phenol and p-cresol, benzene was exceptional in showing weak ECL in the presence of peroxydisulfate ions, in total contrast to its molecular fluorescence. The emission, at 310 nm, is possibly a singlet state excimer emission, implying that the emitting molecule is not benzene at all (Fig. 39). The high instability of anion and cation radicals of benzene in water might explain the weak ECL of benzene.<sup>212</sup> Toluene, phenol, and p-cresol, in turn, exhibit both singlet and triplet state ECL emissions during cathodic pulse polarization of oxide-covered aluminum electrodes in the presence of peroxydisulfate ions (Figs. 42, 43, and 44). Aniline has a low ECL efficiency, probably due to its oxidation-initiated polymerization in peroxydisulfate solutions.



**Fig. 39** Fluorescence excitation and emission (dashed lines) and ECL (solid lines) spectra of aqueous solutions/emulsions of benzene. Conditions: 0.2 M boric acid buffer at pH 9.2,  $3 \times 10^{-3}$  M  $K_2S_2O_8$  (ECL measurements), fluorescence excitation and emission spectra were measured with 2.5 nm excitation and emission slits and ECL measurements with 20 nm emission slits, coulometric pulse generator, pulse charge 200  $\mu$ C, pulse voltage  $-40$  V, pulse frequency 80 Hz, monochromator scanning speed 240 nm/min, concentration of benzene in ECL measurements was  $1 \times 10^{-3}$  M.

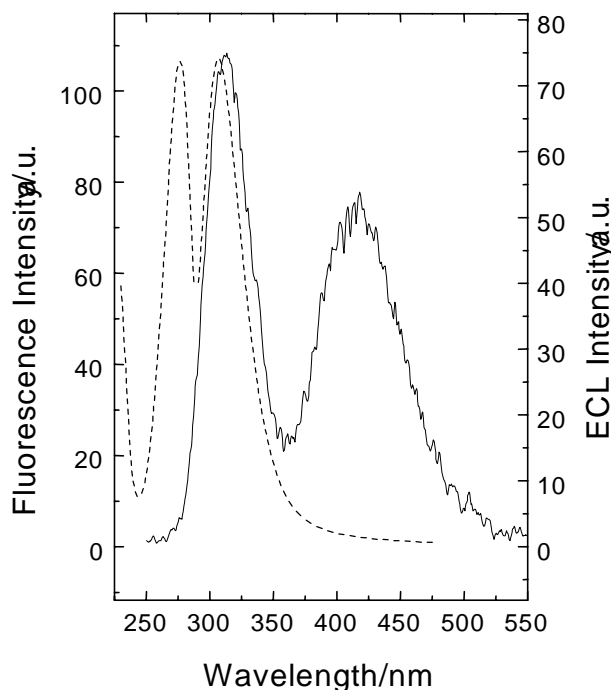


**Fig. 40** Fluorescence excitation and emission (dashed lines) and ECL (solid lines) spectra of aqueous solutions/emulsions of toluene. Conditions as in Fig. 39 and toluene concentration was  $1 \times 10^{-4}$  M in FL and  $7 \times 10^{-4}$  M in ECL measurements..



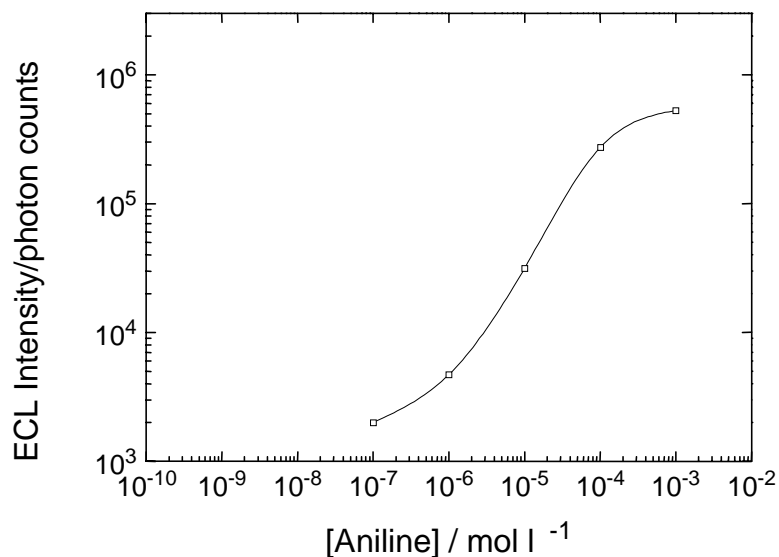
**Fig. 41** Fluorescence excitation and emission (dashed lines) and ECL (solid lines) spectra of aqueous solutions of phenol. Conditions as in Fig. 39 except excitation and emission slits in fluorescence measurements were 15 and 10 nm, respectively. Concentration of phenol was  $1 \times 10^{-4}$  M in both FL and ECL measurements.





**Fig. 42** Fluorescence excitation and emission (dashed lines) and ECL (solid lines) spectra of aqueous solutions of p-cresol. Conditions as in Fig. 41. Concentration of p-cresol was  $1 \times 10^{-4}$  M in both FL and ECL measurements.

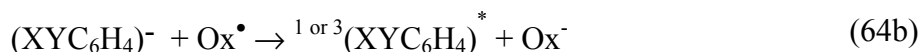
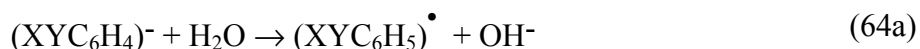
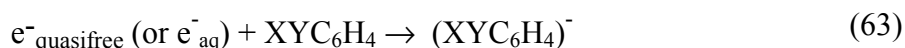
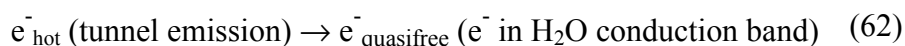
It is worth noting that no ECL of these simple aromatics was observed in the absence of peroxodisulfate ions, although lanthanide (III) chelates containing phenoxide ion as their aromatic moiety are efficiently excited when hydroxyl radical is the oxidizing species in the chemiluminescence system.<sup>45,60,150,230</sup> As an exception, aniline shows a better linear response and calibration curve in the presence of hydrogen peroxide ( $\text{H}_2\text{O}_2$ ) and azide ( $\text{NaN}_3$ ) than in the presence of peroxodisulfate (Fig. 43). In this system, hydroxyl radical is first generated by one-electron reduction of hydrogen peroxide and subsequently converted to azide radical by added azide ions. Azide radical is an efficient one-electron oxidant almost without the side reactions common to hydroxyl radical. Thus aniline ECL response is much better in the presence of azide ion than without it.

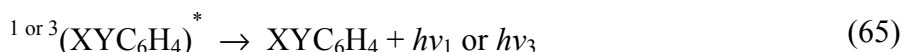


**Fig. 43** Calibration curve of aniline in the presence of  $1 \times 10^{-3}$  M  $\text{H}_2\text{O}_2$  and  $\text{NaN}_3$ . Measured with a photon counter using a filter composed by a Corning 5970 UV-filter and saturated  $\text{NiSO}_4$  solution in 1-cm quartz cuvette resulting in a band-pass filter peaking at 330 nm (3.8 eV) with maximum transmittance 45 % and the half width of the transmission band ca. 35 nm.

In view of the effect of hydrated electron scavengers on the ECL of these aromatics, and the energy diagram of the studied ECL system, the ECL excitation pathways of aromatics in aqueous solutions and emulsions based on redox reactions can be divided into two main routes. Again, these routes involve one-electron reduction or oxidation of the aromatics to a radical species followed by one-electron oxidation or reduction to the original oxidation state so that the aromatic is in its excited state. The redox properties of the aromatic radicals produced in the first step of the excitation pathway (reactions (63), (68) below) and the oxidant/reductant of the second step determine whether the excitation is energetically possible or not. If the enthalpy change in the second step is not sufficiently high, only a ground-state product is formed. Another important point for the predominance of the Red-Ox or the Ox-Red excitation pathway is the stability of the radical formed in the first step.

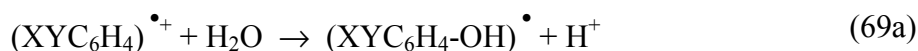
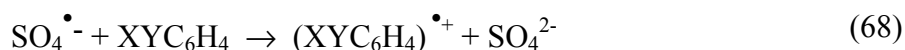
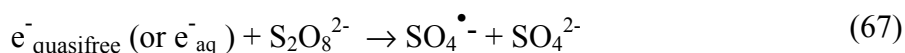
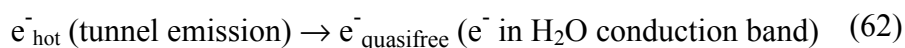
(Red-Ox) pathway with  $\text{Ox}^\bullet$  as a strongly oxidizing radical is obviously as follows:



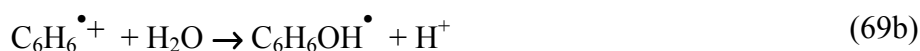


With simple derivatives of benzene, step (64a) is so fast that the anion radical of step (63) has never been reliably observed.<sup>231,232</sup> This means that the Red-Ox excitation pathway is usually blocked by production of cyclohexadienyl-type (CHD-type) radicals by extremely rapid protonation of the formed anion radicals. CHD-type radicals are only weakly reducing and tend to disproportionate and combine, thus being very poor stepping stones for redox luminescence. However, if X or Y is, for example, e.g. benzoyl group, the anion radical may be much more stable and Red-Ox excitation pathway may become important.

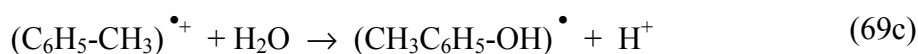
The oxidation-initiated reductive excitation pathway is presented with sulfate radical as oxidant:



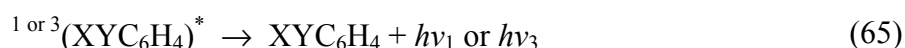
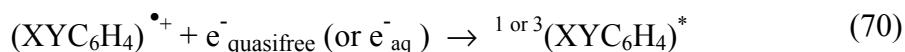
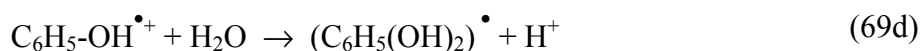
-if X = H and Y = H:



-if X = H and Y = CH<sub>3</sub>:



-if X = H and Y = OH:



Where hydroxyl radical is the oxidant, it always reacts by addition to aromatic rings, and oxidation reaction occurs only if the ring contains electron-donating substituents that assist elimination of hydroxide ion or water.<sup>212</sup> The detailed reactions of the

pathway are presented in paper IX. The properties of the formed hydroxycyclohexadienyl-type (HCHD-type) radicals closely resemble those of CHD-type radicals, and they, too, are poor stepping stones for redox luminescence. Disproportionation and combination of HCHD-type radicals result in production of phenols and derivatives of biphenyl.

In summary, the results show that, in aqueous solutions or emulsions, benzene and its simple aromatic derivatives (toluene, phenol, p-cresol, aniline) emit ECL in the presence of peroxodisulfate, while aniline emits ECL in the presence of azide and hydrogen peroxide. The results also strongly suggest that these simple aromatics, which cannot be oxidized by hydroxyl radical, exhibit ECL only by oxidation-initiated reductive excitation (Ox-Red) route.

#### **6.4.2 Chemiluminescence of Tb(III) chelates induced at aluminum surface in alkaline aqueous solution**

As mentioned in §6.3. the reactive Al/OH-(aq) –interface can be used as a source of chemical energy in the generation of chemiluminescence. It has also been suggested that  $Al^0$ ,  $Al^+$ ,  $Al^{2+}$ , hydrogen atoms, and hydrated electron (in highly alkaline condition) are simultaneously present in solution and act as reductants during dissolution of aluminum metal in alkaline aqueous solution.<sup>208,233,234</sup> Therefore, CL can be generated from compounds that are excited in redox reactions, either in reducing conditions or in a medium that simultaneously contains strongly oxidizing and reducing species.

We have shown very recently elsewhere<sup>235</sup> that aromatic Tb(III) and Eu(III) chelates generate CL during the dissolution of aluminum in alkaline peroxodisulfate solutions. Most of the experiments were carried out with a Tb(III) chelate having a benzophenone as its aromatic backbone because this gave highest CL intensity in the presence of strongly alkaline peroxodisulfate ions.

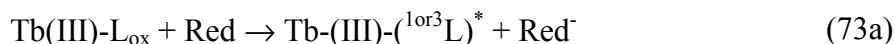
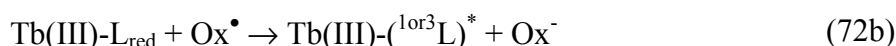
If dissolved oxygen is present in the solution and hydrated electrons or other suitable one-electron donors are present as well, oxyradicals could be generated and consumed as in eqs. (19)-(22) (see §6.1.) at pH 14:

If peroxodisulfate ions are added to the solution, oxidants even stronger than oxyradicals ( $E^\circ(\text{SO}_4^{\bullet-}/\text{SO}_4^{2-}) = 3.4 \text{ V vs. SHE}^{206}$ ) are rapidly generated by monoelectronic reduction<sup>163</sup>:



It is worth noting that atomic hydrogen reduces peroxodisulfate ions relatively slowly ( $k = 2.5 \times 10^7 \text{ l mol}^{-1} \text{ s}^{-1}$ ),<sup>207</sup> and sulfate radical oxidizes water sluggishly ( $k = 60 \text{ l mol}^{-1} \text{ s}^{-1}$ ).<sup>207</sup> The relative stability of sulfate radical thus makes it a usable oxidizing radical in aqueous solutions, even in basic solutions. Its reductive production mediated by hydrated electrons is 400-fold faster than the reductive production mediated by atomic hydrogen<sup>207</sup>.

Briefly, reducing species are produced by the dissolution of aluminum in aqueous alkali hydroxide (denoted by Red in equations 72a and 73b). Oxidizing radicals (denoted by  $\text{Ox}^\bullet$ ), can be produced from peroxodisulfate ion by one-electron reduction, or from dissolved oxygen. Redox luminescence pathways, reduction-initiated oxidation pathways (72a-72b) or oxidation-initiated reduction pathways (73a-73b), are proposed as follows:



In summary, dissolution of aluminum in an aqueous peroxodisulfate solution induces chemiluminescence of some aromatic Tb(III) chelates, although the detectability of these chelates is poorer than that of luminol<sup>208</sup>. Use of the chelates is simpler, however, and they might be useful for some special purposes. In principle, immunoassays can be carried out on the surface of aluminum cups; for the detection step, alkaline peroxodisulfate solution is added and the excited CL of labels is measured. The Tb(III) chelate can also be used for monitoring peroxodisulfate

concentration and for rough determination of aluminum oxide film thicknesses. More generally, the highly reactive  $\text{Al}/\text{OH}^-$ ,  $\text{Al}^0$ ,  $\text{Al}^+$ ,  $\text{Al}^{2+}$ ,  $\text{H}^\bullet$ ,  $\text{e}^-_{\text{aq}}$ -interface may be useful wherever extremely strong reductants in aqueous solution are required<sup>235</sup>.

## 6.5 Immunoassays using ECL labels

The field of immunoassay technology continues to grow although the first use of the principle of competitive inhibition of labeled antigen to antibody was reported as long ago as 1959<sup>236</sup>. Considerable interest has been shown in the use of CL and ECL luminophores as labels in immunoassays and DNA assays<sup>65</sup>. Electrochemiluminescent labels not only possess the same advantages as photoluminescent labels (long shelf life of reagents, no interference with biological compounds, wide dynamic range, high sensitivity), but they also have additional advantages. For instance, the excitation can be achieved with much cheaper instrumentation, and no excitation optics are needed, which should prove very useful in future microanalytical systems. Two applications are reported below.

### 6.5.1 Competitive immunoassay of thyroxine

A homogeneous competitive electrochemiluminoimmunoassay (ECLIA) of thyroxine (T4) was developed on the basis of hot electron electrochemistry<sup>51,54,68,237</sup> (Paper X). In this ECLIA, T4 was first bound to gelatine and after a separation step labeled with Tb-chelate  $(\text{Tb}^{3+}\text{-}N^1\text{-(4-isothiocyanatobenzyl)diethylenetriamine-}N^1,N^2,N^3,N^3\text{-tetraacetate})$  at molar ratio of 1:200. Oxide-covered aluminum electrode coated with antibodies (rabbit immunoglobulins to mouse immunoglobulins) was employed as the working electrode. In a microtiter well, coated aluminum electrode was immersed in a solution containing monoclonal antibody to T4, gelatin-T4-Tb conjugate, and unlabeled standards. After 1 h incubation the ECL signal was measured with a time-resolved electroluminometer.

The ECL dynamic regions of two different free Tb(III) chelate labels were measured in a similar medium to that for heterogeneous immunoassay (Fig. 44). Previous studies<sup>225,238</sup> indicate that Tb(III) chelates are excited by a ligand-sensitized mechanism in which the ligand is first excited by successive one-electron redox steps,

followed by energy transfer to the central ion, and finally emission occurs by  $^5D_4 \rightarrow ^7F_J$  irradiative transitions<sup>238</sup>. The results showed that Tb(III) chelated by 2,6-bis[*N,N*-bis(carboxymethyl)aminomethyl]-4-methylphenol display considerable stronger ECL intensity than the other chelate tested, which is probably mainly due to the shorter energy transfer distance from the aromatic moiety of the ligand to the central ion.

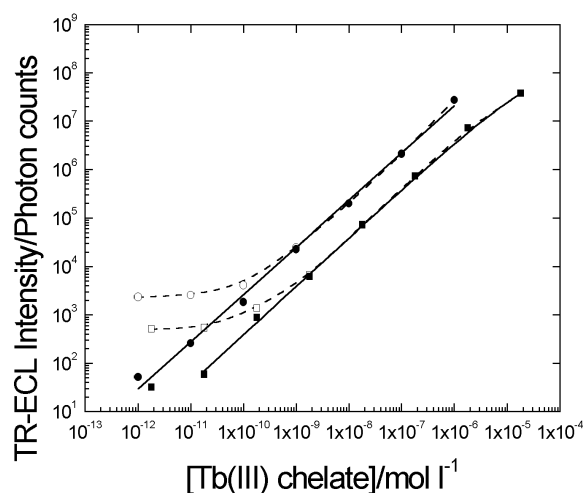


**Fig. 44.** Calibration curves of Tb(III) label chelates. (●)  $Tb^{3+}$ -2,6-bis[*N,N*-bis(carboxymethyl)aminomethyl]-4-methylphenol, (■)  $Tb^{3+}$ - $N^1$ -(*p*-isothiocyanatobenzyl)-diethylene triamine- $N^1, N^2, N^3, N^3$ -tetra acetate. Conditions: 0.2 Mborate buffer, pH 7.75, 0.1% NaN<sub>3</sub>, pulse amplitude-10 V, delay time 50  $\mu$ s, pulse time 240  $\mu$ s. Open circles and squares denote the signal before subtracting the blank.

In the hot electron electrochemistry method, presolvated hot electrons injected into aqueous electrolyte (or subsequently formed hydrated electrons) can reach reducible molecules only at a distance of up to about 200 nm from the oxide film/electrolyte interface. Hence, washing of the unreacted labels away from the assay cell should not be necessary because the amount of the label collected on the electrode surface is mainly a consequence of an immunochemical binding if the assay has reached equilibrium or is close to equilibrium. I.e. the unbound labeled antigens are evenly distributed in the solution and not enriched at the surface of the electrode. A calibration curve of T4 was obtained in 200- $\mu$ l volumes with shaking during incubation in the optimal assay buffer (Fig. 45).

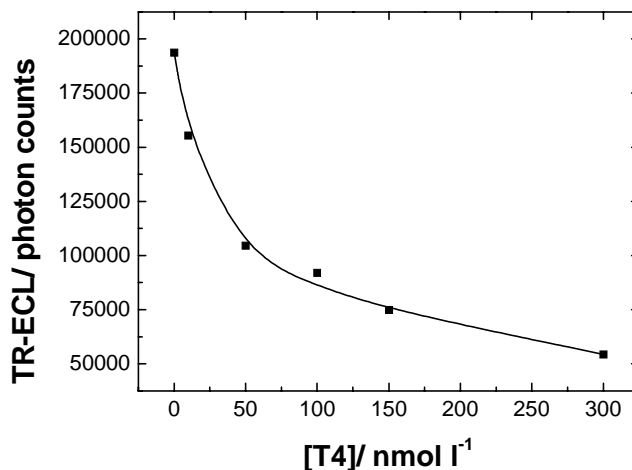


Fig. 45. Calibration curve of homogeneous T4 assay. Conditions: 0.2 M borate buffer, pH 7.75, 0.1 % NaN<sub>3</sub>, bovine gammaglobulin 0.05 %, 0.5 % BSA, Tween 40 0.01 %. Otherwise as in Fig. 44.

### 6.5.2 Non-competitive immunoassay of hTSH

An immunometric sandwich assay for human thyroid stimulating hormone (hTSH) was developed on the basis of hot electron electrochemistry. Briefly, the procedure was as follows: Electrodes were coated with antibody (clone 8661, specific to the alpha chain of hTSH) by physical adsorption. Monoclonal antibody specific to the  $\beta$ -chain of hTSH (clone 5404) was labeled with Tb<sup>3+</sup>-N<sup>1</sup>-(*p*-isothiocyanatobenzyl)-diethylene triamine-N<sup>1</sup>, N<sup>2</sup>, N<sup>3</sup>, N<sup>3</sup>-tetra acetate by allowing the antibody to react with the chelate in molar ratio 1:60 at pH 9.5. Both homogeneous and heterogeneous immunoassays were applied for hTSh.

The signal was considerably weaker in homogeneous assays than in heterogeneous assays (paper X). This is due to the primary radical scavenging effect of proteins (bovine serum albumin, bovine gammaglobulin).<sup>151</sup> However, the correlation with IRMA was still reasonably good ( $r = 0.989$ ,  $n = 6$ , Fig. 46).



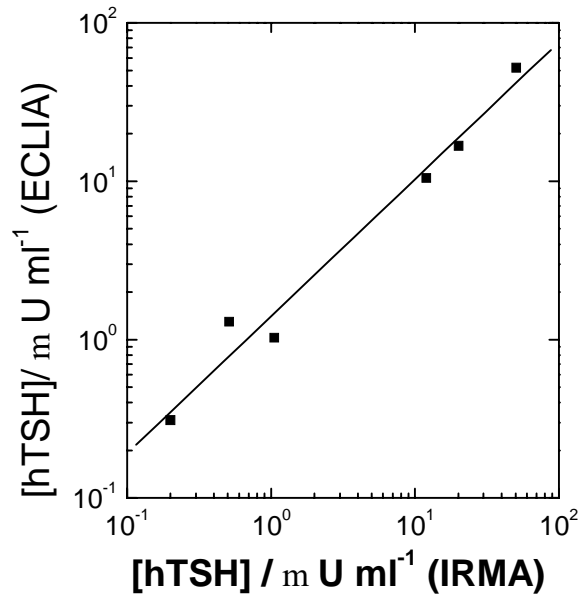


**Fig. 46.** Correlation between hTSH values obtained in homogeneous ECLIA assays and IRMA. Immunoradiometric assays were carried out with Orion Diagnostica IRMA kits (Turku, Finland).

Human TSH was also determined by heterogeneous assays using real patient samples. Fig. 47 displays the calibration curve of standards and Fig. 48 shows the comparison of heterogeneous ECLIA assays and IRMA assays ( $r = 0.977$ ,  $n = 38$ ). The two methods give similar results at higher concentrations, but with a larger deviation at low concentrations.

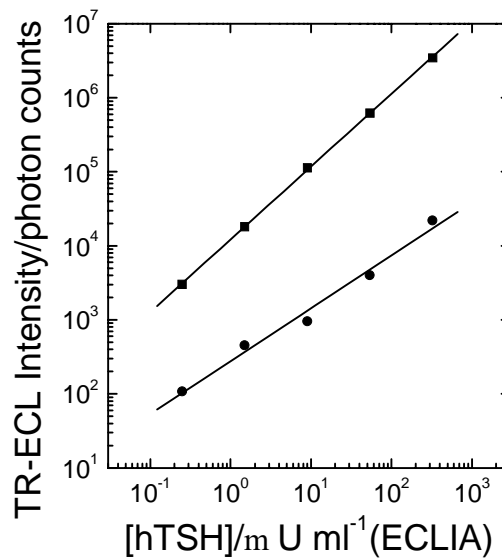


**Fig. 47.** Calibration curves of (a) homogeneous hTSH assay (●) and (b) heterogeneous hTSH assay (■). (a) Conditions: as in Fig. 45 and (b) Conditions: as in Fig. 44.

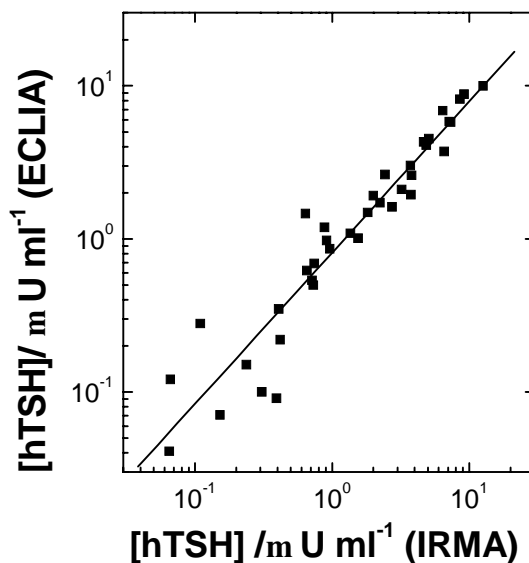


Fig.48. Correlation between hTSH values obtained in heterogeneous ECLIA assays and IRMA.

It is assumed that replacing the working electrodes with oxide-covered silicon electrodes would improve the performance of the ECLIA. This work is in the process in our laboratory. The RSD might be decreased because of the better insulating film coverage on silicon electrode, and incubation time might be decreased by elevating the incubation temperature, which would not be possible for thin aluminum oxide film-covered electrodes because thin aluminum oxide films are unstable in weakly basic conditions at higher temperatures than room temperature.

## 7. Conclusions

Since the first detailed studies in the mid-1960s, ECL methods have become useful and also commercially exploitable techniques in some areas of analytical chemistry. ECL has important advantages over traditional CL because the reagents needed for triggering it can be produced *in situ*, and unstable intermediates can be generated at the electrode and detected simultaneously. The excitation step is low-cost since there is no need for expensive laser or other excitation sources and optics. Construction of small-sized analyzers is thus relatively easy.

The hot electron-induced chemiluminescence method used in this work is a valuable complement to the conventional ECL techniques. It is of greater technical simplicity

for certain applications, such as for low-cost, single-use cells, e.g. for point-of-care or physician's office analysis. High amplitude cathodic pulse polarization of thin oxide film-coated electrodes offers a wider potential window for redox reactions of luminophores than do conventional ECL methods, in which an aqueous solution restricts the usable potential window to a quite narrow range at active metal electrodes. Many luminophores that cannot be excited at active metal electrodes in aqueous solution can be excited at oxide-covered electrodes. Furthermore, the ECL methods described here allow parallel excitation of a variety of luminescent labels with different luminescence lifetimes and emission wavelengths. Both wavelength and time discrimination can be utilized in the separation of the signals produced by different labels. Multi-component analysis and internal standardization become possible on the basis of the present ECL method.

Another striking merit of the hot electron-induced ECL excitation method is that it provides the basis for time-resolved measurements. Thus, novel types of immunoassays and DNA-probe assays can be developed in which time-resolution and wavelength discrimination can be combined for the simultaneous detection of several different labels. The parameter demanding highest sensitivity should be preferentially labeled with long-lived luminescence-displaying Tb(III) chelates, while the other parameters can be labeled with organic luminophores,<sup>60,62</sup> or transition metal chelate<sup>172</sup> or a Eu(III) label.

Although many organic compounds exhibit excellent ECL properties in organic solvents in conventional ECL conditions, they require rigorously purified and deoxygenated nonaqueous solvents. An aqueous medium is essential for immunoassays. Many organic luminophores with distinctive emission properties can be used in connection with the present ECL method in aqueous medium. The presented work thus widens the choice of electrochemiluminescent labels in immunoassays.

All of the presently studied label molecules, except luminol, seem most efficiently to be excited by a route in which the label is first one-electron oxidized or reduced, and the resulting radical is then immediately reduced or oxidized by the primary or secondary radicals of the system. The long-lived ECL emission of luminol is

interesting, but still much more work is required before the emission mechanism is untangled. On the basis of the results obtained with Rhodamine B (paper III) and fluorescein (paper VIII) xanthen dyes in general can be suggested to be worthy of further studies.

**References:**

1. A.K. Campbell (Ed.), *Chemiluminescence: Principles and Applications in Biology and Medicine*, VCH Verlagsgesellschaft, Ellis Horwood, Chichester, England, 1988.
2. E.H.J.M. Jansen, G. Zomer, C. Van Peteghem, *Chemiluminescence Immunoassays in Veterinary and Food Analysis*, in: W.R.G. Baeyens, D. De Keukeleire, K. Korkidis (Eds.), *Luminescence Techniques in Chemical and Biochemical Analysis*, Practical Spectroscopy Series, vol. 12, Marcel Dekker, New York, 1991, pp. 477–504.
3. S.G. Schulman, G. Hochhaus, H.Th. Karnes, *Fluorescence Immunoassay in: W.R.G. Baeyens, D. De Keukeleire, K. Korkidis (Eds.), Luminescence Techniques in Chemical and Biochemical Analysis*, Practical Spectroscopy Series vol. 12, Marcel Dekker, New York, 1991, pp. 341–380.
4. A.W. Knight, *Trends Anal. Chem.* 18 (1999) 47.
5. H.E. Hart, E.D. Greenwald, *Mol. Immunol.* 16 (1979) 265.
6. S. Udenfriend, L.D. Gerber, L. Brink, S. Spector, *Proc. Natl. Acad. Sci. USA* 82 (1985) 8672.
7. P. Skládal, *J. Braz. Chem. Soc.* 14 (2003) 491.
8. J.P. Gosling (Ed.), *Immunoassays: A Practical Approach*, Oxford University Press, Oxford, UK, 2000.
9. I. Hemmilä, S. Webb, *Drug Discov. Today* 2 (1997) 373.
10. H.A.H. Rongen, A. Bult, W.P. van Bennekom, *J. Immunol. Methods*, 200 (1997) 105.
11. K.A. Fahrnich, M. Pravda, G. G. Guilbault, *Talanta*, 54 (2001) 531.
12. F. Lucarelli, G. Marrazza, A. P.E. Turner, M. Mascini, *Biosens. Bioelectron.* 19 (2004) 515.
13. I. Weeks, in: G. Svenhla (Ed.), *Chemiluminescence Immunoassay Wilson's Comprehensive Analytical Chemistry*, vol. 29, Elsevier, Amsterdam, 1992, p.1.
14. G.H.G. Thorpe, L. J. Kricka, *Methods Enzymol.* 133 (1986) 331.
15. L.J. Kricka, *Nucleic Acid Hybridization Test Formats: Strategies and Applications*. In: *Nonisotopic DNA Probe Techniques*, L.J. Kricka (Ed.), San Diego: Academic Press, 1992, p.3-19.
16. C. Dodeigne, L. Thunus, R. Lejeune, *Talanta* 51 (2000) 415.

17. A. Roda, P. Pasini, M. Guardigli, M. Baraldini, M. Musiani, M. Mirasoli, *Fresenius J. Anal. Chem.* 366 (2000) 752.
18. L.J. Kricka, *Anal. Chem.* 71 (1999) 305R.
19. H.Y. Aboul-Enein, R.I. Stefan, J.F. van Stafen, *Crit. Rev. Anal. Chem.*, 29 (1999) 323.
20. M.M. Richter, *Chem. Rev.* 104 (2004) 3003 and references therein.
21. R.T Duffort, D. Nightingale, L.W. Gaddum, *J. Am. Chem. Soc.* 49 (1927) 1858.
22. N. Harvey, *J. Phys. Chem.* 33 (1929) 1456.
23. R.E. Visco, E.A. Chandross, *J. Am. Chem. Soc.* 86 (1964) 5350.
24. D.M. Hercules, *Science* 145 (1964) 808.
25. L.R. Faulkner, *Methods Enzymol.* 57 (1978) 494.
26. L.R. Faulkner, A. J. Bard, *J. Electroanal. Chem.* 10 (1977) 1.
27. S.M. Park, D. A. Tryk, *Rev. Chem. Intermed.* 4 (1981) 43.
28. A.J. Bard, J. D. Dehad, J.K. Leland, G.B. Sigal, J.L. Wilbur, J.N. Wohlstadter, in: *Encyclopedia of Analytical Chemistry*. R.A. Meyers (Ed.), Wiley: Chichester, U.K. 2000; p. 9842.
29. E.A. Chandross, R.E. Visco, *J. Am. Chem. Soc.* 86 (1964) 5350.
30. K.S.V. Santhanam, A.J. Bard, *J. Am. Chem. Soc.* 87 (1965) 139.
31. J.M. Bader, T. Kuman, *J. Electroanal. Chem.* 10 (1965) 104.
32. A.W. Knight, G. M. Greenway, *Analyst* 119 (1994) 879.
33. L.R. Faulkner, H. Tachikawa, A.J. Bard, *J. Am. Chem. Soc.* 94 (1972) 691.
34. A.J. Bard, L. R. Faulkner, *Electrochemical Methods*, Wiley: New York, 1980.
35. A.J. Bard, L. R. Faulkner, *Electrochemical Methods Fundamentals and Applications*, 2nd ed.; Wiley: New York, 2001.
36. J. T. Maloy, K. B. Prater, A. J. Bard, *J. Am. Chem. Soc.* 93 (1971) 5959.
37. G. H. Brilmyer, A. J. Bard, *J. Electrochem. Soc.* 127 (1980) 104.
38. I. Rubinstein, A.J. Bard, *J. Am. Chem. Soc.* 103 (1981) 512.
39. J. K. Leland, M. J. Powell, *J. Electroanal. Chem.* 318 (1991) 91.
40. H.S. White, A. J. Bard, *J. Am. Chem. Soc.* 104 (1981) 6891.
41. D. Egg, W. Becker, A. J. Bard, *Anal. Chem.* 56 (1984) 2413.
42. V.C. Tsafack, C.A. Marquette, F. Pizzolato, L.J. Blum, *Biosens. Bioelectron.* 15 (2000) 125.
43. H.A.H Rongen, R.M.W. Hoetelmans, A. Bult, W.P. Van Bennekom, *J. Pharm. Biomed. Anal.* 12 (1994) 433.

44. W. Koppenol, *Bioelectrochem. Bioenerg.* 18 (1987) 3.
45. S. Kulmala, K. Haapakka, *J. Alloys Compd.* 225 (1995) 502.
46. E.P. Koval'chuk, O.V. Reshetnyak, A.O. Chernyak, Y.S. Kovalyshyn, *Electrochim. Acta* 44 (1999) 4079.
47. Y.E. Sung, F. Gaillard, A.J. Bard, *J. Phys. Chem. B* 102 (1998) 9797.
48. S. Kulmala, T. Ala-Kleme, L. Heikkilä, L. Väre, *J. Chem. Soc. Faraday Trans.* 93 (1997) 3107.
49. T. Ala-Kleme, S. Kulmala, M. Latva, *Acta Chem. Scand.* 51 (1997) 541.
50. S. Kulmala, J. Kankare, K. Haapakka, *Anal. Chim. Acta* 252 (1991) 65.
51. J. Kankare, K. Haapakka, S. Kulmala, V. Näntö, J. Eskola, H. Takalo, *Anal. Chim. Acta* 266 (1992) 205.
52. K. Haapakka, J. Kankare, S. Kulmala, *Anal. Chim. Acta* 209 (1988) 165.
53. S. Kulmala, T. Ala-Kleme, L. Heikkilä, L. Väre, *J. Chem. Soc. Faraday Trans.* 93 (1997) 165.
54. S. Kulmala, A. Kulmala, T. Ala-Kleme, J. Pihlaja, *Anal. Chim. Acta.* 367 (1998) 17.
55. F. Gaidlard, Y.E. Sung, A.J. Bard, *J. Phys. Chem. B* 103 (1999) 667.
56. Y. Pleskov, Z. Rotenberg, in: H. Gerischer, C. Tobias (Eds.), *Advances in Electrochemistry and Electrochemical Engineering*, Wiley, New York, 1978, pp. 3-115.
57. E. Hart, M. Anbar, *The Hydrated Electron*, Wiley, New York, 1970.
58. S. Kulmala, P. Raerinne, H. Takalo, K. Haapakka, *J. Alloys Compd.* 225 (1995) 492.
59. S. Kulmala, A. Hakanen, P. Raerinne, A. Kulmala, K. Haapakka, *Anal. Chim. Acta* 309 (1995) 197.
60. S. Kulmala, M. Helin, T. Ala-Kleme, L. Väre, D. Papkovsky, T. Korpela, A. Kulmala, *Anal. Chim. Acta* 386 (1999) 1-6.
61. S. Kulmala, Doctoral dissertation, Turku, Finland, 1995.
62. P. Canty, L. Väre, M. Håkansson, A.-M. Spehar, D. Papkovsky, T. Ala-Kleme, J. Kankare, S. Kulmala, *Anal. Chim. Acta* 453 (2002) 269.
63. A. Mayer, S. Neuenhofer, *Angew. Chem. Int. Ed.* 33 (1994) 1044.
64. W.Y. Lee, *Mikrochim. Acta* 127 (1997) 19.
65. I. Weeks, *Chemiluminescence Immunoassay*, Elsevier, New York, 1992.

66. J. Suomi, T. Ylinen, M. Hakansson, M. Helin, Q. Jiang, T. Ala-Kleme, S. Kulmala, *J. Electronanal. Chem.* 586 (2006) 49.
67. K. Haapakka, J. Kankare, O. Puhakka, *Anal. Chim. Acta* (1988), 207(1-2), 195.
68. S. Kulmala, J. Suomi, *Anal. Chim. Acta* 500 (2003) 21.
69. G.N. Chen, L. Zhang, R.E. Lin, Z.C. Yang, J.P. Duan, H.Q. Chen, D.B., Hibbert, *Talanta*, 50 (2000) 1275
70. K. Van Dyke, R. Van Dyke, *Luminescence Immunoassay and Molecular Applications*, CRC Press, Boca Raton, 1990.
71. D. Champiat, J.-P. Larpent, *Biochimiluminescence. Principles and applications*, Masson, Paris, 1993.
72. I. Weeks, I. Beheshti, F. McCapra, A.K. Campbell, J.S. Woodhead, *Clin. Chem.* 29 (1983) 1474.
73. H.A.H. Rongen, R.M.W. Hoetelmans, A. Bult, W.P.van Bennekom, *J. Pharm. Biomed. Anal.* 12 (1994) 433.
74. C.A. Marquette, L.J. Blum, *Sens. Actuators B* 51 (1998) 100.
75. K. Nakashima, K. Suetsugu, M. Yoshida, K. Imai, S. Akiyama, *Anal. Sci.* 7 (1991) 815.
76. S. Spurlin, M.M. Cooper, *Anal. Lett.* 19 (1986) 2277.
77. A.R. Bowie, M.G. Sanders, P. J. Worsfold, *J. Biolum. Chemilum.* 11 (1996) 61.
78. S. Girotti, E.N. Ferri, S. Ghini, F. Fini, M. Musiani, G. Carrea, A. Roda, P. Rauch, *Chem. Listy* 91 (1997) 477.
79. M. Yamaguchi, H. Yoshida, H. Nohta, *J. Chromatogr. A*, 950 (2002) 1.
80. K. Nakashima, K. Suetsugu, S. Akiyama, M. Yoshida, *J. Chromatogr.* 530 (1990) 154.
81. K. Nakashima, K. Suetsugu, K. Yoshida, K. Imai, S. Akiyama. *Anal. Sci.* 7 (1991) 815.
82. M. Hashimoto, K. Tsukagoshi, R. Nakajima, K. Kondo, *J. Chromatogr. A* 832 (1999) 191.
83. S.D. Gilman, C.E. Silverman, A.G. Ewing, *J. Microl. Sep.* 6 (1994) 97.
84. K. Arai, K. Takashi, F. Kusu, *Anal. Chem.* 71 (1999) 2237.
85. P. Molz, H.J. Skrzipezyk, T. Kinkel, G. Schnoor, H. Strecker, *J. Biolumin. Chemilumin.* 2 (1988) 238.
86. J.W. Leidy, *J. Immunol. Methods* 172 (1994) 197.
87. S. Alkan, C. Akdis, H. Towbin, *J. Immunoassay* 15 (1994) 217.



88. U.R. Joss, H. Towbin, J. Biolumin. Chemilumin. 9 (1994) 21.
89. S.-K. Oh, S. Luhowskyj, P. Witt, P. Ritch, D. Reitsma, H. Towbin, M. Horisberger, P. von Wussow, B. Bluestein, J. Immunol. Methods 176 (1994) 79.
90. H. Towbin, A. Schmitz, J. Vanoostrum, M. Seitz, B. Dewald, O. Zingel, J. Motz, K. Vosbeck, C. Rordorf, J. Immunol. Methods 170 (1994) 125.
91. S. Kamihira, S. Nakashima, S. Saitoh, M. Kawamoto, Y. Kawashima, M. Shimamoto, Jpn. J. Cancer Res. 84 (1993) 834.
92. T.J. Wu, C. L. Lin, R.L. Taylor, P. C. Kao, Ann. Clin. Lab. Sci. 25 (1995) 467.
93. T.J. Wu, R.L. Taylor, P.C. Kao, Ann. Clin. Lab. Sci. 27 (1997) 384.
94. G. Ogbonna, P.S. Caines, P. Catomeris, R.J. Thibert, K. Adeli, Clin. Biochem. 28 (1995) 117
95. U. Piran, W.J. Riordan, L.A. Livshin, Clin. Chem. 41(1995) 986.
96. H. Sato, H. Mochizuki, Y. Tomita, T. Izako, N. Sato, T. Kanamori, J. Biolumin. Chemilumin. 11 (1996) 23.
97. J.M.A. Schlaeppli, A. Kessler, W. Fory, J. Agric. Food Chem. 42 (1994) 1914.
98. R.C. Hart, L.R. Taaffe, J. Immunol. Methods 101 (1987) 91.
99. S. Batmanghelich, R.C. Brown, J.S. Woodhead, I. Weeks, K. Smith, J. Photochem. Photobiol. B 12 (1992) 193.
100. N.C. Nelson, A.B. Cheikh, E. Matsuda, M.M. Becker, Biochem. 35 (1996) 8429.
101. N.C. Nelson, J.S. Woodhead, I. Weeks, A. B. Cheikh, US Pat. 94-331107 (1994).
102. A. Mazumder, M. Majlessi, M.M. Becker, Nucl. Acids Res. 26 (1998) 1996.
103. F.A. Clifdon-Hadley, Rev. Med. Microbiol. 11 (2000) 47.
104. H. Yu, J.W. Raymonda, T.M. McMahon, A.A. Campagnari, Biosens. Bioelectron. 14 (2000) 829.
105. W.L. Xing, F.H. Chao, Z.H. Jiang, L.R. Ma, Chem. J. Chinese U. 21 (2000) 873.
106. C. Grimshaw, C. Gleason, E. Chojnicki, J. Young, J. Pharmaceut. Biomed. Anal. 16 (1997) 605.
107. A.M. Siddiqi, V.M. Jennings, M.R. Kidd, J.K. Actor, R.L. Hunter, J. Clin. Lab. Anal. 10 (1996) 423.
108. K. Motmans, J. Raus, C. Vandevyver, J. Immunol. Methods 190 (1996) 107.

109. C.D. O'Connell, A. Juhasz, C. Kuo, D.J. Reeder, D.S.B. Hoon, *Clin. Chem.* 44 (1998) 1161.
110. Y.T. Hsueh, R.L. Smith, M.A. Northrup, *Transducers' 95 — Eurosensors IX*, Stockholm, Sweden, June 1995, pp. 768–771.
111. G.F. Blackburn, H.P. Shah, J.H. Kenten, J. Leland, R.A. Kamin, J. Link, J. Peterman, M.J. Powell, A. Shah, D.B. Talley, *Clin. Chem.* 37 (1991) 1534.
112. J.H. Kenten, J. Casedei, J. Link, S. Lupold, J. Willey, M. Powell, A. Rees, R. Massey, *Clin. Chem.* 37 (1991) 1626.
113. S.R. Gudibande, J.H. Kenten, J. Link, R.J. Massey, *Mol. Cell. Probes.* 6 (1992) 495.
114. B. van Gemen, R. van Beuningen, A. Nabbe, D. van Strijp, S. Jurriaans, P. Lens, T. Kietvits, *J. Virol. Meth.* 49 (1994) 157.
115. D.L. Gatto-Menking, H. Yu, J.G. Bruno, M.T. Goode, M. Miller, A.W. Zulich, *Proc. ERDEC Sci. Conf. Chem. Biol. Def. Res.* (1994) 229.
116. D.L. Gatto-Menking, H. Yu, J.G. Bruno, M.T. Goode, M. Miller, A.W. Zulich, *Biosens. Bioelectr.* 10 (1995) 501.
117. T.E. Schutzbank, J. Smith, *J. Clin. Microbiol.* 33 (1995) 2036.
118. M.D. de Jong, J.F.L. Weel, T. Schuurman, P.M. Wertheim-van Dillen, R. Boom, *J. Clin. Biol.* 38 (2000) 2568.
119. S.J.C. Stevens, M.B.H.J. Vervoort, A.J.C. Van den Brule, P.L. Meenhorst, C.J.L.M. Meijer, J.M. Middeldorp, *J. Clin. Microbiol.* 37 (1999) 2852.
120. R.J. Massay, G.F. Blackburn, E.W. Wilkins, J.K. Leland, US Patent, 95-5746974 (1995).
121. R.J. Massay, G.F. Blackburn, E.W. Wilkins, J.K. Leland, U.S. Patent, 94-5770459 (1994).
122. D.R. Deaver, *Nature* 377 (1995) 758.
123. K. Erler, *Wien. Klin. Wochenschr.* 110 (1998) 5.
124. R.J. de Winter, R.W. Koster, J.P. van Straalen, J.P. Gorgels, F.J. Hoek, G.T. Sanders, *Clin. Chem.* 43 (1997) 338.
125. P.C. D'Haese, G.F. Van Landeghem, L.V. Lamberts, V.A. Bekaert, I. Schrooten, M.E. De Broe, *Clin. Chem.* 43 (1997) 121
126. R. Y. Lai, M. Chiba, N. Kitamura, A. J. Bard, *Anal. Chem.* 74 (2002) 551.
127. B. D. Muegge, M. M. Richter, *Anal. Chem.* 74 (2002) 547.
128. D. Bruce, M. M. Richter, *Analyst* 127 (2002) 1492.

129. F. Kanoufi, A. J. Bard, *J. Phys. Chem. B* 103 (1999) 10469.
130. B.L. Waguespack, A. Lillquist, A. Townley, A. Bobbitt, *Anal. Chim. Acta* 441 (2001) 231.
131. M.M. Richter, A.J. Bard, W. Kim, R.H. Schmechl, *Anal. Chem.* 70 (1998) 310.
132. M. Staffilani, E. Hoss, U. Giesen, E. Schneider, F. Hartl, H.-P. Josel, L. De Cola, *Inorg. Chem.* 42 (2003) 7789.
133. H. D. Abruna, *J. Electroanal. Chem.* 175 (1984) 321.
134. D. Bruce, M. M. Richter, K. Brewer, *J. Anal. Chem.* 74 (2002) 3157.
135. C.-W. Lee, J. Ouyang, A. J. Bard, *J. Electroanal. Chem.* 244 (1988) 319.
136. P. Wang, G. Zhu, *Asian J. Chem.* 11 (1999) 1149.
137. G. Xu, S. Dong, *Anal. Chim. Acta* 12 (2000) 235.
138. A. Vogler, H. Kunkely, *Am. Chem. Soc. Symp. Ser.* 333 (1987) 155.
139. G. A. Crosby, R. E. Whan, R. M. Allire, *J. Chem. Phys.* 34 (1961) 743.
140. A. P. B. Sinha, *Spectrosc. Inorg. Chem.* 2 (1971) 255.
141. C.X. Sun, J.H. Yang, L. Li, X. Wu, Y. Liu, S.F. Liu, *J. Chromatogr. B* 803 (2004) 173.
142. E. F. Gudin Dickson, A. Pollak, E.P. Diamandis, *J. Photochem. Photobiol. B; Biol.*, 27 (1995) 3.
143. M. Elbanowski, B. Makowska, *J. Photochem. Photobiol. A; Chem.*, 99 (1996) 85.
144. R.E. Hemingway, S.-M. Park, A. J. Bard, *J. Am. Chem. Soc.* 97 (1975) 2000.
145. P.D. Wildes, E.H. White, *J. Am. Chem. Soc.* 93 (1971) 6286.
146. T. Ala-Kleme, K. Haapakka, M. Latva, *J. Alloys Compd.* 275-277 (1998) 911.
147. M. Paetz, M. Elbanowski, *J. Photochem. Photobiol., A: Chem.* 55 (1990) 63.
148. M. Elbanowski, M. Paetz, *J. Photochem. Photobiol. A: Chem.* 62 (1991) 27.
149. A.I. Voloshin, G.L. Sharipov, V.P. Kazakov, G.A. Tolstikov, *Dokl. Akad. Nauk. SSSR* 315 (1990) 425.
150. J. Kankare, K. Fälden, S. Kulmala, K. Haapakka, *Anal. Chim. Acta* 256 (1992) 17.
151. S. Kulmala, M. Håkansson, A.-M. Spehar, A. Nyman, J. Kankare, K. Loikas, T. Ala-Kleme, J. Eskola, *Anal. Chim. Acta*, 458 (2002) 271.
152. M. Helin, L. Vare, M. Håkansson, P. Canty, H.-P. Hedman, L. Heikkilä, T. Ala-Kleme, J. Kankare, S. Kulmala, *J. Electroanal. Chem.* 524-525 (2002) 176.
153. A. Despic, V.P. Parkhutik, *Modern Aspects of Electrochemistry*, 20 (1989) 401.

154. J. Diggle, T. Downie, C. Goulding, *Chem. Rev.* 69 (1969) 365.
155. D. Diesing, S. Russe, A. Otto, M. Lohrengel, *Ber. Bunsenges. Phys. Chem.* 99 (1995) 1402.
156. S. Kulmala, T. Ala-Kleme, *Ber. Bunsenges. Phys. Chem.* 101 (1997) 758.
157. C. Morrison, *Electrochemistry at Semiconductor and Oxidized Metal Electrodes*, Plenum Press, New York, 1980. (a) pp. 299-334; (b) p.6. (c) p. 114.
158. S. Chang, N. Johnson, S. Lyon, *Appl. Phys. Lett.* 44 (1984) 317.
159. D. DiMaria, E. Cartier, *J. Appl. Phys.* 78 (1995) 3883.
160. S. Kulmala, T. Ala-Kleme, H. Joela, A. Kulmala, *J. Radioanal. Nucl. Chem.* 232 (1998) 91.
161. J. Luttmmer, A. Bard, *J. Electrochem. Soc.* 125 (1978) 1423.
162. N. Klein, M. Albert, *J. Appl. Phys.* 53 (1982) 5840.
163. G. Buxton, C. Greenstock, W. Helman, A. Ross, *J. Phys. Chem. Ref. Data* 17 (1988) 513 and the references therein.
164. S. Kulmala, A. Kulmala, M. Latva, K. Haapakka, *Anal. Chim. Acta* 347 (1997) 333.
165. A. Bernas, D. Grand, E. Anoyal, *J. Phys. Chem.* 84 (1980) 1259.
166. W. Koppenol, J. Butler, *Adv. Free. Bio. Med.* 1 (1985) 91.
167. M.M. Richter, *Chem. Rev.* 104 (2004) 3003 and references therein.
168. Y. Yoshimi, H. Haramoto, T. Miyasaka, K. Sakai, *J. Chem. Eng. Jpn.* 29 (5) (1996) 851.
169. T. Miyasaka, K. Endo, K. Sakai, *J. Artif. Organs.* 5 (2002) 18.
170. C. Zhang, H. Zhang, M. Feng, *Anal. Lett.* 36 (2003) 1103.
171. S. Kulmala, T. Ala-Kleme, A. Kulmala, D. Papkovsky, K. Loikas, *Anal. Chem.* 70 (1998) 1112.
172. T. Ala-Kleme, S. Kulmala, L. Väre, M. Helin, *Anal. Chem.* 71 (1999) 5538.
173. J. J. Yourick, R. L. Bronaugh, *J. Appl. Toxicol.* 17 (1997) 153.
174. R. D. H. Murray, J. Mendez, S. A. Brown, *Progress in the chemistry of organic natural products*, 72 (1997) 1.
175. S. R. Trenor, A. R. Shultz, B.J. Love, T.E. Long, *Chem. Rev.* 104 (2004) 3059.
176. I. Hemmilä, *Applications of Fluorescence in Immunoassays*, John Wiley & Sons, New York, 1991, and the references therein.
177. S. Fujita, N. Kagyama, M. Momyama, Y. Kondo, *Jpn. Kokai Tokyo Koho* (1996) JP 08029422.


178. G.J. Keating, J.G. Quinn, R. O'Kennedy, *Anal. Lett.* 32 (1999) 2136.
179. B. Deasy, E. Dempsey, M.R. Smyth, D. Egan, D. Bogan, R. O'Kennedy, *Anal. Chim. Acta*, 294 (1994) 291.
180. R.C. Wong, J.F. Burd, R.J. Carrico, R.T. Buckler, J. Thoma, R.C. Boguslaski, *Clin. Chem.* 25 (1979) 686.
181. R. A. Houghten, T. C. Dooley, J. R. Appel, *Bioorganicmedic. Chem. Lett.* 14 (2004) 1947.
182. K. Sommermeyer, V.B. Birkwald, W. Pruetz, *Strahlentherapie* 116 (1961) 354.
183. K. Sommermeyer, W. Pruetz, *Zeitschrift für Naturforschung, Teil A: Astrophysik, Physik und Physikalische Chemie* 21 (1966) 1081.
184. W. Pruetz, K. Sommermeyer, E.J. Land, *Nature* 212 (1966) 1043.
185. P.S. Rao, E. Hayon, *J. Am. Chem. Soc.* 96 (1974) 1287.
186. S. Park, A.J. Bard, *J. Electroanal. Chem.* 77 (1977) 137.
187. D. Stanbury, *Adv. Inorg. Chem. Rad. Chem.* 33 (1989) 69.
188. W. Prutz, E.J. Land, *Biophysik*, 3 (1967) 349.
189. E. Kucherenko, L.A. Kartasheva, A. Pikaev, *High Energy Chem.* 16 (1982) 168.
190. K.D. Legg, D.M. Hercules, *J. Am. Chem. Soc.* 91 (1969) 1902.
191. Y.G. Sun, H. Cui, X.Q. Lin, *J. Lumin.* 92 (2001) 205.
192. C. Zhang, H. Qi, *Anal. Sci.* 18 (2002) 819.
193. I. Minkenbergh, E. Ferber, *J. Immunol. Methods* 71 (1984) 61.
194. H. Gyllenhammar, *J. Immunol. Methods* 97 (1989) 209.
195. H. Gyllenhammar *J. Clin. Lab. Immunol.* 28 (1989) 97.
196. H. Sasamoto, M. Maeda, A. Tsuji, *Anal. Chim. Acta* 310 (1995) 347.
197. Y.Y. Su, J. Wang, G. Che, *Talanta* 65 (2005) 531.
198. J.M. Lin, M. Yamada, *Microchem. J.* 58 (1998) 105.
199. G.N. Chen, L. Zhang, R.E. Lin, Z.C. Yang, J.P. Duan, H.Q. Chen, D.B. Hibbert, *Talanta* 50 (2000) 1275.
200. R. Maskiewicz, D. Sogah, T.C. Bruice, *J. Am. Chem. Soc.* 101 (1979) 5355.
201. R. Maskiewicz, D. Sogah, T.C. Bruice, *J. Am. Chem. Soc.*, 101 (1979) 5347.
202. T. Okajima, T. Ohsaka, *J. Electroanal. Chem.* 534 (2002) 181.
203. K. Papadopoulos, T. Triantis, D. Dimotikali, J. Nikokavouras, *J. Photochem. Photobiol. A: Chem.*, 124 (1999) 85.
204. S. Kulmala, A. Kulmala, M. Helin, I. Hyppänen, *Anal. Chim. Acta*, 359 (1998) 71.

205. R. D. Gerardi, N. W. Barnett, S. W. Lewis, *Anal. Chim. Acta*, 378 (1999) 1.
206. R. Memming, *J. Electrochem. Soc.* 116 (1969) 785.
207. P. Neta, R. Huie, A. Ross, *J. Phys. Chem. Ref. Data* 17 (1988) 1027.
208. S. Kulmala, C. Matachescu, A. Kulmala, D. Papkovsky, M. Hakansson, H. Ketamo, P. Canty, *Anal. Chim. Acta*, 453 (2002) 253.
209. J. Thomas, S. Gordon, E. Hart, *J. Phys. Chem.* 68 (1964) 1524.
210. C. Jørgensen, *Theoretical Chemistry of Rare Earths*, in K. Gschneider, Jr. and L. Eyring (Eds.), *Handbook on the Physics and Chemistry of Rare Earths*, Vol. 3, North-Holland, Amsterdam, 1979, p. 111.
211. S. Steenken, *Top. Curr. Chem.* 177 (1996) 125.
212. S. Steenken, *J. Chem. Soc. Faraday Trans. I* 83 (1987) 113.
213. G. Reynolds, *J. Lumin.* 54 (1992) 43, and references therein.
214. A. Bard, R. Pearsons, J. Jordan (Eds.), *Standard Potentials in Aqueous solutions*, Marcel Dekker Inc., New York, 1985, pp. 618–629 and 555–585.
215. H. Aida, I. Epelboin, M. Garreau, *J. Electrochem. Soc.* 118 (1971) 243.
216. A. Juris, V. Balzani, F. Barigelletti, S. Campagna, P. Belser, A. Zelewsky, *Coord. Chem. Rev.* 84 (1988) 85.
217. D.M. Hercules, F.E. Lytle, *J. Am. Chem. Soc.* 88 (1966) 4745.
218. E. Terpetschnig, H. Szmecinski, J. R. Lakowicz, *Anal. Biochem.* 227 (1995) 140.
219. P.E. Michel, N.F. de Rooij, M. Koudelka-hep, K. A. Fahrnich, C.K. O'Sullivan, G.G. Guilbault, *J. Electroanal. Chem.* 474 (1999) 192.
220. A. J. Bard, G. M. Whiteside, PCT. WO86/02734 (1986).
221. C. M. Elliott, E. J. Hershenhart, *J. Am. Chem. Soc.* 104 (1982) 7519.
222. T. Saji, S. Aoyagui, *J. Electroanal. Chem. Interfac. Electrochem.* 58 (1975) 401.
223. S. Kulmala, T. Ala-Kleme, M. Latva, K. Loikas, H. Takalo, *J. Fluoroscence.* 8 (1998) 59.
224. E. Soini, T. Lövgren, *CRC Crit. Rev. Anal. Chem.* 18 (1987) 105 and references therein.
225. M.M. Richter, A.J. Bard, *Anal. Chem.* 68 (1996) 2641.
226. W. Carnall, *The Absorption and Fluorescence Spectra of Rare Earth Ions in Solution*, in: K. Gschneider, Jr. and L. Eyring (Eds.), *Handbook on the Physics and Chemistry of Rare Earths*, Vol. 3, North-Holland, Amsterdam, 1979, pp. 171-208.

227. A. Hakanen, E. Laine, K. Haapakka, *Europhys. Lett.* 39 (1997) 311.
228. J. Kankare, A. Karppi, H. Takalo, *Anal. Chim. Acta* 295 (1994) 27.
229. J. Birks, *Photophysics of Aromatic Molecules*, Wiley, London, 1970, pp.397-399.
230. T. Ala-Kleme, *Doctoral Dissertation*, Turku, Finland, 2002.
231. S. K. Schmidt, E. Hart, J. Edwin, *J. Phys. Chem.* 81 (1977) 104.
232. M. Sauer, B. Ward, *J. Phys. Chem.* 71 (1967) 3971.
233. D. Walker, *ACS Advan. Chem.* 81 (1968) 49.
234. J. Kalecinsky, *Bull. Acad. Pol. Ser. Chim.* 18 (1970) 263.
235. M. Håkansson, Q. Jiang, A.-M. Spehar, J. Suomi, S. Kulmala, *J. Lumin.* in press.
236. R. Yalow, S. Berson, *Nature* 184 (1959) 1648.
237. J. Kankare, K. Haapakka, GB2217007, patent filed 21.3.1989.
238. R. Reisfeld, *J. Res. Natl. Bur. Stand. U.S., Sect. A*, 76 (1972) 613.

## **Reprints of original publications**





ISBN 951-22-8106-6  
ISBN 951-22-8107-4 (PDF)  
ISSN 1795-2239  
ISSN 1795-4584 (PDF)